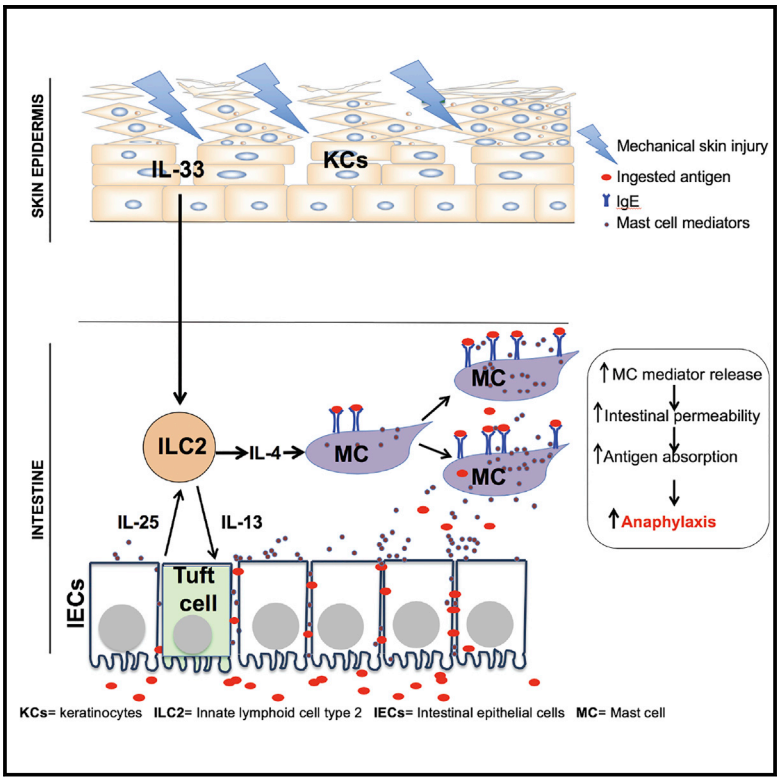
Article

Immunity

# Mechanical Skin Injury Promotes Food Anaphylaxis by Driving Intestinal Mast Cell Expansion

## Graphical Abstract




## Highlights

- Mechanical skin injury promotes intestinal mast-cell expansion
- Intestinal mast-cell expansion requires skin-derived IL-33 and gut-derived IL-25
- Intestinal mast-cell expansion requires ILC2 activation by IL-33 and IL-25
- ILC2-derived IL-4 and IL-13 directly cause intestinal mast-cell expansion

## Authors

Juan-Manuel Leyva-Castillo, Claire Galand, Christy Kam, ..., Isaac Chiu, K. Frank Austen, Raif S. Geha

## Correspondence

raif.geha@childrens.harvard.edu

## In Brief

Atopic dermatitis is a pruritic inflammatory skin disease highly associated with food allergy. Leyva-Castillo and colleagues demonstrate that a skin-to-gut crosstalk initiated by mechanical skin injury promotes food anaphylaxis by increasing mast cells in the gut.

Leyva-Castillo et al., 2019, Immunity *50*, 1–14
May 21, 2019 © 2019 Elsevier Inc.
https://doi.org/10.1016/j.immuni.2019.03.023

CellPress

Please cite this article in press as: Leyva-Castillo et al., Mechanical Skin Injury Promotes Food Anaphylaxis by Driving Intestinal Mast Cell Expansion, Immunity (2019), https://doi.org/10.1016/j.immuni.2019.03.023



CellPress

# Mechanical Skin Injury Promotes Food Anaphylaxis by Driving Intestinal Mast Cell Expansion

Juan-Manuel Leyva-Castillo,[1,11] Claire Galand,[1,11,12] Christy Kam,[1] Oliver Burton,[1,13] Michael Gurish,[2,14] Melissa A. Musser,[3] Jeffrey D. Goldsmith,[4] Elizabeth Hait,[5] Samuel Nurko,[5] Frank Brombacher,[6] Chen Dong,[7] Fred D. Finkelman,[8] Richard T. Lee,[9] Steven Ziegler,[10] Isaac Chiu,[3] K. Frank Austen,[2] and Raif S. Geha[1,15,*]

[1]Division of Immunology, Boston Children's Hospital, Harvard Medical School, Boston, MA, USA
[2]Division of Rheumatology, Immunology and Allergy, Brigham and Women's Hospital, Harvard Medical School, Boston, MA, USA
[3]Department of Microbiology and Immunobiology, Harvard Medical School, Boston, MA 02115, USA
[4]Department of Pathology, Boston Children's Hospital, Boston, MA, USA
[5]Division of Gastroenterology, Boston Children's Hospital, Boston, MA, USA
[6]International Center for Genetic Engineering and Biotechnology & University of Cape Town & South Africa Medical Research Council, South Africa
[7]Institute for Immunology and School of Medicine, Tsinghua University, Beijing, China
[8]Department of Internal Medicine and Division of Immunobiology, Cincinnati Children's Hospital Medical Center, Cincinnati, OH, USA
[9]Department of Stem Cell and Regenerative Biology, Harvard University, Cambridge, MA, USA
[10]Immunology Program, Benaroya Research Institute, Seattle, WA, USA
[11]These authors contributed equally
[12]Present address: Agenus, Inc., 3 Forbes Rd, Lexington, MA 02421, USA
[13]Present address: VIB-KU Leuven Center for Brain & Disease Research, Leuven, Belgium
[14]Deceased
[15]Lead Contact
*Correspondence: raif.geha@childrens.harvard.edu
https://doi.org/10.1016/j.immuni.2019.03.023

## SUMMARY

**Mast cell (MC) mediator release after crosslinking of surface-bound IgE antibody by ingested antigen underlies food allergy. However, IgE antibodies are not uniformly associated with food allergy, and intestinal MC load is an important determinant. Atopic dermatitis (AD), characterized by pruritis and cutaneous sensitization to allergens, including foods, is strongly associated with food allergy. Tape stripping mouse skin, a surrogate for scratching, caused expansion and activation of small intestinal MCs, increased intestinal permeability, and promoted food anaphylaxis in sensitized mice. Tape stripping caused keratinocytes to systemically release interleukin-33 (IL-33), which synergized with intestinal tuft-cell-derived IL-25 to drive the expansion and activation of intestinal type-2 innate lymphoid cells (ILC2s). These provided IL-4, which targeted MCs to expand in the intestine. Duodenal MCs were expanded in AD. In addition to promoting cutaneous sensitization to foods, scratching may promote food anaphylaxis in AD by expanding and activating intestinal MCs.**

## INTRODUCTION

Food allergy affects 6% of children and 3% of adults in the US and is on the rise (Sicherer and Sampson, 2009). The life-threatening symptom of food allergy is anaphylaxis. The physiopathology of anaphylaxis involves mast cell (MC) degranulation and release of mediators and cytokines after recognition of antigen by immunoglobulin E (IgE) antibodies bound to high-affinity IgE receptors (FcεRI) on MCs (Galli and Tsai, 2012). Not all individuals who have food-specific IgE antibodies react upon oral challenge, and food-specific IgE serum concentrations do not necessarily predict the severity of food allergy (Fleischer et al., 2011). Thus, additional factors other than IgE antibody are required for food anaphylaxis. An important such factor is intestinal MC load, which controls intestinal permeability (Lee et al., 2013) and, thereby, systemic absorption of antigen, which is essential for food anaphylaxis (Strait et al., 2011). Importantly, gut MC expansion is associated with increased susceptibility to oral anaphylaxis (Vaali et al., 2012), and intestinal MC load modulates the severity of oral anaphylaxis (Ahrens et al., 2012). Cutaneous exposure to food allergens in infants and mice predisposes to IgE-mediated food allergy (Bartnikas et al., 2013; Lack et al., 2003), implicating the skin as an important route of sensitization. There is a high prevalence of IgE antibodies to foods in atopic dermatitis (AD), a chronic pruritic inflammatory skin disease affecting ~15% of children in the United States (Spergel, 2010). The association between IgE sensitization to food and food anaphylaxis is substantially higher in patients with AD than in the population at large (Salo et al., 2014). Intestinal $IgE^+$ cell numbers are increased in patients with AD (Caffarelli et al., 2001; Kalimo et al., 1988), but the nature of these $IgE^+$ cells is ill defined. Furthermore, intestinal permeability is increased in AD patients (Pike et al., 1986). Tape stripping the skin of mice is a surrogate for scratching. Intestinal MC expansion is observed after application of saline to tape-stripped skin (Bartnikas et al., 2013), suggesting a link between mechanical skin injury and intestinal MC expansion. In the present study,

we demonstrate that tape stripping mouse skin causes selective MC expansion in the small intestine (SI), increases intestinal permeability, and promotes food anaphylaxis. Interleukin (IL)-33 released by keratinocytes synergized with IL-25 released by intestinal tuft cells to expand intestinal type-2 innate lymphoid cells (ILC2s) and increase their expression of *Il4* and/or *Il13*. ILC2-derived IL-4 and IL-13 targeted MCs to cause their expansion in the SI. We demonstrated that duodenal MCs are expanded in children with AD, independent of overt food allergy. Our observations document a skin-to-gut crosstalk in which mechanical skin injury promotes food anaphylaxis by driving intestinal MC expansion, in addition to facilitating sensitization to food allergens. Thus, our results are directly relevant to food allergy in patients with AD.

## RESULTS

### Mechanical Skin Injury Elicits Expansion of Intestinal Mast Cells

To mimic mechanical skin injury caused by scratching, the shaved back skin of BALB/c mice was tape stripped six times on day 0 and three times on day 3, and the mice were studied on day 14 (Figure 1A). Tape stripping resulted in a 2-fold increase in chloroacetate esterase positive ($CAE^+$) MCs in the jejunum, including MCs in the submucosa, as well as the lamina propria (LP) (Figure 1B). Immunohistochemical staining demonstrated that tape stripping the skin caused an increase in mast cell protease-$1^+$ ($mMCPT1^+$) MCs and $mMCPT6^+$ MCs in the jejunum (Figure S1A). The increase in MC expansion in the jejunal LP of tape-stripped mice was confirmed by flow cytometric analysis of $CD45^+Lin^-$ $c\text{-}Kit^+IgE^+$ cells (Figure 1C). Tape stripping also caused MC expansion in the duodenum but not in the colon (Figure S1B). The total number of $CD45^+$ cells in the SI did not increase in tape-stripped mice (Figure S1C). MCs expanded at the site of tape stripping but not in distant skin sites, lungs, or spleen (Figure 1D).

Tape stripping the skin caused an increase in the granularity of jejunal $c\text{-}Kit^+IgE^+$ MCs (Figure 1E) and upregulated their surface expression of c-Kit and IgE binding (Figure 1F), as well as their expression of *Il13*, *Hdc*, *Alox5*, *Kit*, and *Fcer1a* but not *Il4* (Figure 1G). *Il5* and *Il9* mRNAs were not detectable in jejunal MCs. These results indicate that tape stripping causes selective expansion of mucosal and submucosal MCs in the SI with an increase in MC granularity, maturation, and potential ability to produce IL-13, histamine, and leukotrienes.

Expansion of intestinal MCs after mechanical skin injury was not specific to the BALB/c strain, as it was observed in C57BL/6 mice (Figures S1D and S1E). Furthermore, it was independent of the mouse housing facility. A comparable ~2-fold increase in jejunal MCs was observed after tape stripping the skin of BALB/c mice obtained from Taconic Biosciences (Figure S1E). Importantly, jejunal MC expansion induced by tape stripping was independent from the microbiota, as it was preserved in germ-free BALB/c mice (Figure S1E). Because of the differences in baseline numbers of intestinal MCs between mice of different strains and mice housed in different facilities, we subsequently expressed the numbers of intestinal MCs in tape-stripped mice relative to their numbers in genetically matched unmanipulated controls.

### Tape Stripping Increases Intestinal Permeability and Promotes Oral Anaphylaxis

MC numbers in mouse intestine correlate with intestinal permeability (Ahrens et al., 2012). Tape stripping mouse skin caused an increase in intestinal permeability, as evidenced by an increase in serum horseradish peroxidase (HRP) concentration after oral gavage of HRP (Figure 2A). The increase in intestinal permeability was dependent on MCs and, in particular, on intestinal MCs, as it was not observed in $Kit^{W\text{-}sh/W\text{-}sh}$ mice, which globally lack MCs, or $Itgb7^{-/-}$ mice, which are selectively deficient in intestinal MCs (Gurish et al., 2001) (Figure 2A).

We investigated whether the expansion, increased granularity, and activation of intestinal MCs elicited by mechanical skin injury was associated with enhancement of oral anaphylaxis. To that end, mice were tape stripped and i.p. immunized with ovalbumin (OVA) or saline in alum, then challenged orally with OVA (Figure 2B). As expected, mice i.p. immunized with OVA, but not saline, demonstrated a drop in body temperature and an increase in serum mMCPT1 concentrations after oral OVA challenge (Figure 2B). Tape stripping of the skin enhanced oral anaphylaxis in mice i.p. immunized with OVA, as evidenced by a greater drop in core body temperature and higher serum mMCPT1 concentrations after oral OVA challenge compared to non-tape-stripped controls (Figure 2B). Neither non-tape-stripped nor tape-stripped i.p.-immunized $Itgb7^{-/-}$ mice exhibited a drop in body temperature after oral OVA challenge (data not shown), demonstrating the critical role of intestinal MCs in food anaphylaxis. MC expansion after tape stripping was comparable in mice immunized with OVA and in controls injected with saline (Figure S2A). Tape stripping had no detectable effect on the IgE anti-OVA response to i.p. immunization (Figure S2B). These results indicate that that the more severe oral anaphylaxis in tape-stripped mice was not due to a greater IgE antibody response to OVA.

To circumvent other potential effects of tape stripping on the response to OVA immunization, we examined whether tape stripping of the skin enhances IgE-mediated passive food anaphylaxis. Mice were tape stripped and passively sensitized by i.v. administration of IgE anti-TNP (2,4,6-trinitrophenol) or saline as control, then challenged orally with TNP-BSA (bovine serum albumin) (Figure 2C). Mice sensitized with IgE anti-TNP, but not unsensitized controls, demonstrated a drop in body temperature and an increase in serum mMCPT1 concentrations after oral TNP-BSA challenge (Figure 2C). Anaphylaxis to oral antigen challenge following passive sensitization was more severe in tape-stripped mice compared to unmanipulated controls, as evidenced by a greater drop in core body temperature and higher serum concentrations of MCTP1 (Figure 2C). These results suggest that expansion of intestinal MCs after mechanical skin injury increases intestinal absorption of antigen and promotes oral anaphylaxis.

### Keratinocyte-Derived IL-33 and Intestinal-Cell-Derived IL-25 Are Essential for Intestinal MC Expansion Elicited by Mechanical Skin Injury

Keratinocytes upregulate the expression and/or release of the cytokines IL-33, thymic stromal lymphopoietin (TSLP), and IL-25 in response to injury (Leyva-Castillo et al., 2013; Oyoshi et al., 2010). Receptors for these cytokines are expressed by

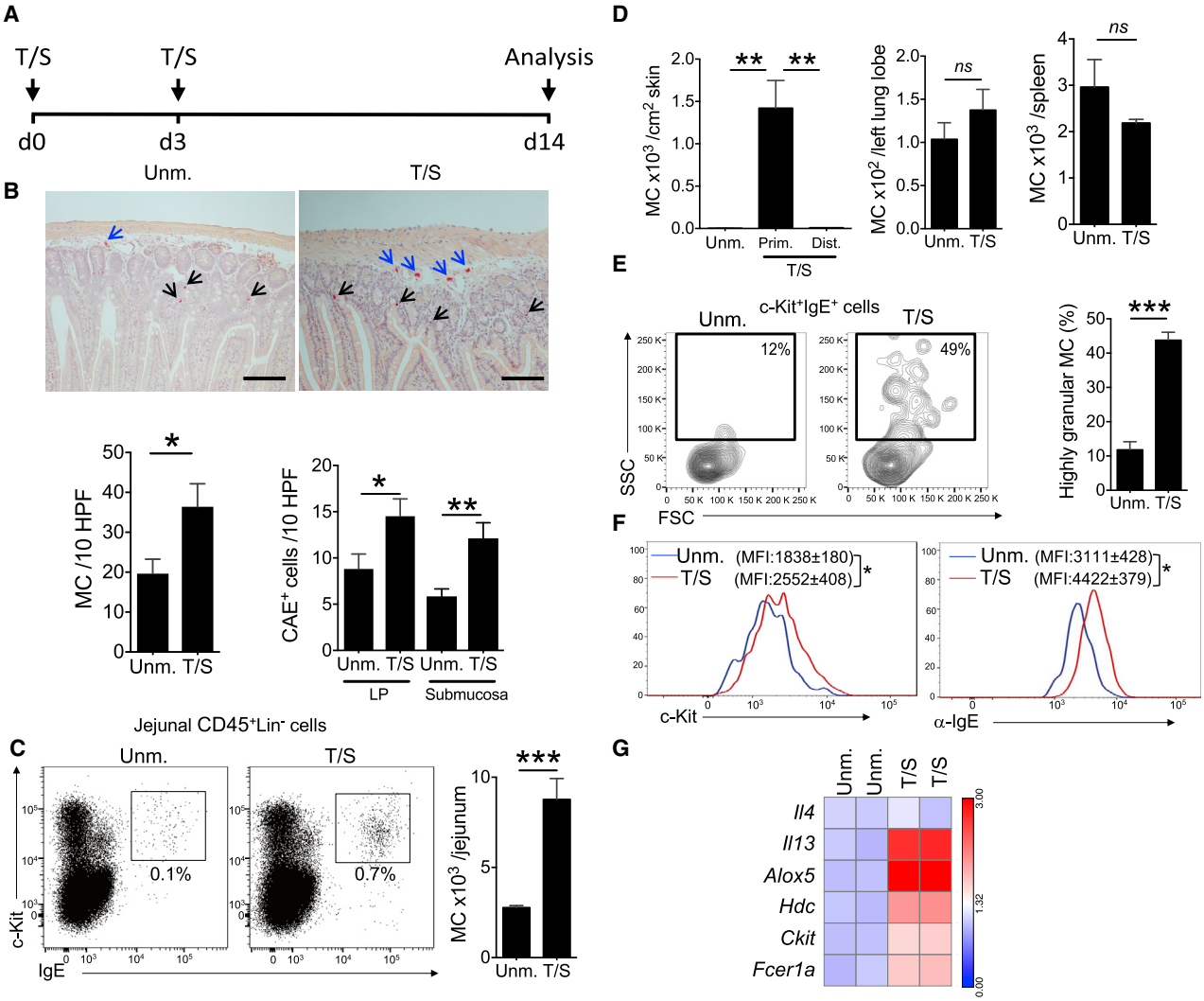



**Figure 1. Tape Stripping Mouse Skin Causes Expansion of Mast Cells (MCs) in the Small Intestine**

(A) Experimental protocol. BALB/C mouse skin was tape stripped (T/S) 6 times on day 0 and 3 times on day 3 using Tegaderm; mice were analyzed on day 14.

(B) Representative chloroacetate esterase (CAE) staining of jejunal sections, with scale bars representing 100 μM (top) and quantitation of MC numbers per 10 HPF in jejunum (bottom left) and jejunal LP and submucosa (bottom right) of T/S mice and unmanipulated (Unm.) controls. Results are derived from 2 independent experiments, each with 3 to 5 mice/group.

(C) Representative flow cytometry analysis of c-Kit$^+$IgE$^+$ MCs in the CD45$^+$Lin$^-$ fraction of jejunal LP cells from T/S mice and Unm. controls (left), and absolute numbers of jejunal CD45$^+$Lin$^-$c-Kit$^+$IgE$^+$ MCs (right). Results are derived from 2 independent experiments, each with 4 mice/group.

(D) Numbers of CD45$^+$Lin$^-$c-Kit$^+$IgE$^+$ MCs in primary (Prim.) skin sites subjected to tape stripping, distant (Dist.) skin site (left), lungs (middle), and spleen (right) of T/S mice and Unm. controls. Data are representative of 2 independent experiments, each with 3 to 4 mice/group.

(E) Representative flow cytometry analysis of the granularity (side scatter) and size (forward scatter) of CD45$^+$Lin$^-$c-Kit$^+$IgE$^+$ MCs (left) and percentage of SSC$^{high}$c-Kit$^+$IgE$^+$ MCs (right) in the jejunum of T/S mice and Unm. controls. Results are derived from 2 independent experiments, each with 4 mice/group.

(F) Representative flow cytometry analysis of surface expression of c-Kit or CD117 (left) and FcεR1 detected as IgE binding (right) by CD45$^+$Lin$^-$c-Kit$^+$IgE$^+$ MCs from the lamina propria (LP) of T/S mice and Unm. controls. Results are representative of 2 independent experiments, each with 4 mice/group.

(G) qPCR analysis of mRNA expression of select genes by CD45$^+$Lin$^-$c-Kit$^+$IgE$^+$ MCs sorted from the LP of T/S mice and Unm. controls expressed relative to the mean of Unm. controls. The lanes correspond to the groups from 2 different experiments in which MCs were pooled from 4 to 5 mice/group.

Columns and bars in B–E represent SEM. **p < 0.01, ***p < 0.001, ns: not significant. Please see also Figure S1.

ILC2s, MCs, and subsets of T cells (Saenz et al., 2008), rendering epithelial cytokines potential candidates for communicating signals from injured skin to the intestine. mRNA expression of *Il33* and *Tslp*, but not *Il25*, increased in mouse skin 6 h after tape stripping (Figure 3A). Explants of tape-stripped mouse skin released more IL-33 and TSLP than explants from unmanipulated skin, but no detectable amounts of IL-25 (Figure 3B). Importantly, there was a ~3-fold rise in the serum concentration of IL-33, but not TSLP, 1 h after tape stripping the skin (Figure 3C). IL-25 was not detected in the serum. IL-33 release by skin explants and the increase in IL-33 serum concentrations after tape stripping were abolished in *K14-cre*$^{Tg/0}$*Il33*$^{flox/flox}$

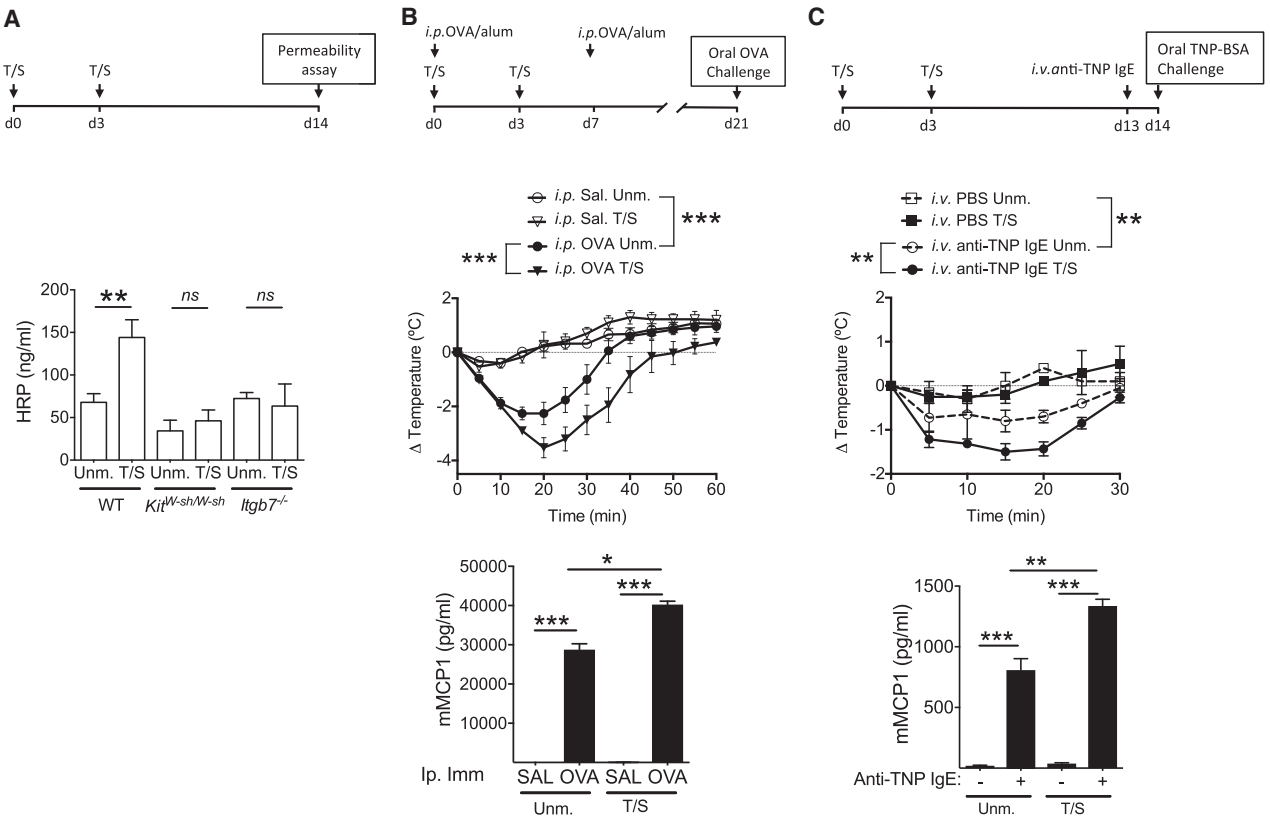



**Figure 2. Tape Stripping of the Skin Increases Intestinal Permeability and Promotes Anaphylaxis to Oral Antigen Challenge**

(A) Effect of tape stripping (T/S) the skin on intestinal permeability. Upper panel: Experimental protocol. Lower panel: serum HRP concentrations in T/S and Unm. wild-type (WT,) *Kit*$^{W\text{-}sh/W\text{-}sh}$, and *Itgb7*$^{-/-}$ mice. Results are derived from 3 independent experiments, each with 4 to 5 mice/group.

(B) Effect of tape stripping the skin on food anaphylaxis in i.p.-immunized T/S and Unm. WT mice. Upper panel: experimental protocol. Middle panel: change in core body temperature following oral OVA challenge. Lower panel: serum mMCPT1 concentrations. Data are representative of 2 independent experiments, each with 4 to 5 mice/group.

(C) Effect of tape stripping the skin on food anaphylaxis in T/S and Unm. mice passively sensitized with IgE anti-TNP. Upper panel: experimental protocol. Middle panel: change in core body temperature after oral challenge with TNP-BSA. Lower panel: serum mMCPT1 concentrations.

Data are representative of 2 independent experiments each with 4 to 5 mice/group. Columns and bars in (A) and symbols and bars in (B) and (C) represent SEM. **p < 0.01, ***p < 0.001, ns: not significant. Please see also Figure S2.

mice, which lack IL-33 specifically in keratinocytes (Figure 3D). These results suggest that mechanical injury to mouse skin results in the systemic release of the epithelial cytokine IL-33 from keratinocytes. In addition to keratinocytes, the *K14* transgene is expressed in mouse thymic epithelial cells (TECs) and oral epithelium (Li et al., 2001). We cannot rule out a potential contribution of these tissues in our model.

Expansion of intestinal MCs was abolished in *Il1rl1*$^{-/-}$ mice that lack the IL-33R and in *Il17rb*$^{-/-}$ mice that lack the high-affinity ligand-binding chain of the IL-25R but was preserved in *Tslpr*$^{-/-}$ mice (Figure 3E), indicating that IL-33 and IL-25, but not TSLP, play essential and non-redundant roles in intestinal MC expansion elicited by mechanical skin injury. Expansion of intestinal MCs was abolished in tape-stripped *K14-cre*$^{Tg/0}$ *Il33*$^{flox/flox}$ mice (Figure 3F). In contrast, it was preserved in *K14-cre*$^{Tg/0}$*Il25*$^{flox/flox}$ mice (Figure 3F). These results demonstrate that keratinocytes are the source of the IL-33, but not the IL-25, essential for intestinal MC expansion elicited by mechanical skin injury.

Tuft cells constitutively express IL-25 and are the only identified source of IL-25 in the intestine (von Moltke et al., 2016). They are characterized by intracellular expression of doublecortin like kinase 1 (DCLK1) and surface expression of epithelial cell adhesion molecule (EpCAM) and the C-type lectin receptor SiglecF (von Moltke et al., 2016). Immunofluorescence analysis of the jejunum revealed that tape stripping caused a ~2-fold increase in the number of DCLK1$^{+}$ tuft cells (Figure 3G). This was confirmed by flow cytometry analysis of CD45$^{-}$EpCAM$^{+}$SiglecF$^{+}$ tuft cells in jejunal IECs (Figure 3H). Tape stripping also caused a ~3-fold increase in *Il25* mRNA expression in jejunal IECs (Figure 3I). Upregulation of *Il25* mRNA expression after tape stripping of the skin was selective to IECs, as it was not observed in lung epithelial cells or skin epidermal layer (Figure S3). Importantly, expansion of jejunal MCs after tape stripping was abolished in *Vil1-cre*$^{Tg/0}$*Il25*$^{flox/flox}$ mice, which lack IL-25 in their IECs (von Moltke et al., 2016) (Figure 3J). These results demonstrate that tape stripping of the skin causes tuft-cell expansion and increased *Il25* expression by IECs and that IEC-derived

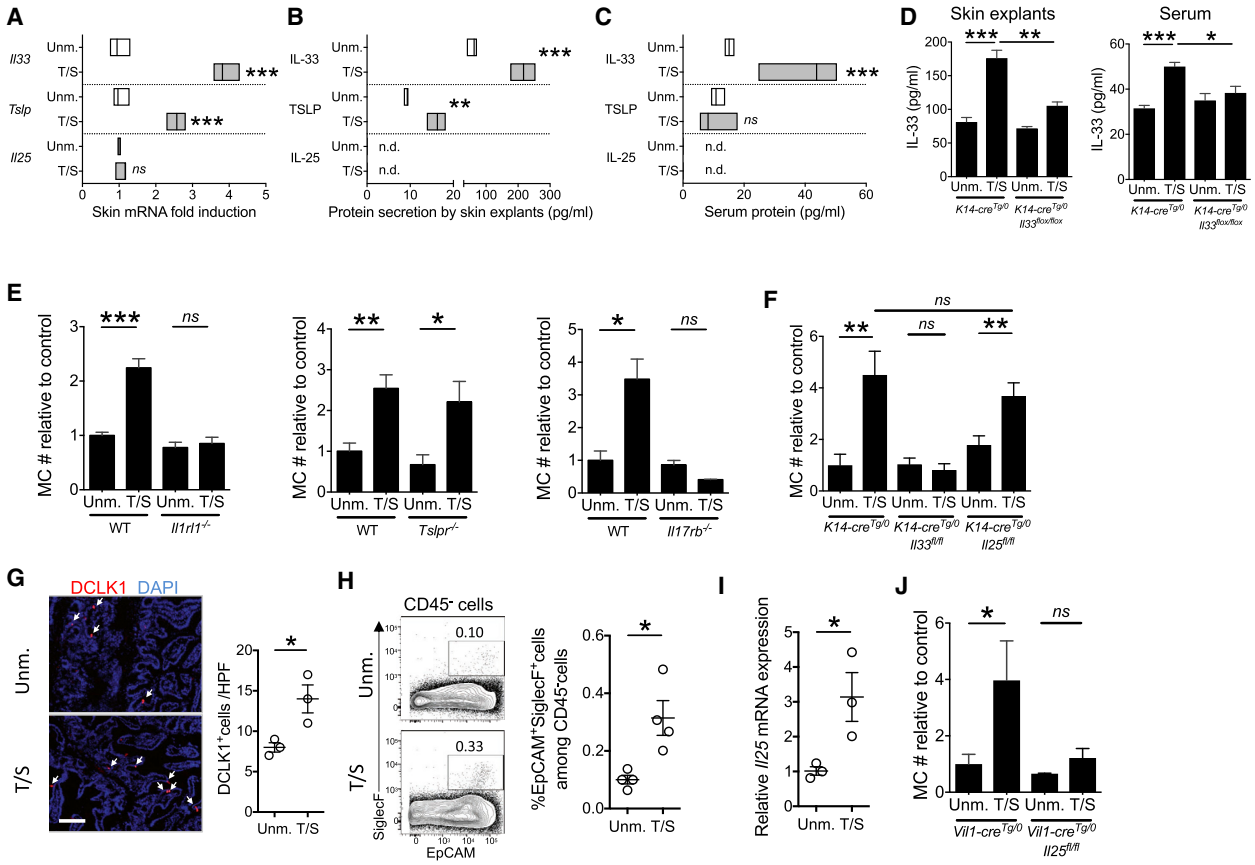



**Figure 3. Keratinocyte-Derived IL-33 and IEC-Derived IL-25 Are Necessary for Intestinal MC Expansion Elicited by Tape Stripping the Skin**

(A) *Il33*, *Tslp*, and *Il25* mRNA expression in skin. Values represent fold induction in tape-stripped skin relative to unmanipulated (Unm.) skin. Data are representative of 2 independent experiments, each with 3 mice/group.

(B) IL-33, TSLP, and IL-25 concentrations in the supernatants of skin explants from T/S and Unm. skin.

(C) Serum concentrations of IL-33, TSLP, and IL-25 in mice 1 h after tape stripping the skin and in Unm. controls. Data representative of 2 independent experiments, each with 3 mice/group.

(D) IL-33 concentrations in the supernatants of skin explants (left) and serum (right) of T/S and Unm*K14-cre*$^{Tg/0}$*Il33*$^{flox/flox}$ mice and *K14-cre*$^{Tg/0}$ controls.

(E) Jejunal MC numbers (#) in T/S and Unm. *Il1rl1*$^{-/-}$, *Tslpr* $^{-/-}$, and *Il17rb*$^{-/-}$ mice and genetically matched WT controls relative to the mean of unmanipulated controls. Results are derived from 2 independent experiments with 3 to 5 mice/group.

(F) Jejunal MC numbers (#) in T/S and Unm. *K14- cre*$^{Tg/0}$*Il33*$^{flox/flox}$, *K14-cre*$^{Tg/0}$*Il25*$^{flox/flox}$, and *K14-cre*$^{Tg/0}$ mice relative to the mean of the unmanipulated *K14-cre*$^{Tg/0}$ controls. Results are derived from 2 independent experiments with 3 to 5 mice/group.

(G) Representative immunofluorescence staining of jejunal sections for DCLK1 in red and DAPI in blue (left) and quantitation of DCLK1$^{+}$ tuft cells per HPF (right) in T/S WT mice and Unm. controls. Results are derived from 2 independent experiments, each with 1 and 2 mice/group, respectively.

(H) Representative flow cytometry analysis (left) and quantitation of the percentage (right) of SiglecF$^{+}$EPCAM$^{+}$ cells gating on CD45$^{-}$ cells from the jejunal epithelial layer. Results are derived from 2 independent experiments, each with 2 mice/group.

(I) *Il25* mRNA expression in intestinal epithelial cells from T/S WT mice and Unm. controls. Values represent fold induction relative to the mean of unmanipulated mice. Results are derived from 2 independent experiments, each with 1 and 2 mice/group, respectively.

(J) Jejunal MC numbers (#) in T/S and Unm. *Vil1-cre*$^{Tg/0}$*Il25*$^{flox/flox}$ mice and *Vil1-cre*$^{Tg/0}$ controls relative to unmanipulated *Vil1-cre*$^{Tg/0}$ controls. Results are derived from 2 independent experiments with 2 to 3 mice/group.

Circles in (G)–(I) represent individual mice. Floating bars in (A)–(C), columns and bars in (D)–(F) and (J), and horizontal lines and bars in (G)–(I) represent mean and SEM. *p < 0.05, **p <0.01, ***p< 0.001, ns: not significant. Please see also Figure S3.

IL-25 is essential for intestinal MC expansion elicited by mechanical skin injury.

## ILC2s Are Essential for Intestinal MC Expansion Elicited by Tape Stripping the Skin

ILC2s and adaptive Th2 cells are targets for IL-33 and IL25 (Saenz et al., 2008). Tape stripping of the skin caused intestinal MC expansion in *Rag2*$^{-/-}$ mice, which are deficient in mature T and B cells but sufficient in ILCs (Figure 4A). In contrast, it caused no expansion of intestinal MCs in *Rag2*$^{-/-}\gamma c^{-/-}$ mice, which, in addition, lack ILCs (Figure 4B). Tape stripping also failed to cause intestinal MC expansion in *Il7ra*$^{-/-}$ mice, which lack ILCs and are deficient in T and B cells (Figure 4B). These results indicate that ILCs, but not mature T or B cells, are important for the expansion of intestinal MCs elicited by mechanical skin injury.

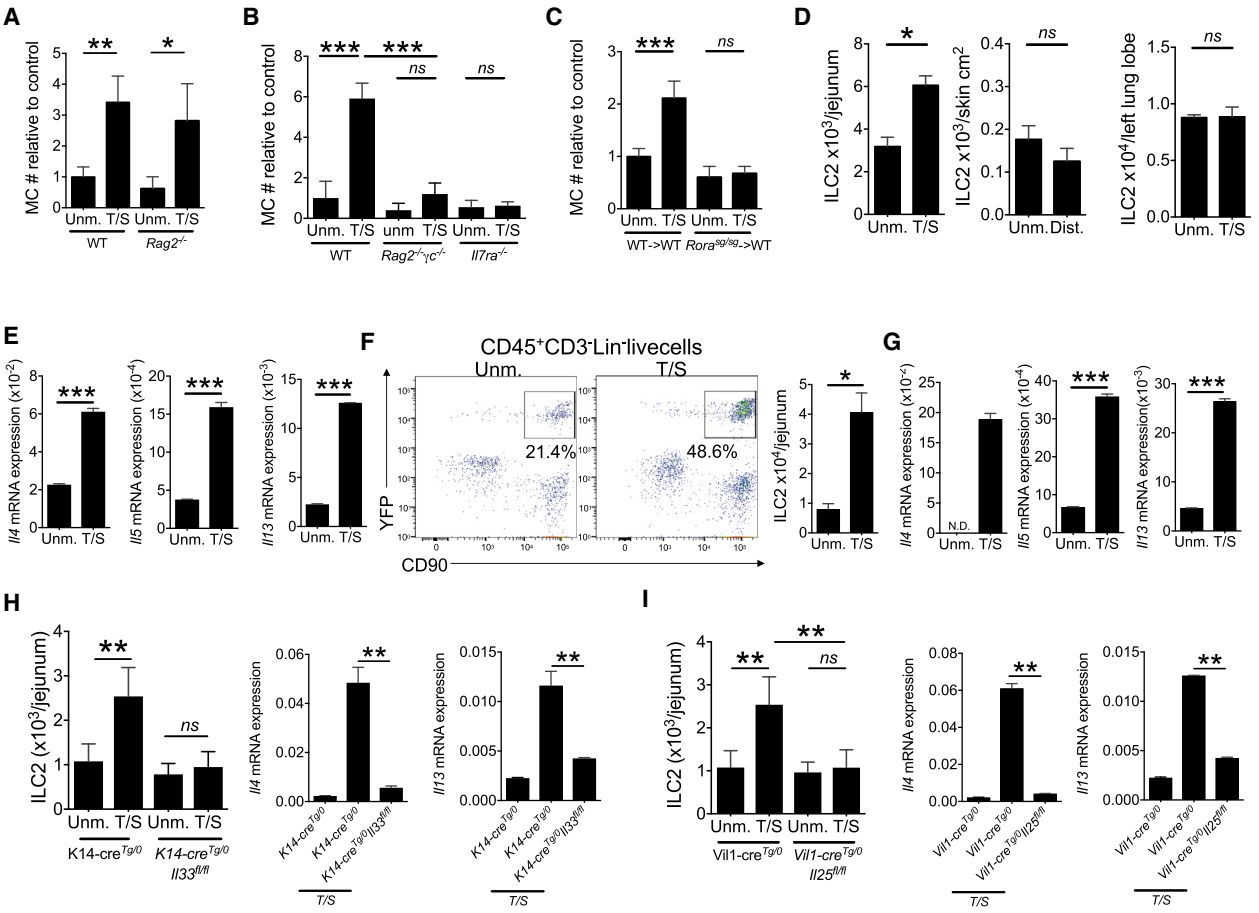



**Figure 4. ILC2s Are Necessary for Intestinal MC Expansion Elicited by Tape Stripping the Skin**

(A and B) Jejunal MC numbers in tape stripped (T/S) and unmanipulated (Unm.) *Rag2*$^{-/-}$, *Rag2*$^{-/-}\gamma c^{-/-}$, and *Il7ra*$^{-/-}$ mice (B) and genetically matched WT controls relative to the mean value of the unmanipulated control group. Results are derived from 2 independent experiments with 2 to 5 mice/group.

(C) Jejunal MC numbers (#) in T/S and Unm. *Rora*$^{sg/sg}\rightarrow$WT and WT$\rightarrow$WT chimeras, relative to the mean value of the unmanipulated WT$\rightarrow$WT chimera group. Results are derived from 2 independent experiments, each with 2 to 3 mice/group.

(D) ILC2 numbers in the jejunum (left), distant skin (middle), and lungs (right) in T/S BALB/c mice and Unm. controls. Data pooled from 2 independent experiments, each with 3 to 4 mice/group.

(E) Cytokine mRNA expression, relative to *B2m* in sorted CD45$^{+}$Lin$^{-}$CD90$^{+}$ ILCs from the jejunum of T/S mice and Unm. controls. Data pooled from 2 independent experiments, each with 3 to 4 mice/group.

(F) Representative flow cytometry analysis (left) and quantitation (right) of CD90$^{+}$YFP$^{+}$ ILC2s gating on CD45$^{+}$Lin$^{-}$ live cells from the jejunum of T/S and Unm. *Rora*$^{cre/cre}$*ROSA*$^{YFP}$ mice.

(G) Cytokine mRNA expression, relative to *B2m*, in Lin$^{-}$CD90$^{+}$YPF$^{+}$ cells (ILC2s) sorted from the jejunum of T/S and Unm. *Rora*$^{cre/cre}$*ROSA*$^{YFP}$ mice. Data pooled from 2 independent experiments, each with 3 to 4 mice/group.

(H and I) ILC2 numbers (left) and *Il4* and *Il13* mRNA expression, relative to *B2m*, in sorted CD45$^{+}$Lin$^{-}$CD90$^{+}$ ILCs (right) from the jejunum of T/S and Unm. *K14-cre*$^{Tg/0}$*Il33*$^{flox/flox}$ mice and *K14-cre*$^{Tg/0}$ controls (H) and T/S and Unm. *Vil1-cre Il25*$^{flox/flox}$ mice and *Vil1-cre* controls (I). Results are derived from 2 independent experiments with 3 to 5 mice/group.

Columns and bars represent mean and SEM. *p < 0.05, **p < 0.01, ***p < 0.001, ns: not significant. Please see also Figures S5 and S6.

ILC2s, but not ILC1s or ILC3s, express IL-25R and IL-33R (Spits et al., 2013). We directly examined the role of ILC2s in intestinal MC expansion after tape stripping of the skin. The transcription factor RAR-related orphan receptor alpha (RORα) is expressed selectively in ILC2s but not ILC1s or ILC3s (Spits et al., 2013). It is also expressed in cerebellar Purkinje cells and a subset of Th2 cells. *Rora*$^{sg/sg}$ mice carry a deletion that introduces a frameshift in the exon that encodes the ligand-binding domain of RORα (Dussault et al., 1998) and have no detectable ILC2s. However, they have neurologic abnormalities and a severely reduced lifespan. We therefore examined *Rora*$^{sg/sg}\rightarrow$ wild-type (WT) bone-marrow radiation chimeras, which are healthy and have a normal lifespan (Wong et al., 2012). GATA-3 is a transcription factor expressed in ILC2s but not ILC1s or ILC3s (Spits et al., 2013), allowing their identification by flow cytometry analysis as CD45$^{+}$Lin$^{-}$CD90$^{+}$CD3$^{-}$GATA-3$^{+}$ cells (Figure S4A). Intestinal ILC2s were virtually undetectable in *Rora*$^{sg/sg}\rightarrow$WT chimeras, but their numbers in control WT$\rightarrow$WT chimeras were comparable to those in WT mice (Figure S4B). Tape stripping caused no expansion of intestinal

MCs in *Rora*$^{sg/sg}$→WT chimeras but caused intestinal MC expansion in WT→WT chimeras comparable in magnitude to that in WT mice (Figure 4C). Because T cells are dispensable for intestinal MC expansion after tape stripping, these results indicate that ILC2s are critical for this expansion.

## Keratinocyte-Derived IL-33 and IEC-Derived IL-25 Drive the Expansion and Activation of Intestinal ILC2s after Mechanical Skin Injury

Tape stripping the skin caused a ~2-fold increase in the numbers of CD45$^+$Lin$^-$CD90$^+$CD3$^-$GATA-3$^+$ ILC2s in the LP of the jejunum of WT mice (Figure 4D). ILC2 expansion after mechanical skin injury was selective to the jejunum, because ILC2 numbers did not increase in distant skin sites, lungs, blood, skin draining lymph nodes, spleens, or visceral adipose tissue of tape-stripped mice (Figures 4D and S4C). We observed a 2-fold increase in ILC2s in tape-stripped skin (Figure S4D). Treatment with the sphingosine-1-phosphate (S1P) analogue FTY720 did not abolish the intestinal MC expansion induced by tape stripping (Figure S4E), suggesting that migration of ILC2s from tape-stripped skin is not required in our model.

There was an increase in Ki67$^+$ intestinal ILC2s at day 10, but not day 7, of our tape-stripping protocol (Figure S4F), suggesting that ILC2s are proliferating locally. IL-33 promotes the egress of ILC2 progenitors from the bone marrow (BM) (Stier et al., 2018). There was a decrease in Lin$^-$Sca1$^+$IL-25R$^+$CD25$^+$CD127$^+$ ILC2 progenitors (ILC2ps) in the BM at day 7, but not day 10, of our tape-stripping protocol (Figure S4G), but there was no increased expression of the gut-homing receptors CCR9 and integrin beta7 by these ILC2ps (data not shown). ILC2p mobilization from the BM may contribute to the ILC2 expansion in our model.

Activated ILC2s express type 2 cytokines (McKenzie et al., 2014; Spits et al., 2013). Tape stripping the skin upregulated expression of *Il4*, *Il5*, and *Il13* mRNA in CD45$^+$Lin$^-$CD90$^+$CD3$^-$ ILCs sorted from the jejunal LP (Figure 4E) but not in ILCs sorted from distant skin (Figure S4H). *Il4*, *Il5*, and *Il13* mRNA was not detectable in CD45$^+$Lin$^-$CD90$^+$CD3$^-$ ILCs sorted from the lungs. *Il9* mRNA was undetectable in jejunal ILCs (data not shown). In addition, tape stripping did not increase lung or visceral-adipose-tissue ILC2 numbers or their expression of IL-5 or IL-13 on day 7, 10, or 14 (Figures S4I and S4J; data not shown). Because CD45$^+$Lin$^-$CD90$^+$CD3$^-$ cells include ILCs other than ILC2s, we examined *Rora*$^{cre/cre}$*ROSA26*$^{YFP}$ mice in which ILC2s are identified as CD45$^+$Lin$^-$CD90$^+$CD3$^-$YFP$^+$ cells. Tape stripping the skin caused an increase in the numbers of CD45$^+$Lin$^-$CD90$^+$YFP$^+$ jejunal ILC2s in *Rora*$^{cre/cre}$*ROSA26*$^{YFP}$ mice (Figure 4F) and upregulated *Il4*, *Il5*, and *Il13* mRNA expression in yellow fluorescent protein$^+$ (YFP$^+$) ILC2s sorted from the jejunum of these mice (Figure 4G). *Il4*, *Il5*, and *Il13* mRNAs were not detectable in CD45$^+$Lin$^-$CD90$^+$CD3$^-$YFP$^-$ cells from the jejunum of tape-stripped *Rora*$^{cre/cre}$*ROSA26*$^{YFP}$ mice (data not shown). Serum IL-4 and IL-13 concentrations were increased 2-fold on day 4 after tape stripping, when jejunal expansion and activation are not yet observed, but returned to normal on day 7, before jejunal ILC2s were expanded and activated (Figure S4K; data not shown).

Jejunal ILC2 expansion and increased expression of *Il4* and *Il13* by ILCs were abolished in tape-stripped *K14-cre*$^{Tg/0}$ *Il33*$^{flox/flox}$ mice and *Vil1-cre*$^{Tg/0}$*Il25*$^{flox/flox}$ mice (Figures 4H and 4I), demonstrating that keratinocyte-derived IL-33 and IEC-derived IL-25 play non-redundant roles in the expansion and activation of jejunal ILC2s elicited by mechanical skin injury.

## IL-33 and IL-25 Act Directly on ILC2s to Cause Their Expansion and Activation after Mechanical Skin Injury

IL-33 and IL-25 act directly on ILC2s to cause proliferation and expression of type 2 cytokines (Spits et al., 2013). We investigated whether IL-33 and IL-25 act directly on ILC2s to cause their expansion in the intestines of tape-stripped mice. Tape stripping the skin caused a ~3-fold expansion of jejunal ILC2s and an increase in the expression of *Il4* and *Il13* mRNAs by jejunal ILCs in *Rora*$^{cre/cre}$ mice but not in *Rora*$^{cre/cre}$*Il17rb*$^{flox/flox}$ mice and *Rora*$^{cre/cre}$*Il1rl1*$^{flox/flox}$ mice, which lack IL-25R and IL-33R, respectively, in *Rora*-expressing cells (Figures 5A and 5B). Furthermore, tape stripping caused expansion of jejunal MCs in *Rora*$^{cre/cre}$ mice but not *Rora*$^{cre/cre}$*Il17rb*$^{flox/flox}$ or *Rora*$^{cre/cre}$*Il1rl1*$^{flox/flox}$ mice (Figure 5C). These results demonstrate that keratinocyte-derived IL-33 and IEC-derived IL-25 act directly and non-redundantly on intestinal ILC2s to cause their expansion and activation and to promote intestinal MC expansion after mechanical skin injury. YFP expression was detected in less than 2% of Beta III tubulin$^+$ intestinal neurons and was undetectable in intestinal MCs of *Rora*$^{cre/cre}$*ROSA26*$^{YFP}$ mice (Figure S5), demonstrating that *Rora*-driven *cre*-mediated ablation of gene expression is not operative in these cells.

Flow cytometry analysis demonstrated that IL-25R is expressed robustly on jejunal ILC2s and weakly on lung ILC2s, whereas IL-33R was expressed robustly on lung ILC2s and less strongly on intestinal ILC2s (Figure 5D). The strong expression of IL-25R on jejunal ILC2s, together with the selective increase in *Il25* mRNA in IECs after tape stripping of the skin, likely contributes to the selective expansion of ILC2s and MCs in the jejunum after mechanical skin injury.

## A Feedforward Loop Drives the Expansion and Activation of Intestinal ILC2s and Tuft Cells after Mechanical Skin Injury

Recent reports demonstrate the existence of a feedforward loop involving intestinal ILC2s and tuft cells in which IL-13 derived from ILC2s promotes the expansion of intestinal tuft cells and their expression of IL-25, which drives ILC2 expansion and activation (von Moltke et al., 2016). We used *Rora*$^{cre/cre}$*Il4/13*$^{flox/flox}$ and *Rag2*$^{-/-}$ mice to investigate whether expansion of intestinal tuft cells after tape stripping of the skin is dependent on ILC2-derived IL-13 and/or IL-4. Tape stripping of the skin caused expansion of EpCAM$^+$SiglecF$^+$ jejunal tuft cells, increased IL-25 mRNA expression by IECs, and expansion of ILC2s in *Rora*$^{cre/cre}$ mice but not *Rora*$^{cre/cre}$*Il4/13*$^{flox/flox}$ mice (Figures 5E–5G). Expansion of jejunal tuft cells, as well as expansion of intestinal ILC2s and their upregulation of *Il4* and *Il13* expression after tape stripping of the skin, was preserved in *Rag2*$^{-/-}$ mice (Figure 5H). Together with the dependence of intestinal ILC2 expansion and activation on IEC-derived IL-25 (Figure 4I), these results suggest that, after mechanical skin injury, IL-13 and/or IL-4 produced by ILC2s in response to keratinocyte-derived IL-33 activate a feedforward loop in which expansion and upregulation of IL-25 by tuft cells drives further the expansion and activation of small intestinal ILC2s. Injection of rIL-33 caused

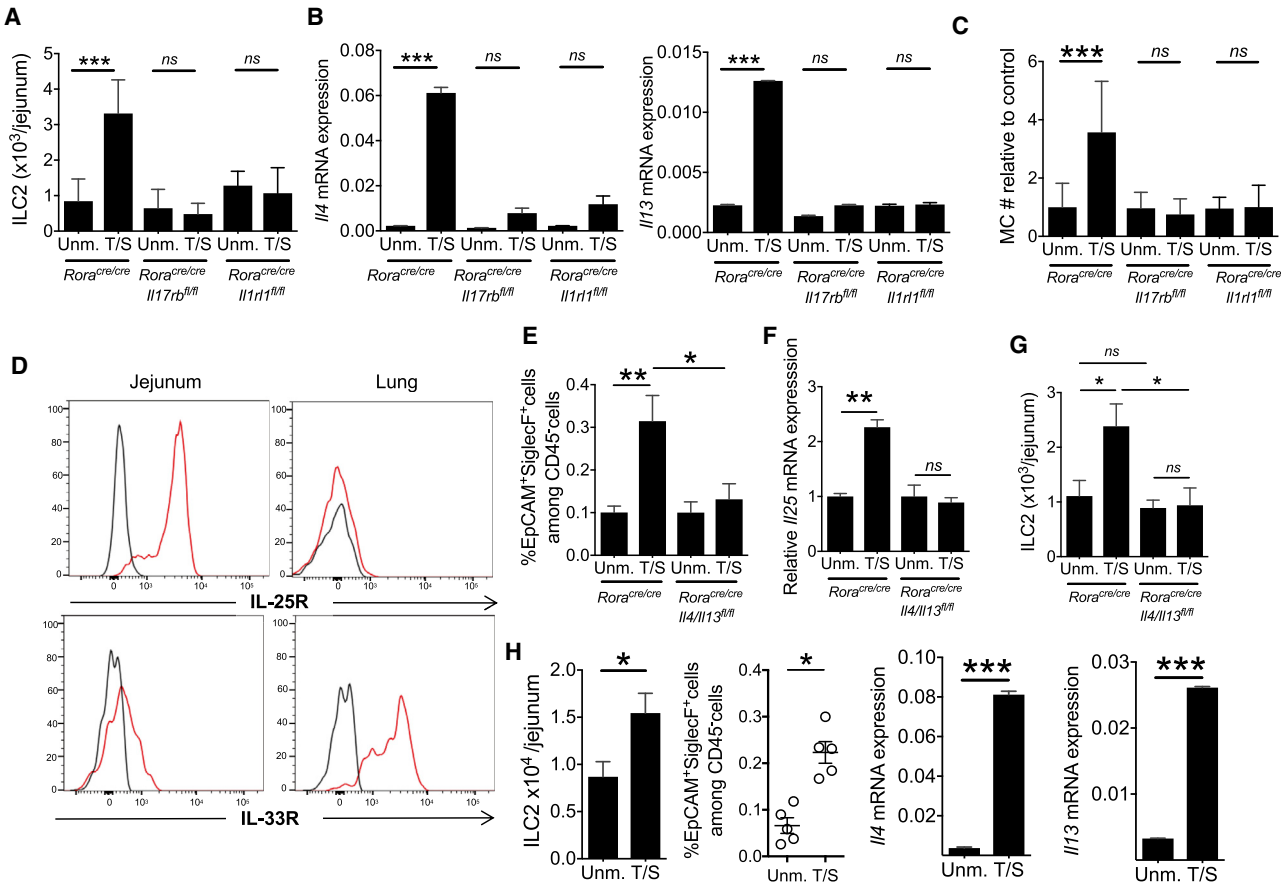



**Figure 5. IL-33 and IL-25 Directly Target ILC2s to Cause Their Expansion and to Activate a Feedforward ILC2 and Tuft-Cell Loop in the Intestine of Tape-Stripped Mice**

(A–C) ILC2 numbers (A), *Il4* and *Il13* mRNA expression relative to *B2m* in sorted CD45$^+$Lin$^-$CD90$^+$ ILCs (B) and MC numbers (C) in the jejunum of T/S and Unm. *Rora*$^{cre/cre}$*Il17rb*$^{flox/flox}$, *Rora*$^{cre/cre}$*Il1rl1*$^{flox/flox}$, and *Rora*$^{cre/cre}$ mice relative to Unm. *Rora*$^{cre/cre}$ controls. Results are derived from 3 independent experiments with 2 to 4 mice/group.

(D) Representative flow cytometry analysis of IL-25R (left) and IL-33R (right) expression by jejunal and lung CD45$^+$Lin$^-$ CD90$^+$YFP$^+$ ILC2s from *Rora*$^{cre/cre}$ *ROSA*$^{YFP}$ mice. Black lines represent isotype control. Similar results were obtained in two other independent experiments.

(E–G) Quantitation of the percentage of SiglecF$^+$EPCAM$^+$ cells gating on CD45$^-$ cells from the epithelial layer (E), *Il25* mRNA expression in IECs (F), and ILC2s numbers (G) in the jejunum of T/S and Unm. *Rora*$^{cre/cre}$*Il4/13*$^{flox/flox}$ mice and *Rora*$^{cre/cre}$ controls. Results are derived from 3 independent experiments with 2 to 4 mice/group.

(H) ILC2 numbers (left), percentage SiglecF$^+$EPCAM$^+$ cells gating on CD45$^-$ cells from the jejunal epithelial layer (center), and *Il4* and *Il13* mRNA expression relative to *B2m* in sorted CD45$^+$Lin$^-$CD90$^+$ ILCs (right) in the jejunum of T/S and Unm. *Rag2*$^{-/-}$ mice. Results are derived from 2 independent experiments with 3 to 4 mice/group.

Columns and bars represent mean and SEM. *p < 0.05, ***p< 0.001, ns: not significant. Please see also Figure S5.

an increase in the number of jejunal tuft cells, ILC2s, and MCs in WT mice that was abolished or markedly less in *Il17rb*$^{-/-}$ mice (Figures S6A–S6C), whereas injection of rIL-25 caused a comparable increase in the number of jejunal MCs in WT mice and *Il1rl1*$^{-/-}$ mice but no increase in *Il17rb*$^{-/-}$ mice (Figure S6D). These findings support the notion that keratinocyte-derived IL-33 initiates the intestinal ILC2-tuft-cell feedforward loop that results in intestinal MC expansion in our model.

## IL-4 and IL-13 Produced by ILC2s Target MCs to Cause MC Expansion after Mechanical Skin Injury

IL-4, IL-5, IL-9, and IL-13 promote the proliferation of bone-marrow-derived MCs *in vitro* (Okayama and Kawakami, 2006), whereas IL-4 and IL-9 can drive the expansion of MCs *in vivo* (Burton et al., 2013). Intestinal MC expansion elicited by tape stripping the skin of WT mice was abolished by administration of neutralizing monoclonal antibody (mAb) to IL-4 and IL-13 but not IL-5 and IL-9 (Figure 6A), indicating that IL-4 and IL-13 play essential and non-redundant roles in small intestinal MC expansion after mechanical skin injury.

To investigate whether ILC2s are the source of IL-4 and IL-13 important for intestinal MC expansion elicited by tape stripping the skin, we used *Rora*$^{cre/cre}$*Il4/13*$^{flox/flox}$ mice. Tape stripping caused no intestinal MC expansion in these mice but caused a ~2-fold expansion of intestinal MCs in *Rora*$^{cre/cre}$ controls (Figure 6B). The lack of intestinal MC expansion in *Rora*$^{cre/cre}$ *Il4/13*$^{flox/flox}$ mice was accompanied by attenuation of anaphylaxis in response to oral OVA challenge after i.p. sensitization

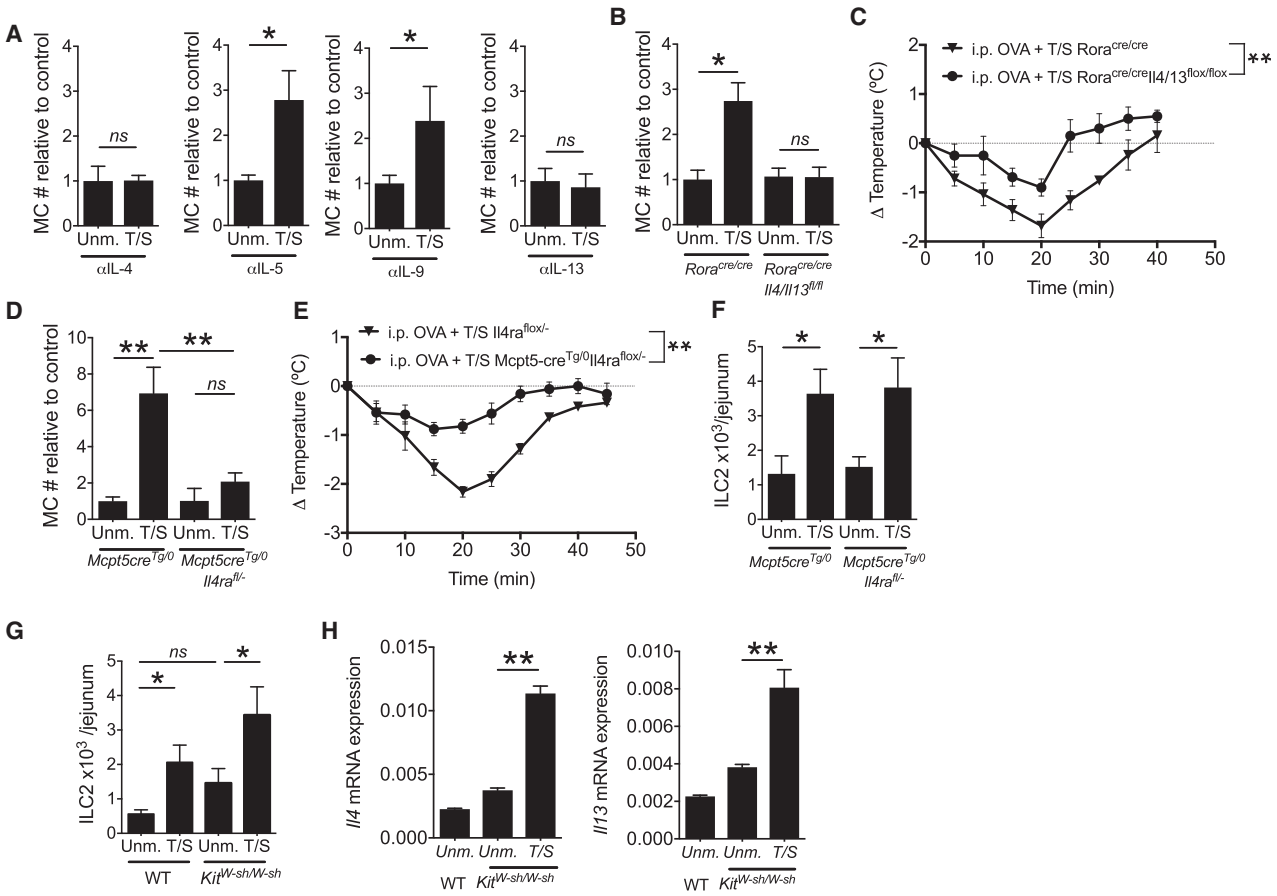



**Figure 6. ILC2-Derived IL-4 and IL-13 Directly Target MCs to Cause Their Expansion in the Intestine of Tape-Stripped Mice**

(A) Jejunal MC numbers (#) in T/S and Unm. WT mice treated with neutralizing anti-IL-4, anti-IL-5, anti-IL-9, or anti-IL-13 mAbs. MC values are relative to the mean value of the unmanipulated control group. Results are derived from 3 independent experiments with 2 to 4 mice/group.

(B) MC numbers relative to Unm. *Rora*$^{cre/cre}$ controls in the jejunum of T/S and Unm. *Rora*$^{cre/cre}$*Il4/13*$^{flox/flox}$ and *Rora*$^{cre/cre}$ mice. Results are derived from 3 independent experiments with 2 to 4 mice/group.

(C) Change in core body temperature after oral OVA challenge in T/S *Rora*$^{cre/cre}$*Il4/13*$^{flox/flox}$ mice and *Rora*$^{cre/cre}$ controls i.p. sensitized with OVA. Results are derived from 2 independent experiments with 3 to 5 mice/group.

(D and E) MC numbers relative to Unm. *Mcpt5-cre*$^{Tg/0}$ (D) and ILC2 numbers (E) in the jejunum of T/S and Unm. *Mcpt5-cre*$^{Tg/0}$*Il4ra*$^{flox/-}$ mice and *Mcpt5-cre*$^{Tg/0}$ mice. Results are derived from 2 independent experiments with 3 to 5 mice/group.

(F) Change in core body temperature following oral OVA challenge in T/S *Mcpt5-cre*$^{Tg/0}$*Il4ra*$^{flox/-}$ mice and *Mcpt5-cre*$^{Tg/0}$ controls i.p. sensitized with OVA. Results are derived from 2 independent experiments with 3 to 5 mice/group.

(G and H) ILC2 numbers (G) and *Il4* and *Il13* mRNA expression in sorted CD45$^+$Lin$^-$CD90$^+$ ILCs (H) in the jejunum of T/S and Unm. *Kit*$^{W\text{-}sh/W\text{-}sh}$ mice and genetically matched controls. Results are derived from 2 independent experiments with 3 to 5 mice/group.

Columns and bars represent mean and SEM. *p < 0.05, **p < 0.01, ns: not significant.

(Figure 6C). Given that intestinal MC expansion after tape stripping is maintained in *Rag2*$^{-/-}$ mice, these results suggest that ILC2-derived IL-4 and/or IL-13 are essential for intestinal MC expansion elicited by mechanical skin injury.

To examine whether IL-4 and/or IL-13 target MCs directly to mediate their expansion in the intestines of tape-stripped mice, we used *Mcpt5-cre*$^{Tg/0}$*Il4ra*$^{flox/-}$ mice, which selectively lack IL-4Rα and, thus, both IL-4R and IL-13R, in MCs. Tape stripping the skin caused no significant intestinal MC expansion in *Mcpt5-cre*$^{Tg/0}$*Il4ra*$^{flox/-}$ mice but caused robust intestinal MC expansion in *Mcpt5-cre*$^{Tg/0}$ controls (Figure 6D). Together with our previous findings, this result strongly suggests that IL-4 and/or IL-13 derived from intestinal ILC2s directly target intestinal MCs to cause their expansion. The lack of intestinal MC expansion in *Mcpt5-cre*$^{Tg/0}$*Il4ra*$^{flox/-}$ mice was accompanied by a decrease in food anaphylaxis in response to oral OVA challenge after i.p. sensitization (Figure 6E).

MCs release molecules that can drive the expansion and activation of ILC2s (Shimokawa et al., 2017). Intestinal ILC2 expansion after tape stripping of the skin was comparable in *Mcpt5-cre*$^{Tg/0}$*Il4ra*$^{flox/-}$ mice and *Mcpt5-cre*$^{Tg/0}$ controls (Figure 6F). Importantly, intestinal ILC2 expansion and increased expression of *Il4* and *Il13* mRNAs after tape stripping of the skin was comparable in MC-deficient *Kit*$^{W\text{-}sh/W\text{-}sh}$ mice and WT controls (Figures 6G and 6H). These results demonstrate that

A

**Characteristics of AD patients and non-AD controls**

| Subject | AD | Age (years) | Sex | Clinical Food Sensitivity | IgE (U/ml) | Food specific IgE |
|---|---|---|---|---|---|---|
| 1 | + | 3 | F | Anaphylaxis to milk | 1517 | + |
| 2 | + | 8 | F | Eosinophilic Esophagitis | 2348 | - |
| 3 | + | 13 | F | None | 41 | n.d. |
| 4 | + | 2 | M | None | 285 | + |
| 5 | - | 15 | F | None | n.d. | n.d. |
| 6 | - | 13 | F | None | n.d. | n.d. |
| 7 | - | 10 | M | Anaphylaxis to wheat | 784 | + |
| 8 | - | 4 | M | Eosinophilic Esophagitis | 715 | + |

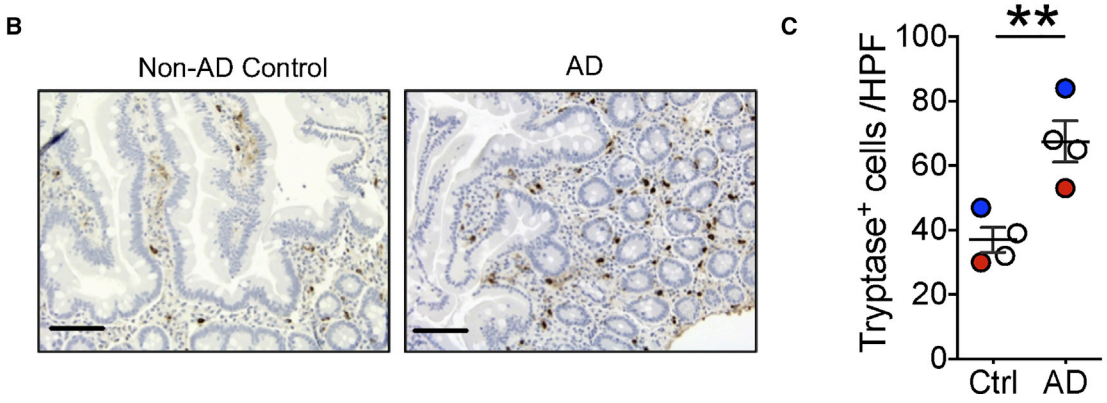



**Figure 7. Duodenal Mast Cells Are Increased in Patients with AD**

(A) Characteristics of AD patients and non-AD controls, n.d.: not done.

(B) Representative immunohistochemistry staining of duodenal sections with anti-tryptase mAb, with scale bars representing 100 μm (left) and numbers of tryptase$^+$ cells per HPF in the duodenum (right) of 4 children with active AD and scratching and 4 children with no AD and no scratching.

Circles represent individual patients. Open circle: no history of food sensitivity, red circle: anaphylaxis to food, blue circle: eosinophilic esophagitis. Horizontal lines and bars in (C) represent mean and SEM. **$p < 0.01$.

intestinal ILC2 expansion and activation after mechanical skin injury is independent of MCs.

## Duodenal Mast Cells Are Increased in Patients with AD

We next investigated whether intestinal MCs are increased in patients with AD. We examined MCs in archived duodenal biopsies from four children with active AD and four non-AD age-matched children. All patients underwent endoscopy with biopsy of the esophagus, stomach, and duodenum because of a history of recurrent upper abdominal pain and/or vomiting. History of food sensitivity, IgE serum concentrations, and IgE antibodies to food allergens in the patients are shown in Figure 7A. Two AD patients and two non-AD patients had no history of sensitivity to foods. One AD patient and one non-AD patient had a history of food anaphylaxis and IgE antibodies to the offending allergens but were on an avoidance diet and had no food allergy symptoms at the time of the study. One AD patient and one non-AD patient have been diagnosed clinically with eosinophilic esophagitis (EoE) and had IgE antibodies to multiple food allergens. MCs were identified in tissue sections by staining for the MC-specific enzyme tryptase. The number of tryptase-positive MCs in the LP of the duodenal mucosa was higher in

AD compared to non-AD controls (Figures 7B and 7C). Duodenal biopsies did not include the submucosa. Except for the increased MC numbers in the AD patients and the confirmation of the clinical diagnosis of EoE in one AD patient and one non-AD patient by the presence of more than 15 eosinophils per HPF in the esophagus LP, no other abnormalities were evident in the patients' biopsies. IgE can promote MC proliferation (Oettgen and Burton, 2015). The increased number of MCs in the duodenums of AD patients could not be simply due to higher serum IgE concentrations, because two of the four AD patients had lower serum IgE than the two non-AD patients on whom serum IgE concentrations were determined, one AD patient had a serum IgE in the normal range, and the mean serum IgE concentrations were not significantly different between the AD and non-AD patients: mean ± SEM, 1048 ± 540 IU/mL for AD patients, n = 4, versus 750 ± 35 IU/mL for non-AD patients, n = 2 ($p = 0.73$, unpaired t test). These results suggest that AD is associated with intestinal MC expansion independent of the presence of food allergy or EoE and that this expansion is not simply the result of elevated serum IgE.

## DISCUSSION

We unraveled the mechanisms of a crosstalk between skin and gut in which mechanical skin injury elicits expansion of intestinal MCs and thereby promotes IgE-mediated food anaphylaxis.

Tape stripping of the skin caused selective expansion of both mucosal and submucosal MCs in the jejunum, independently of the microbiota. This suggests that danger signals released in response to mechanical skin injury activate a skin-gut crosstalk that culminates in the expansion of intestinal MCs. Expansion of intestinal MCs was accompanied by phenotypic changes that included increased MC granularity; maturation, with increased c-Kit and FcεRI expression; and activation, with increased expression of genes that encode for IL-13 and enzymes involved in histamine and leukotriene synthesis.

MCs regulate homeostatic intestinal epithelial barrier function (Groschwitz et al., 2009). Tape stripping the skin increased intestinal permeability. This was dependent on intestinal MCs, as no increase in permeability was observed in tape-stripped *Igtb7*$^{-/-}$ mice that lack these cells. More importantly, tape stripping the skin concurrently with i.p. immunization with OVA potentiated anaphylaxis to oral antigen challenge. This was not due to an effect on the IgE antibody response to OVA or other aspects of the immune response to OVA immunization, because tape stripping also potentiated anaphylaxis to oral antigen challenge in mice that were passively sensitized with IgE antibodies. The finding that intestinal MC expansion after mechanical skin injury was associated with increased severity of anaphylaxis to oral challenge is consistent with previous reports that intestinal MC numbers control the severity of oral anaphylaxis (Ahrens et al., 2012). MC-mediated intestinal permeability predisposes to oral antigen hypersensitivity (Forbes et al., 2008). Thus, increased intestinal permeability associated with MC expansion likely contributed to the increased susceptibility to oral anaphylaxis caused by mechanical skin injury.

Tape stripping the skin caused increased local expression of the epithelial cytokine genes *Il33* and *Tslp*, but not *Il25*, and release of IL-33 and TSLP; however, only IL-33 was released systemically into the blood. Examination of *K14-cre*$^{Tg/0}$ *Il33*$^{flox/flox}$ mice revealed that keratinocytes were the source of the increased IL-33 released by skin explants and increased serum IL-33 in tape-stripped mice. Experiments using receptor-deficient mice demonstrated that both IL-33 and IL-25 are required for intestinal MC expansion after mechanical skin injury. Studies in mice with selective deficiency of IL-33 or IL-25 in keratinocytes demonstrated that keratinocyte-derived IL-33 was important for elicitation of intestinal MC expansion by mechanical skin injury. In contrast, keratinocyte-derived IL-25 played no evident role, consistent with the failure to detect IL-25 in the blood. Intestinal MC expansion after tape stripping was abolished in *Vil1-cre*$^{Tg/0}$*Il25*$^{flox/flox}$ mice, which lack IL-25 in their IECs, demonstrating that tuft cells, the only IECs known to produce IL-25, are the relevant source of IL-25 in our model. The finding that tape stripping caused an increase in the numbers of intestinal tuft cells and upregulated *Il25* mRNA expression by IECs suggests that mechanical skin injury causes proliferation and activation of tuft cells.

ILC2s were essential mediators of skin-to-gut crosstalk in our model. This was evidenced by the observation that lack of ILC2s in *Rora*$^{sg/sg}$ → WT BM chimeras abrogated the ability of tape stripping the skin to elicit intestinal MC expansion. Tape stripping caused expansion of intestinal ILC2s and their activation, as evidenced by marked upregulation of expression of the type 2 cytokines *Il4*, *Il5*, and *Il13*. rIL-33 and rIL-25 synergize to cause ILC2 expansion *in vivo* and ILC2 proliferation and cytokine secretion *in vitro* (Salimi et al., 2013). Expansion and activation of intestinal ILC2 after tape stripping was abrogated in *Rora*$^{cre/cre}$*Il17rb*$^{flox/flox}$ mice and *Rora*$^{cre/cre}$*Il1rl1*$^{flox/flox}$ mice that lack IL-33R or IL-25R, respectively, in ILC2s. This demonstrates that IL-33 and IL-25 play non-redundant roles in our model, suggesting that *in vivo* synergy between these two cytokines is necessary to optimally drive intestinal ILC2 expansion and activation in our model. Importantly, intestinal MC expansion after tape stripping was also abrogated in *Rora*$^{cre/cre}$*Il17rb*$^{flox/flox}$ mice and *Rora*$^{cre/cre}$*Il1rl1*$^{flox/flox}$ mice, indicating that expansion and activation of intestinal ILC2s is required for intestinal MC expansion. The selective upregulation of *Il25* expression in IECs and the high expression of IL-25R by intestinal ILC2s, but not in lung or skin ILC2s (Ricardo-Gonzalez et al., 2018), may underlie the selective expansion and activation of ILC2s in the small intestine after tape stripping. IL-33 acts on MCs to promote food anaphylaxis (Galand et al., 2016). IL-33 action on MCs cannot account by itself for the MC expansion and activation in tape-stripped mice, as these are strictly dependent on IL-4. However, IL-33 could act in synergy with IL-4 on MCs in our model.

We provide evidence that, after mechanical skin injury, intestinal ILC2s and tuft cells participate in a feedforward loop that amplifies their expansion and activation. We propose that, after tape stripping the skin, increased serum IL-33 activates intestinal ILC2s to produce IL-13 and IL-4, which drive the expansion of tuft cells and upregulate their production of IL-25, which amplifies ILC2 production of IL-13 and IL-4 in a feedforward loop. ILC2-derived IL-4 then drives intestinal MC expansion and activation. Such a feedforward loop has been demonstrated in intestinal helminth infection (Howitt et al., 2016; von Moltke

et al., 2016) and may have evolved to protect the intestine from helminths that infect it directly or via the skin as a portal of entry, as in the case of hookworms, and to provide concomitant immunity. In line with this hypothesis, oral administration of sodium succinate, a metabolite from protists and helminths, promotes expansion of intestinal-tuft-cell ILC2s and intestinal mast cells (Schneider et al., 2018; data not shown). ILC2-derived IL-4 and/or IL-13 drove intestinal MC expansion in our model by directly targeting MCs, as intestinal MC expansion after tape stripping was abolished in *Rora*$^{cre/cre}$*Il4/13*$^{flox/flox}$ mice and *Mcpt5-cre*$^{Tg/0}$*Il4ra*$^{flox/-}$ mice.

MCs play a protective role against microbes and helminths (Mukai et al., 2017). The crosstalk that we describe between mechanically injured skin and intestine may have evolved as a system to alert the gut to react to agents breaching the skin barrier. Importantly, intestinal MC expansion elicited by mechanical skin injury is likely relevant to food anaphylaxis in patients with AD. We tape stripped ~10% of the mouse body surface area in our model. A similar or greater percentage of body area is commonly affected and subject to scratching in patients with AD (Sugarman et al., 2003). Skin and serum IL-33 concentrations are increased in our model and in patients with AD (Galand et al., 2016; Savinko et al., 2012), and *Il33* mRNA expression increases in the skin of healthy individuals after scratching (Galand et al., 2016). We observed intestinal MC expansion in patients with AD, independent of food allergy history, serum IgE, or the presence of EOE. Moreover, increased intestinal permeability has been documented in patients with AD (Caffarelli et al., 2001; Kalimo et al., 1988). Taken together, our findings suggest that increased intestinal MCs and permeability elicited by mechanical skin injury inflicted by scratching may play an important role in promoting food anaphylaxis in patients with AD. Interventions that inhibit scratching may be useful in dampening the severity of food allergy in these patients by decreasing their intestinal MC load.

## STAR★METHODS

Detailed methods are provided in the online version of this paper and include the following:

- KEY RESOURCES TABLE
- CONTACT FOR REAGENT AND RESOURCE SHARING
- EXPERIMENTAL MODEL AND SUBJECT DETAILS
  - Mice
  - Human Subjects
- METHOD DETAILS
  - Mechanical Skin Injury, EC Sensitization, and Oral Antigen Challenge
  - Passive Sensitization
  - Intraperitoneal Sensitization
  - Histology
  - Cell Suspension Preparation and Flow Cytometry Analysis
  - Intestinal Permeability
  - *Il33, Il25,* and *Tslp* mRNA Expression and Its Release Upon Tape Stripping
- QUANTIFICATION AND STATISTICAL ANALYSIS

## SUPPLEMENTAL INFORMATION

Supplemental Information can be found online at https://doi.org/10.1016/j.immuni.2019.03.023.

## ACKNOWLEDGMENTS

We thank Dr. T. Chatila for his gift of *Mcpt5-cre*$^{Tg/0}$ mice; Dr. Andrew N.J. McKenzie for his gift of *Il1rl1*$^{-/-}$ and *Il17rb*$^{-/-}$ mice; Dr. Dennis O'Leary for his gift of *Rora*$^{cre/cre}$ mice; Dr. Nicolas Severe for help in immunofluorescence imaging; and Drs. T. Chatila, H. Oettgen, and J. Chou for reading the manuscript and for useful discussions. This work was supported by NIH grants AI113294-01A1 and U19 AI117673. J.-M.L.-C. is supported by NIAID T32 training grant (5T32AI007512).

## AUTHOR CONTRIBUTIONS

J.-M.L.-C., C.G., and R.S.G designed experiments. J.-M.L.-C., C.G., C.K., O.B., M.G., J.G., E.H., and S.N. performed experiments and analyzed data. F.B., C.D., F.D.F., R.T.L., S.Z. and K.F.A. contributed with critical reagents, mice, or analytic tools. J.-M.L.-C., C.G. and R.S.G interpreted data and wrote the manuscript.

## DECLARATION OF INTERESTS

The authors declare no competing interests.

Received: August 17, 2018
Revised: January 17, 2019
Accepted: March 25, 2019
Published: April 23, 2019

## REFERENCES

Ahrens, R., Osterfeld, H., Wu, D., Chen, C.Y., Arumugam, M., Groschwitz, K., Strait, R., Wang, Y.H., Finkelman, F.D., and Hogan, S.P. (2012). Intestinal mast cell levels control severity of oral antigen-induced anaphylaxis in mice. Am. J. Pathol. *180*, 1535–1546.

Al-Shami, A., Spolski, R., Kelly, J., Keane-Myers, A., and Leonard, W.J. (2005). A role for TSLP in the development of inflammation in an asthma model. J. Exp. Med. *202*, 829–839.

Angkasekwinai, P., Chang, S.H., Thapa, M., Watarai, H., and Dong, C. (2010). Regulation of IL-9 expression by IL-25 signaling. Nat. Immunol. *11*, 250–256.

Bartnikas, L.M., Gurish, M.F., Burton, O.T., Leisten, S., Janssen, E., Oettgen, H.C., Beaupre, J., Lewis, C.N., Austen, K.F., Schulte, S., et al. (2013). Epicutaneous sensitization results in IgE-dependent intestinal mast cell expansion and food-induced anaphylaxis. J Allergy Clin Immunol *131*, 451–460.e1–6.

Burton, O.T., Darling, A.R., Zhou, J.S., Noval-Rivas, M., Jones, T.G., Gurish, M.F., Chatila, T.A., and Oettgen, H.C. (2013). Direct effects of IL-4 on mast cells drive their intestinal expansion and increase susceptibility to anaphylaxis in a murine model of food allergy. Mucosal Immunology *6*, 740–750.

Caffarelli, C., Cavagni, G., Romanini, E., Caruana, P., and de Angelis, G. (2001). Duodenal IgE-positive cells and elimination diet responsiveness in children with atopic dermatitis. Ann. Allergy Asthma Immunol. *86*, 665–670.

Chou, S.J., Babot, Z., Leingärtner, A., Studer, M., Nakagawa, Y., and O'Leary, D.D. (2013). Geniculocortical input drives genetic distinctions between primary and higher-order visual areas. Science *340*, 1239–1242.

Dussault, I., Fawcett, D., Matthyssen, A., Bader, J.A., and Giguère, V. (1998). Orphan nuclear receptor ROR alpha-deficient mice display the cerebellar defects of staggerer. Mech. Dev. *70*, 147–153.

Fleischer, D.M., Bock, S.A., Spears, G.C., Wilson, C.G., Miyazawa, N.K., Gleason, M.C., Gyorkos, E.A., Murphy, J.R., Atkins, D., and Leung, D.Y. (2011). Oral food challenges in children with a diagnosis of food allergy. J Pediatr *158*, 578–583.e1.

Forbes, E.E., Groschwitz, K., Abonia, J.P., Brandt, E.B., Cohen, E., Blanchard, C., Ahrens, R., Seidu, L., McKenzie, A., Strait, R., et al. (2008). IL-9- and mast

cell-mediated intestinal permeability predisposes to oral antigen hypersensitivity. J. Exp. Med. *205*, 897–913.

Galand, C., Leyva-Castillo, J.M., Yoon, J., Han, A., Lee, M.S., McKenzie, A.N.J., Stassen, M., Oyoshi, M.K., Finkelman, F.D., and Geha, R.S. (2016). IL-33 promotes food anaphylaxis in epicutaneously sensitized mice by targeting mast cells. J. Allergy Clin. Immunol. *138*, 1356–1366.

Galli, S.J., and Tsai, M. (2012). IgE and mast cells in allergic disease. Nat. Med. *18*, 693–704.

Gerbe, F., Sidot, E., Smyth, D.J., Ohmoto, M., Matsumoto, I., Dardalhon, V., Cesses, P., Garnier, L., Pouzolles, M., Brulin, B., et al. (2016). Intestinal epithelial tuft cells initiate type 2 mucosal immunity to helminth parasites. Nature *529*, 226–230.

Groschwitz, K.R., Ahrens, R., Osterfeld, H., Gurish, M.F., Han, X., Abrink, M., Finkelman, F.D., Pejler, G., and Hogan, S.P. (2009). Mast cells regulate homeostatic intestinal epithelial migration and barrier function by a chymase/Mcpt4-dependent mechanism. Proc. Natl. Acad. Sci. USA *106*, 22381–22386.

Gurish, M.F., Tao, H., Abonia, J.P., Arya, A., Friend, D.S., Parker, C.M., and Austen, K.F. (2001). Intestinal mast cell progenitors require CD49dbeta7 (alpha4beta7 integrin) for tissue-specific homing. J. Exp. Med. *194*, 1243–1252.

Herbert, D.R., Hölscher, C., Mohrs, M., Arendse, B., Schwegmann, A., Radwanska, M., Leeto, M., Kirsch, R., Hall, P., Mossmann, H., et al. (2004). Alternative macrophage activation is essential for survival during schistosomiasis and downmodulates T helper 1 responses and immunopathology. Immunity *20*, 623–635.

Howitt, M.R., Lavoie, S., Michaud, M., Blum, A.M., Tran, S.V., Weinstock, J.V., Gallini, C.A., Redding, K., Margolskee, R.F., Osborne, L.C., et al. (2016). Tuft cells, taste-chemosensory cells, orchestrate parasite type 2 immunity in the gut. Science *351*, 1329–1333.

Kalimo, K., Lammintausta, K., Klemi, P., Leino, R., Panula, P., and Kalimo, H. (1988). Mast cells and IgE in intestinal mucosa in adult atopic dermatitis patients. Br. J. Dermatol. *119*, 579–585.

Lack, G., Fox, D., Northstone, K., and Golding, J.; Avon Longitudinal Study of Parents and Children Study Team (2003). Factors associated with the development of peanut allergy in childhood. N. Engl. J. Med. *348*, 977–985.

Lee, H., Park, J.H., Park, D.I., Kim, H.J., Cho, Y.K., Sohn, C.I., Jeon, W.K., Kim, B.I., and Chae, S.W. (2013). Mucosal mast cell count is associated with intestinal permeability in patients with diarrhea predominant irritable bowel syndrome. J. Neurogastroenterol. Motil. *19*, 244–250.

Leisten, S., Oyoshi, M.K., Galand, C., Hornick, J.L., Gurish, M.F., and Geha, R.S. (2013). Development of skin lesions in filaggrin-deficient mice is dependent on adaptive immunity. J Allergy Clin Immunol *131*, 1247–1250.

Leyva-Castillo, J.M., Hener, P., Jiang, H., and Li, M. (2013). TSLP produced by keratinocytes promotes allergen sensitization through skin and thereby triggers atopic march in mice. J. Invest. Dermatol. *133*, 154–163.

Li, M., Chiba, H., Warot, X., Messaddeq, N., Gérard, C., Chambon, P., and Metzger, D. (2001). RXR-alpha ablation in skin keratinocytes results in alopecia and epidermal alterations. Development *128*, 675–688.

Mathias, C.B., Hobson, S.A., Garcia-Lloret, M., Lawson, G., Poddighe, D., Freyschmidt, E.J., Xing, W., Gurish, M.F., Chatila, T.A., and Oettgen, H.C. (2011). IgE-mediated systemic anaphylaxis and impaired tolerance to food antigens in mice with enhanced IL-4 receptor signaling. J Allergy Clin Immunol *127*, 795–805.e1–6.

McKenzie, A.N.J., Spits, H., and Eberl, G. (2014). Innate lymphoid cells in inflammation and immunity. Immunity *41*, 366–374.

Mukai, K., Karasuyama, H., Kabashima, K., Kubo, M., and Galli, S.J. (2017). Differences in the Importance of Mast Cells, Basophils, IgE, and IgG versus That of $CD4^+$ T Cells and ILC2 Cells in Primary and Secondary Immunity to Strongyloides venezuelensis. Infect. Immun. *85*, e00053-17.

Oettgen, H.C., and Burton, O.T. (2015). IgE and Mast Cells: The Endogenous Adjuvant. Adv. Immunol. *127*, 203–256.

Okayama, Y., and Kawakami, T. (2006). Development, migration, and survival of mast cells. Immunol. Res. *34*, 97–115.

Oyoshi, M.K., Larson, R.P., Ziegler, S.F., and Geha, R.S. (2010). Mechanical injury polarizes skin dendritic cells to elicit a T(H)2 response by inducing cutaneous thymic stromal lymphopoietin expression. J Allergy Clin Immunol *126*, 976–984.

Pike, M.G., Heddle, R.J., Boulton, P., Turner, M.W., and Atherton, D.J. (1986). Increased intestinal permeability in atopic eczema. J. Invest. Dermatol. *86*, 101–104.

Ricardo-Gonzalez, R.R., Van Dyken, S.J., Schneider, C., Lee, J., Nussbaum, J.C., Liang, H.E., Vaka, D., Eckalbar, W.L., Molofsky, A.B., Erle, D.J., and Locksley, R.M. (2018). Tissue signals imprint ILC2 identity with anticipatory function. Nat. Immunol. *19*, 1093–1099.

Rickel, E.A., Siegel, L.A., Yoon, B.-R.P., Rottman, J.B., Kugler, D.G., Swart, D.A., Anders, P.M., Tocker, J.E., Comeau, M.R., and Budelsky, A.L. (2008). Identification of functional roles for both IL-17RB and IL-17RA in mediating IL-25-induced activities. J Immunol *181*, 4299–4310.

Saenz, S.A., Taylor, B.C., and Artis, D. (2008). Welcome to the neighborhood: epithelial cell-derived cytokines license innate and adaptive immune responses at mucosal sites. Immunol. Rev. *226*, 172–190.

Salimi, M., Barlow, J.L., Saunders, S.P., Xue, L., Gutowska-Owsiak, D., Wang, X., Huang, L.C., Johnson, D., Scanlon, S.T., McKenzie, A.N., et al. (2013). A role for IL-25 and IL-33-driven type-2 innate lymphoid cells in atopic dermatitis. J. Exp. Med. *210*, 2939–2950.

Salo, P.M., Arbes, S.J., Jr., Jaramillo, R., Calatroni, A., Weir, C.H., Sever, M.L., Hoppin, J.A., Rose, K.M., Liu, A.H., Gergen, P.J., et al. (2014). Prevalence of allergic sensitization in the United States: results from the National Health and Nutrition Examination Survey (NHANES) 2005-2006. J. Allergy Clin. Immunol. *134*, 350–359.

Savinko, T., Matikainen, S., Saarialho-Kere, U., Lehto, M., Wang, G., Lehtimäki, S., Karisola, P., Reunala, T., Wolff, H., Lauerma, A., and Alenius, H. (2012). IL-33 and ST2 in atopic dermatitis: expression profiles and modulation by triggering factors. J. Invest. Dermatol. *132*, 1392–1400.

Schneider, C., O'Leary, C.E., von Moltke, J., Liang, H.E., Ang, Q.Y., Turnbaugh, P.J., Radhakrishnan, S., Pellizzon, M., Ma, A., and Locksley, R.M. (2018). A Metabolite-Triggered Tuft Cell-ILC2 Circuit Drives Small Intestinal Remodeling. Cell *174*, 271–284.

Scholten, J., Hartmann, K., Gerbaulet, A., Krieg, T., Müller, W., Testa, G., and Roers, A. (2008). Mast cell-specific Cre/loxP-mediated recombination in vivo. Transgenic Res. *17*, 307–315.

Shimokawa, C., Kanaya, T., Hachisuka, M., Ishiwata, K., Hisaeda, H., Kurashima, Y., Kiyono, H., Yoshimoto, T., Kaisho, T., and Ohno, H. (2017). Mast Cells Are Crucial for Induction of Group 2 Innate Lymphoid Cells and Clearance of Helminth Infections. Immunity *46*, 863–874.e4.

Sicherer, S.H., and Sampson, H.A. (2009). Food allergy: recent advances in pathophysiology and treatment. Annu. Rev. Med. *60*, 261–277.

Spergel, J.M. (2010). From atopic dermatitis to asthma: the atopic march. Ann Allergy Asthma Immunol *105*, 99–106.

Spits, H., Artis, D., Colonna, M., Diefenbach, A., Di Santo, J.P., Eberl, G., Koyasu, S., Locksley, R.M., McKenzie, A.N., Mebius, R.E., et al. (2013). Innate lymphoid cells–a proposal for uniform nomenclature. Nat. Rev. Immunol. *13*, 145–149.

Stier, M.T., Zhang, J., Goleniewska, K., Cephus, J.Y., Rusznak, M., Wu, L., Van Kaer, L., Zhou, B., Newcomb, D.C., and Peebles, R.S., Jr. (2018). IL-33 promotes the egress of group 2 innate lymphoid cells from the bone marrow. J. Exp. Med. *215*, 263–281.

Strait, R.T., Mahler, A., Hogan, S., Khodoun, M., Shibuya, A., and Finkelman, F.D. (2011). Ingested allergens must be absorbed systemically to induce systemic anaphylaxis. J Allergy Clin Immunol *127*, 982–989.e1.

Sugarman, J.L., Fluhr, J.W., Fowler, A.J., Bruckner, T., Diepgen, T.L., and Williams, M.L. (2003). The objective severity assessment of atopic dermatitis score: an objective measure using permeability barrier function and stratum corneum hydration with computer-assisted estimates for extent of disease. Arch. Dermatol. *139*, 1417–1422.

Townsend, M.J., Fallon, P.G., Matthews, D.J., Jolin, H.E., and McKenzie, A.N. (2000). T1/ST2-deficient mice demonstrate the importance of T1/ST2 in developing primary T helper cell type 2 responses. J Exp Med *191*, 1069–1076.

Vaali, K., Lappalainen, J., Lin, A.H., Mäyränpää, M.I., Kovanen, P.T., Berstad, A., and Eklund, K.K. (2012). Imatinib mesylate alleviates diarrhea in a mouse model of intestinal allergy. Neurogastroenterol. Motil. *24*, e325–e335.

von Moltke, J., Ji, M., Liang, H.E., and Locksley, R.M. (2016). Tuft-cell-derived IL-25 regulates an intestinal ILC2-epithelial response circuit. Nature *529*, 221–225.

Wong, S.H., Walker, J.A., Jolin, H.E., Drynan, L.F., Hams, E., Camelo, A., Barlow, J.L., Neill, D.R., Panova, V., Koch, U., et al. (2012). Transcription factor RORα is critical for nuocyte development. Nat. Immunol. *13*, 229–236.

# STAR★METHODS

## KEY RESOURCES TABLE

| REAGENT or RESOURCE | SOURCE | IDENTIFIER |
|---|---|---|
| Antibodies | | |
| eBioscience Fixable Viability Dye eFluor 506 | Thermo Fisher | Cat# 65-0866-18 |
| Alexa Fluor 700 anti-mouse CD45 Antibody | Biolegend | Cat# 103128; RRID: AB_493715 |
| Biotin anti-mouse/human CD45R/B220 Antibody | Biolegend | Cat# 103204; RRID: AB_312989 |
| Biotin anti-mouse/human CD11b Antibody | Biolegend | Cat# 101204; RRID: AB_312787 |
| CD11c Monoclonal Antibody (N418), Biotin, | Thermo Fisher | Cat# 13-0114-85; RRID: AB_493715 |
| CD19 Monoclonal Antibody (eBio1D3 [1D3]) | Thermo Fisher | Cat# 13-0193-85; RRID: AB_657658 |
| F4/80 Monoclonal Antibody (BM8), Biotin | Thermo Fisher | Cat# 13-4801-85; RRID: AB_466658 |
| Ly-6G/Ly-6C Monoclonal Antibody (RB6-8C5), Biotin | Thermo Fisher | Cat# 13-5931-85; RRID: AB_466801 |
| CD335 (NKp46) Monoclonal Antibody (29A1.4), Biotin, | Thermo Fisher | Cat# 13-3351-82; RRID: AB_2572784 |
| CD3 Monoclonal Antibody (17A2), PerCP-eFluor 710 | Thermo Fisher | Cat# 46-0032-82; RRID: AB_1834427 |
| CD117 (c-Kit) Monoclonal Antibody (ACK2) | Thermo Fisher | Cat# 17-1172-83; RRID: AB_469434 |
| BV421 Rat Anti-Mouse IgE | BD Biosciences | Cat# 564207; RRID: AB_2738668 |
| CD31 (PECAM-1) Monoclonal Antibody (390), PE-Cyanine7 | Thermo Fisher | Cat# 25-0311-82; RRID: AB_2716949 |
| PE Rat Anti-Mouse Siglec-F | BD Biosciences | Cat# 552126; RRID: AB_394341 |
| Rabbit anti-DCAMKL1 | Abcam | Cat# ab31704; RRID: AB_873537 |
| Biological Samples | | |
| anti-trinitrophenyl (TNP) IgE monoclonal antibody | Finkelman FD | PMID: 22465213 |
| Chemicals, Peptides, and Recombinant Proteins | | |
| Peroxidase from horseradish | Sigma | P8375 |
| Albumin from chicken egg white | Sigma | A5503 |
| Imject Alum Adjuvant | Thermo Fisher | 77161 |
| Sodium succinate hexahydrate | Alfa Aesar | Cat# 41983 |
| Critical Commercial Assays | | |
| RNeasy Micro Kit | QIAGEN | Cat# 74004 |
| MCPT-1 (mMCP-1) Mouse Uncoated ELISA Kit | Thermo fisher | Cat# 7400488-7503-86 |
| Mouse/Rat IL-33 Quantikine ELISA Kit | R&D | Cat# 74004M3300 |
| Mouse TSLP Quantikine ELISA Kit | R&D | Cat# 74004MTLP00 |
| RNAqueous Total RNA Isolation Kit | Thermo Fisher | Cat# 74004AM1912 |
| Experimental Models: Organisms/Strains | | |
| Mouse, BALB/cAnNCrl | Charles River | Strain code: 028 |
| Mouse, C57BL/6NCrl | Charles River | Strain code: 027 |
| Mouse, BALB/cAnNTac | Taconic | Model# BALB-F |
| Mouse, Balb/c *Kit*$^{W\text{-}sh/W\text{-}sh}$ | Michael Stassen, Johannes Gutenberg University | N/A |
| Mouse, Balb/c *Itgb7*$^{-/-}$ | In this paper | N/A |
| *K14-Cre*$^{Tg/0}$*Il33*$^{flox/flox}$ | In this paper | N/A |
| Mouse, Balb/c *Il1rl1*$^{-/-}$ | Andrew N.J. McKenzie | N/A |
| Mouse, Balb/c *Il17rb*$^{-/-}$ | Amgen | N/A |
| Mouse, Balb/c *Tslpr*$^{-/-}$ | Steve F. Ziegler | N/A |
| *K14-Cre*$^{Tg/0}$*Il25*$^{flox/flox}$ | In this paper | N/A |
| *Vil1-Cre*$^{Tg/0}$*Il25*$^{flox/flox}$ | In this paper | N/A |
| Mouse, Balb/c *Rag2*$^{-/-}$ | Taconic | 601 |
| *Rag2*$^{-/-}\gamma c^{-/-}$ | Taconic | 4111 |

(*Continued on next page*)

**Continued**

| REAGENT or RESOURCE | SOURCE | IDENTIFIER |
|---|---|---|
| *Il7ra*$^{-/-}$ | JAX | Stock Number 002295 |
| *Rora*$^{sg/sg}$ | JAX | 000237 |
| *Rora*$^{Cre/Cre}$*ROSA26*$^{YFP}$ | Raif Geha, Boston Children's Hospital | N/A |
| *Rora*$^{Cre/Cre}$*Il17rb*$^{flox/flox}$ | In this paper | N/A |
| *Rora*$^{Cre/Cre}$*Il1rl1*$^{flox/flox}$ | In this paper | N/A |
| *Rora*$^{Cre/Cre}$ | Dennis O'Leary | N/A |
| *Rora*$^{Cre/Cre}$*Il4/13*$^{flox/flox}$ | In this paper | N/A |
| Mouse, Balb/c *Mcpt5-Cre*$^{Tg/0}$*Il4ra*$^{flox/-}$ | In this paper | N/A |
| Mouse, Balb/c *Mcpt5-Cre*$^{Tg/0}$ | Talal Chatila, Boston Children's Hospital | N/A |
| Oligonucleotides | | |
| Hdc TaqMan Assays | Thermo Fisher | Assay ID Mm00456104_m1 |
| Alox5 TaqMan Assays | Thermo Fisher | Mm01182747_m1 |
| Il13 TaqMan Assays | Thermo Fisher | Mm00434204_m1 |
| Kit TaqMan Assays | Thermo Fisher | Mm00445212_m1 |
| Fcerla TaqMan Assays | Thermo Fisher | Mm00438867_m1 |
| Il4 TaqMan Assays | Thermo Fisher | Mm00445259_m1 |
| Il9 TaqMan Assays | Thermo Fisher | Mm00434305_m1 |
| Il33 TaqMan Assays | Thermo Fisher | Mm00505403_m1 |
| TSLP TaqMan Assays | Thermo Fisher | Mm01157588_m1 |
| Il25 TaqMan Assays | Thermo Fisher | Mm00499822_m1 |
| Il5 TaqMan Assays | Thermo Fisher | Mm00439646_m1 |
| Software and Algorithms | | |
| GraphPad Prism 7 | GraphPad Software | N/A |
| FlowJo 10.4.2 | Tree Star | https://www.flowjo.com/solutions/flowjo/downloads |
| Morpheus | Broad Institute | https://software.broadinstitute.org/morpheus/ |

## CONTACT FOR REAGENT AND RESOURCE SHARING

Further information and requests for resources and reagents should be directed to and will be fulfilled by the Lead Contact, Raif S. Geha (raif.geha@childrens.harvard.edu).

## EXPERIMENTAL MODEL AND SUBJECT DETAILS

### Mice

WT BALB/c, C57BL/6, and B6.SJL mice were purchased from Charles River Laboratories. BALB/c, Rag2-deficient mice, Rag2-gamma chain-deficient mice were obtained from Taconic. ST2-deficient *Il1rl1*$^{-/-}$ mice obtained from Dr. Andrew N.J. McKenzie (Townsend et al., 2000); IL-25R-deficient *Il17rb*$^{-/-}$ mice obtained from Amgen (Rickel et al., 2008); IL-25R-floxed *Il17rbfl/fl* mice and TSLPR-deficient mice (Al-Shami et al., 2005) were obtained from Dr. Steve F. Ziegler; Il4Rα-floxed mice were obtained from Dr. Frank Brombacher on BALB/c background (Herbert et al., 2004). Mcpt5-cre mice (Scholten et al., 2008), obtained from Dr. Talal Chatila, were derived for >6 generations on BALB/c background. Integrin beta7 *Itgb7*$^{-/-}$, *K14-creTg/0*, *Vil1-cre Tg/0*, Il7R -deficient, RORα-deficient mice, on C57Bl/6 background and IL-4Rα-deficient mice, on a Balb/c background, were obtained from Jax. Integrin beta7 *Itgn7*$^{-/-}$ were derived for >6 generations on BALB/c background in the laboratory. ST2-floxed *Il1rl1fl/fl* mice and IL-33-floxed mice obtained from Dr. Richard T Lee; IL-25-floxed mice obtained from Dr. Chen Dong (Angkasekwinai et al., 2010); and Rora-cre mice obtained from Dr. Dennis O'Leary (Chou et al., 2013), on a C57Bl/6 background were crossed once with mice on BALB/c background. All mice were housed in a specific pathogen-free environment and fed an OVA-free diet. All procedures were performed in accordance with the Animal Care and Use Committee of Boston Children's Hospital.

### Human Subjects

Excess of duodenal biopsy samples from children endoscoped because of abdominal pain, were collected during routine clinical care. Subjects were divided in 2 groups: active AD and scratching and subjects with no AD and no scratching based on history and clinical examination recorded by their gastroenterologist (E.H.). Samples were submitted in a blinded fashion to the pathologist (J.G.).

## METHOD DETAILS

### Mechanical Skin Injury, EC Sensitization, and Oral Antigen Challenge

Mechanical skin injury consists in two cycles of tape stripping, one at day 0 and one at day 3 (scheme in Figure 1A). For the first cycle, 6- to 8-week-old female mice were anesthetized; their back skin was shaved and tape-stripped with a film dressing (TegadermTM, 3M) 6 times. For the other cycle, mice were tape stripped 3 times. Finally, mice were sacrificed at different time points.

### Passive Sensitization

6- to 8-week-old female mice were injected intravenously with 10 μg of anti-trinitrophenyl (TNP) IgE monoclonal antibody (mAb). The following day, mice were challenged intragastrically with 12.5mg of TNP conjugated bovine serum albumin (TNP-BSA). Temperature changes were measured every 5 min following OVA challenge using the DAS-6001 Smart Probe and IPTT-300 transponders (Bio Medic Data Systems) injected subcutaneously.

### Intraperitoneal Sensitization

6- to 8-week-old female mice were injected intraperitoneally (i.p.) with 50 μg of OVA and 1 mg of alum at day 0 and day 7. At day 14, mice were challenged intragastrically with 100 mg of OVA. Temperature changes were measured as described above.

### Histology

For the chloroacetate esterase (CAE) staining, 1 cm pieces of mouse jejunum were fixed in 4% paraformaldehyde overnight at 4°C and embedded in paraffin. Paraffin sections were stained with CAE. $CAE^+$ cells were counted by an investigator who was blinded to the experimental groups. For the tryptase staining, duodenal biopsy samples were stained with an anti-tryptase antibody. Ten HPFs in areas of high-density MCs were evaluated blinded per the criteria used in evaluating EOE. For DCLK1 staining, the whole SI were treated as previously described (von Moltke et al., 2016), rolled and frozen in OCT. 10μM slices were first incubated with rat serum then stained with purified mAb anti-DCLK1 (ab31704) from Abcam, and with secondary Ab anti-rabbit IgG. Slices were fixed with a mounting medium containing DAPI (Prolon Gold) from ThermoFisher Scientific.

### Cell Suspension Preparation and Flow Cytometry Analysis

Cell isolation from the jejunum was performed as previously described (Galand et al., 2016). In brief, the jejuna were harvested, flushed with PBS supplemented with 2% fetal calf serum, opened longitudinally, and cut in 1 cm long pieces. Then, intestinal pieces were incubated in HBSS without Ca2+ and Mg2+ supplemented with 10 mM EDTA, 10 mM HEPES, 0.5% fetal calf serum, and 1.5 mM DTE, for 20 min at 37°C twice. Intestinal pieces were digested in HBSS with Ca2+ and Mg2+, 20% fetal calf serum, 100 U/mL collagenase VIII (Sigma-Aldrich), and 5 μg/mL DNase (Sigma-Aldrich) for 60 min at 37°C. Immune cells were purified with a 40% Percoll gradient (GE Healthcare).

Cell isolation from the skin was performed as previously described (Leisten et al., 2013). One-centimer squares of back skin were harvested; the layer of fat under the dermis was scrapped. Lower left lobes of lung were harvested. Skin remaining tissue and lung lobes were chopped finely and incubated for 60 and 30 min, respectively, at 37°C in complete RPMI media complemented with 100U Liberase DL (Roche) and 5 μg/mL DNase (Sigma-Aldrich). Red blood cells of the lung suspensions were lysed with ACK buffer. The cell suspensions were washed, incubated with TruStain FcX (anti-CD16/32 antibody; 10 μg/ml; Biolegend) and stained with the eF506 viability dye from eBioscience to exclude dead cells and the following murine fluorochrome labeled-monoclonal antibodies: B220 (RA3-6B2), CD3 (17A2), CD4 (GK1.5), CD11c (N418), CD19 (1D3), CD45 (30F11), CD90.2 (53-2.1), c- Kit (ACK2), Gr1 (RB6-8C5), IL-13Rα1 (13MOKA), ST2 (RMST2-2) from eBioscience, CD11b (M1/70), F4/80 (BM8), FcεRI (MAR-1), IgE (RME-1) and IL-17RB (9B10) from Biolegend. BV605 Streptavidin from Biolegend was used to detect biotinylated antibodies. For transcription factor staining, cells were fixed and permeabilized (eBiosicence fix/perm kit) and stained in permeabilization solution with GATA-3 (TWAJ) and Rorc (B2D) antibodies from eBioscience. For cytokine staining, cells were stimulated with Ionomycin (0.5ug/ml; Sigma), Phorbol 12,13- dibutyrate (1ug/ml; Sigma), Brefeldin A (eBioscience), Monensin (eBioscience) in complete RPMI for 3 h before surface staining. Then, cells were fixed and permeabilized (BD Biosciences Cytofix/Cytoperm) and stained in permeabilization solution with IL-4 (11B11), IL-5 (TRFK5), IL-9 (RM9A4) antibodies from Biolegend and IL-13 (eBio13A) antibodies from eBioscience. Cells were analyzed by flow cytometry using an LSRFortessa machine (BD Biosciences). The data were analyzed with FlowJo software.

### Intestinal Permeability

Intestinal permeability was determined as previously (Mathias et al., 2011). Briefly, mice were gavaged at day 14 with 400 μl of a 1 mg/ml horseradish peroxidase solution (HRP, MW 44 kDa; Sigma). Blood was obtained 4h later and the concentration of HRP was measured in the serum using the TMB substrate system.

### *Il33, Il25,* and *Tslp* mRNA Expression and Its Release Upon Tape Stripping

The back skin of anesthetized mice was shaved and subjected to tape stripping six times with a film dressing (TegadermTM, 3M). 6 h later, RNA was extracted from the skin with Total RNA isolation kit (Ambion). Intestinal epithelial cells were isolated from the duodenum as previously described (Gerbe et al., 2016). cDNA was prepared with iscript cDNA synthesis kit (Biorad). Quantitative real-time PCR was done with the Taqman gene expression assay, universal PCR master mix and ABI prism 7300 sequence detection system (Applied Biosystems). *Il25*, *Il33* and *tslp* mRNA fold induction was calculated using delta-delta ct with normalization to the internal control *β2microglobulin*. An arbitrary unit of 1 was assigned to the mean value of unmanipulated skin samples or intestinal epithelial cells from unmanipulated mice. For measuring IL-33, IL-25 and TSLP release, patches of ~1cm2 skin were excised from unmanipulated back or immediately post-tape stripping. Subcutaneous fat was removed, and the patches were cultured for 1 hr in complete RPMI. IL-25, IL-33 and TSLP in the supernatant and the sera, harvested 1 hr after tape stripping, was measured using Quantikine ELISA kit (R&D Systems) for IL-33 and Ready-set- go ELISA kit (eBioscience) for IL-25 and TSLP.

## QUANTIFICATION AND STATISTICAL ANALYSIS

All experiments were performed using randomly assigned mice without investigator blinding. Results of allergen challenge studies were analyzed using two-way ANOVA. Other results were analyzed by one-way ANOVA or non-parametric t tests using Prism 7 (GraphPad). A p value of less than 0.05 was considered significant.

**Immunity, Volume *50***

## Supplemental Information

# Mechanical Skin Injury Promotes Food Anaphylaxis by Driving Intestinal Mast Cell Expansion

**Juan-Manuel Leyva-Castillo, Claire Galand, Christy Kam, Oliver Burton, Michael Gurish, Melissa A. Musser, Jeffrey D. Goldsmith, Elizabeth Hait, Samuel Nurko, Frank Brombacher, Chen Dong, Fred D. Finkelman, Richard T. Lee, Steven Ziegler, Isaac Chiu, K. Frank Austen, and Raif S. Geha**

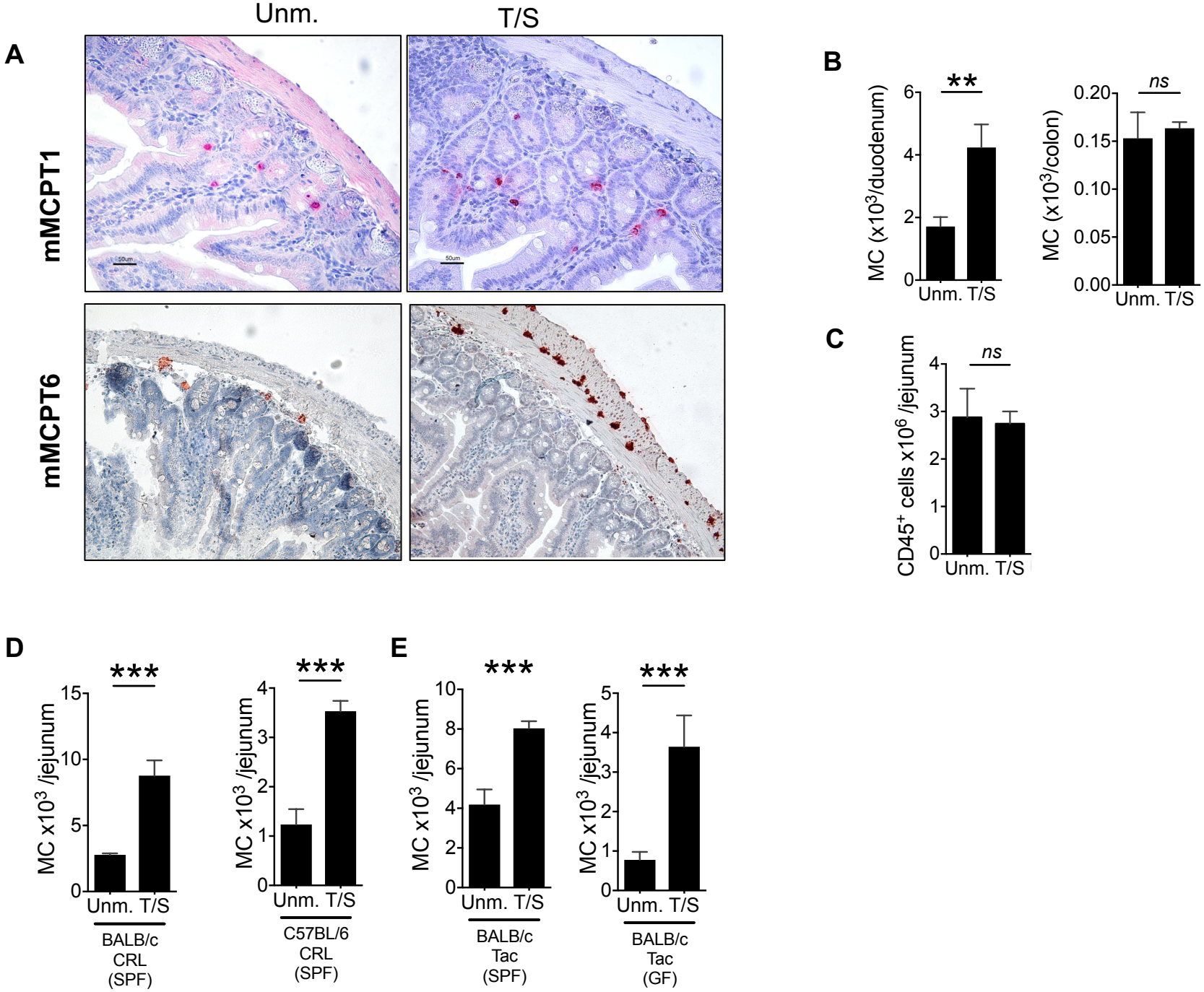

A
Unm.
T/S
mMCPT1
mMCPT6
B
**
ns
MC (x10³/duodenum)
MC (x10³/colon)
Unm. T/S
C
ns
CD45⁺ cells x10⁶ /jejunum
Unm. T/S
D
***
***
MC x10³ /jejunum
Unm. T/S
BALB/c CRL (SPF)
C57BL/6 CRL (SPF)
E
***
***
MC x10³ /jejunum
Unm. T/S
BALB/c Tac (SPF)
BALB/c Tac (GF)

**Figure S1**

**Figure S1. Tape stripping causes expansion of intestinal submucosal and mucosal MCs and of intestinal MCs in different mice strains and independently of the microbiota, related to Figure 1. A.** Representative immunohistochemistry staining for mMCPT1 (top) and mMCPT6 (bottom) of jejunal sections from tape stripped (T/S) mice and unmanipulated (Unm.) controls. **B.** Absolute numbers of c-kit$^+$IgE$^+$ MCs in duodenum (left) and colon (right) of T/S mice and Unm. controls. Results are derived from 2 independent experiments with 3 to 5 mice/group. **C.** Numbers of CD45$^+$ cells in the jejunum of T/S mice and Unm. controls. Results are derived from 2 independent experiments with 3 to 5 mice/group. **D.** Absolute numbers of jejunal c-kit$^+$IgE$^+$ MCs in T/S and Unm. BALB/c (left) and C57BL/6 (right) mice from Charles River Labs (CRL) kept at Children's Hospital Boston specific pathogen free (SPF) facility. Data representative of 2 independent experiments each with 3 to 4 mice/group. **E.** Absolute numbers of jejunal c-kit$^+$IgE$^+$ MCs in T/S and Unm. BALB/c mice from Taconic Biosciences (Tac) kept at Children's Hospital Boston SPF (left) or germ free (GF) facility. Data representative of 2 independent experiments each with 3 to 4 mice/group. Columns and bars represent mean and SEM. ** = $p < 0.01$, *** = $p < 0.001$, ns: not significant.

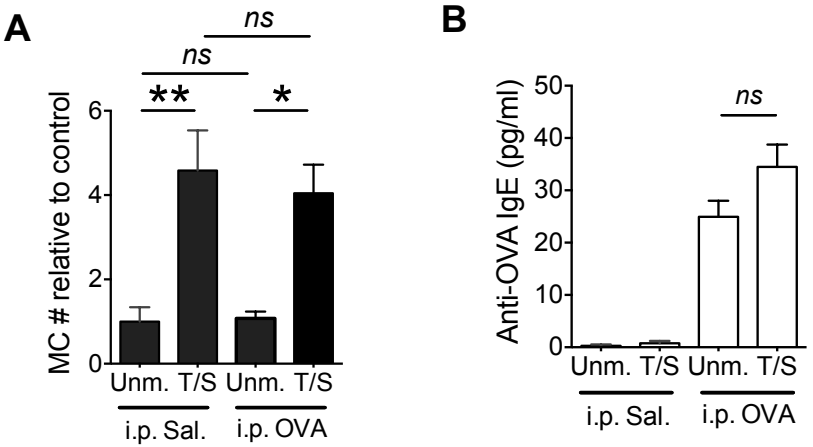

A
ns
ns
**
*
MC # relative to control
6
4
2
0
Unm.
T/S
Unm.
T/S
i.p. Sal.
i.p. OVA
B
ns
Anti-OVA IgE (pg/ml)
50
40
30
20
10
0
Unm.
T/S
Unm.
T/S
i.p. Sal.
i.p. OVA

**Figure S2**

**Figure S2. Intestinal MC expansion and antigen specific IgE in mice tape stripped and i.p. immunized with OVA, related to Figure 2. A-B.** Relative numbers (#) of jejunal MCs (A) and Serum anti-OVA IgE antibody concentrations (B) in WT BALB/c mice *i.p.* immunized with OVA or saline and tape stripped (T/S) or left unmanipulated (Unm.) as per the protocol in Fig. 2B. Data representative of 2 independent experiments each with 4-5 mice/group. Columns and bars represent mean and SEM. * = $p < 0.05$, ** = $p < 0.01$, ns: not significant.

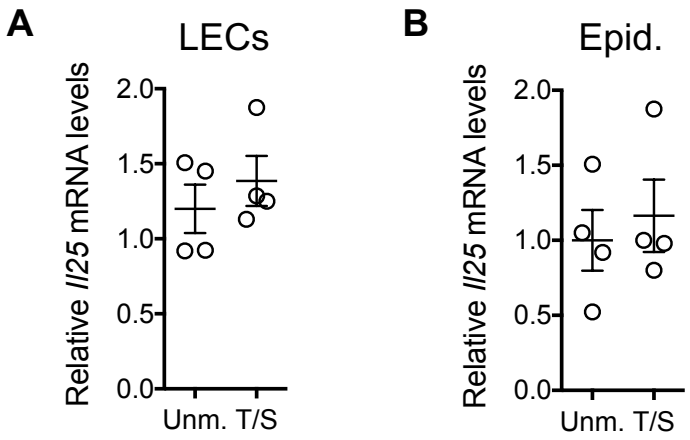

A
LECs
Relative Il25 mRNA levels
2.0
1.5
1.0
0.5
0.0
Unm.
T/S
B
Epid.
Relative Il25 mRNA levels
2.0
1.5
1.0
0.5
0.0
Unm.
T/S

**Figure S3**

**Figure S3**. **Effect of tape stripping on *Il25* mRNA expression in lung and skin epithelial cells, related to Figure 3. A.** *Il25* mRNA expression in lung epithelium cells (LECs) and skin epidermal layer (Epid.) from ears of mice tape stripped on back skin or unmanipulated controls. ns: not significant. Values represent fold induction relative to the mean value in unmanipulated mice. Results are derived from 2 independent experiments each with respectively 3 -5 mice/group.

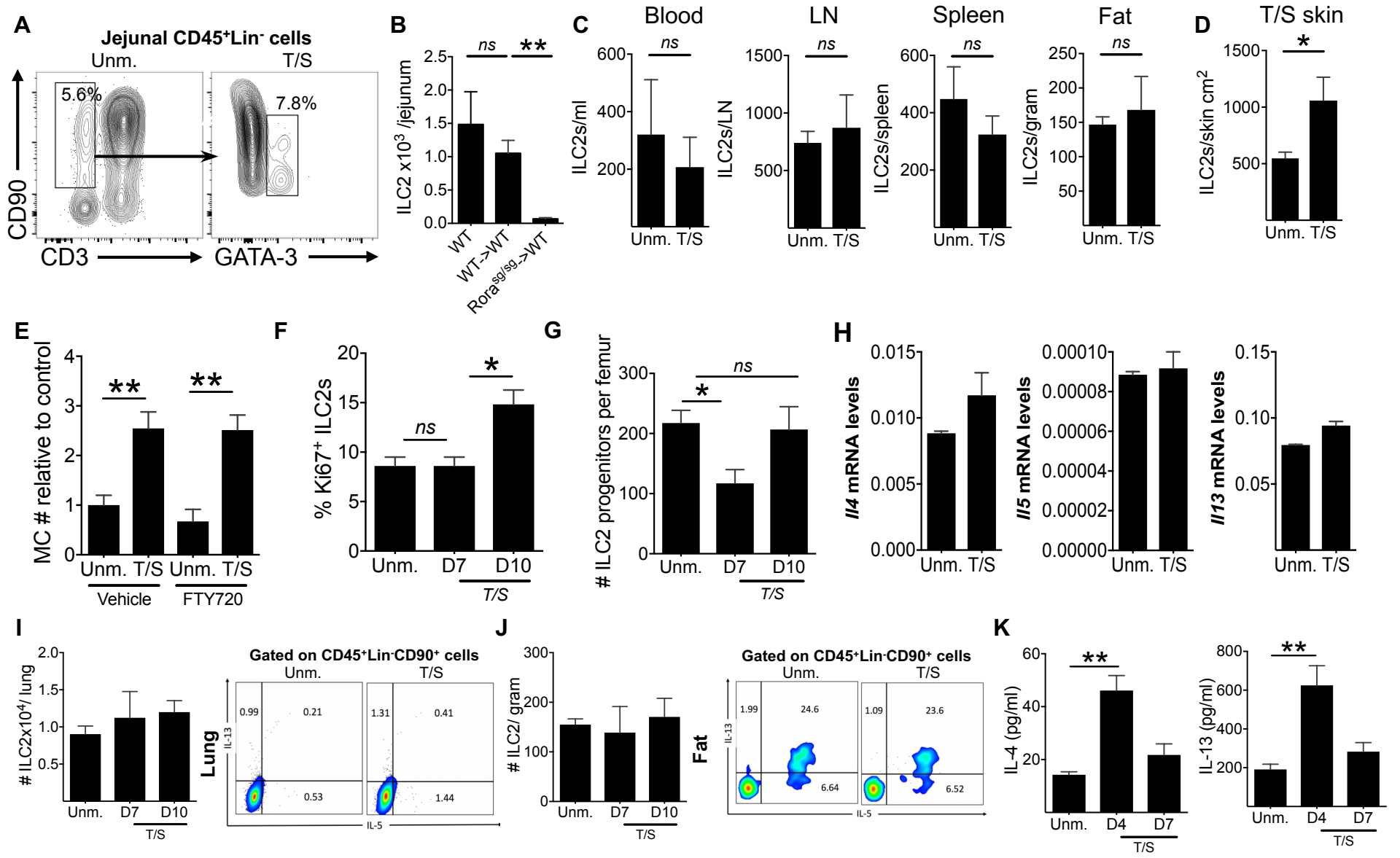
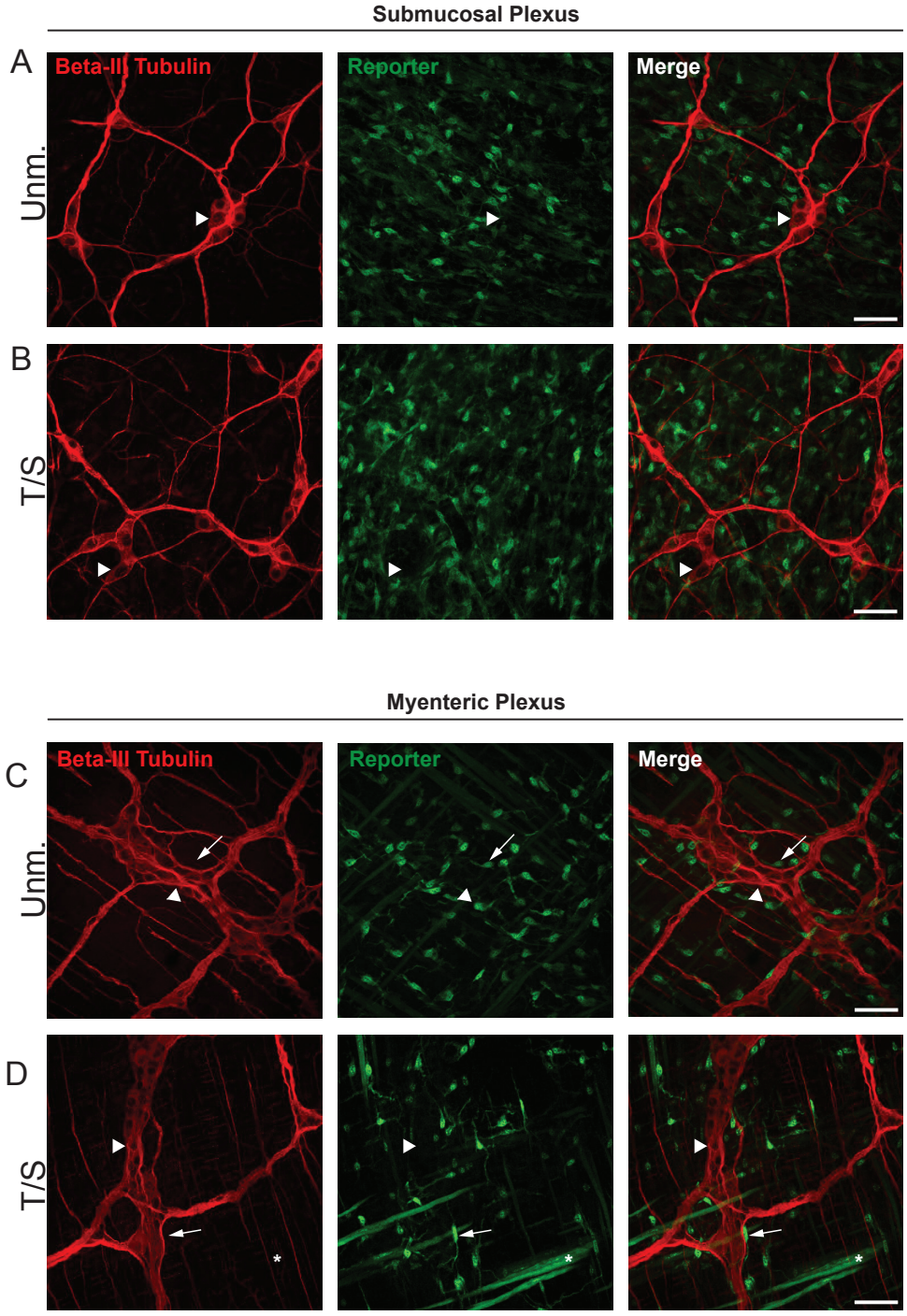

A
Jejunal CD45+Lin- cells
Unm.
T/S
5.6%
7.8%
CD90
CD3
GATA-3
B
ILC2 x10^3 /jejunum
ns
**
WT
WT->WT
Rora sg/sg->WT
C
Blood
LN
Spleen
Fat
ILC2s/ml
ILC2s/LN
ILC2s/spleen
ILC2s/gram
ns
Unm. T/S
D
T/S skin
ILC2s/skin cm2
*
E
MC # relative to control
**
Unm. T/S Unm. T/S
Vehicle
FTY720
F
% Ki67+ ILC2s
ns
*
Unm. D7 D10
T/S
G
# ILC2 progenitors per femur
ns
*
Unm. D7 D10
T/S
H
Il4 mRNA levels
Il5 mRNA levels
Il13 mRNA levels
Unm. T/S
I
# ILC2x10^4/ lung
Unm. D7 D10
T/S
Gated on CD45+Lin-CD90+ cells
Unm.
T/S
Lung
IL-13
IL-5
0.99
0.21
0.53
1.31
0.41
1.44
J
# ILC2/ gram
Unm. D7 D10
T/S
Gated on CD45+Lin-CD90+ cells
Unm.
T/S
Fat
IL-13
IL-5
1.99
24.6
6.64
1.09
23.6
6.52
K
IL-4 (pg/ml)
IL-13 (pg/ml)
**
Unm. D4 D7
T/S

**Figure S4**

**Figure S4**. **Gating strategy for intestinal ILC2s, absence of ILC2s in the intestine of *Rora*$^{sg/sg}$->WT, number of ILC2s in different tissues, effect of the sphingosine-1-phosphate (S1P) analogue FTY720 on intestinal MC expansion , effect of tape stripping on proliferation of jejunal ILC2s and mobilization of ILC2 progenitors from the bone marrow, type 2 cytokine expression in ILCs from distant skin sites, lungs and fat and Serum IL-4 and IL-13 are increased by tape stripping prior to intestinal ILC2 expansion related to Figure 4. A.** Representative flow cytometry analysis of CD90$^+$CD3$^-$GATA-3$^+$ ILC2s in the CD45$^+$Lin$^-$ fraction of LP cells from the jejunum. **B.** Numbers of jejunal ILC2s in unmanipulated *Rora*$^{sg/sg}$->WT chimeras, WT-WT chimeras and WT mice controls. **C-D.** Numbers of CD45$^+$Lin$^-$CD90$^+$GATA3$^+$ ILC2s in blood, lymph node (LN), spleen, visceral adipose tissue (C) and in the unmanipulated and tape stripped skin (D) of unmanipulated (Unm) and tape stripped (T/S) WT BALB/c mice. **E.** Jejunal MC numbers (#) in unmanipulated (Unm) and tape stripped (T/S) BALB/c mice treated with FTY720 or vehicle. **F.** Percentage of CD45$^+$Lin$^-$CD90$^+$GATA3$^+$Ki67$^+$ cells in the jejunum of unmanipulated (Unm) and tape stripped (T/S) WT mice. **G.** Numbers (right) of Lin$^-$Sca1$^+$IL-25R$^+$CD25$^+$CD127$^+$ ILC2 progenitors (ILC2p) in bone marrow cells from T/S or Unm. mice. **H.** *Il4, Il5 and Il13 mRNA* expression, relative to *B2m*, in sorted CD45$^+$Lin$^-$CD90$^+$ ILCs from distant skin sites of T/S mice and skin from Unm. controls. Data pooled from 2 independent experiments each with 3-4 mice/group. Columns and bars represent mean and SEM. **I-J.** ILC2 quantitation in lungs and visceral adipose tissue of WT BALB/c mice mice on Days 0, 7 and 10 post tape stripping (left panels) and representative flow cytometry analysis of the expression of IL-5 and IL-13 by CD45$^+$Lin$^-$CD90$^+$ ILCs in the lungs and visceral adipose tissue of Unmanipulated (Unm) mice and mice on Day 7 after tape stripping (right panels).

**K.** Serum concentration of IL-4 (left) and IL-13 (right) in tape stripped (T/S) or left unmanipulated (Unm.) WT mice at different time points. Results are derived from 2 independent experiments.


Submucosal Plexus
A
Unm.
Beta-III Tubulin
Reporter
Merge
B
T/S
Myenteric Plexus
C
Unm.
Beta-III Tubulin
Reporter
Merge
D
T/S

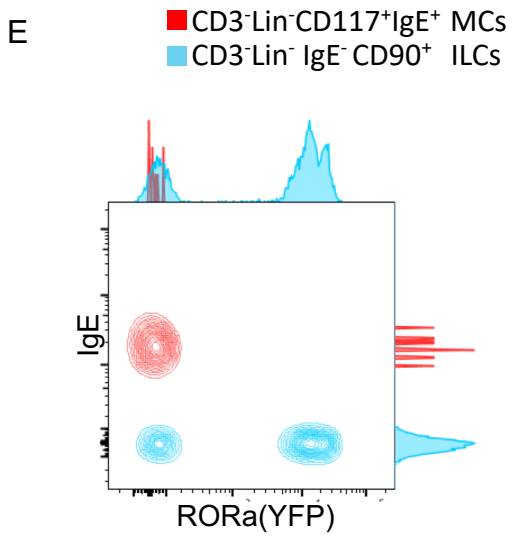

E
CD3⁻Lin⁻CD117⁺IgE⁺ MCs
CD3⁻Lin⁻ IgE⁻ CD90⁺ ILCs
IgE
RORa(YFP)

**Figure S5**

**Figure S5. RORα is not expressed in intestinal neurons or MCs, related to Figure 5. A-D.** Representative images from jejunum of tape stripped unmanipulated (Unm) and tape stripped (T/S) *Rora*$^{cre/cre}$*ROSA*$^{YFP}$ mice. Beta-III tubulin is a pan-neuronal marker, labeling neuron bodies and processes. In the submucosal plexus, YFP expression rarely, if ever, overlapped with Beta-III tubulin expression in (A) T/S mouse submucosal plexus vs (B) Unm. mouse submucosal plexus (arrowheads). Similar to the submucosal plexus, reporter expression very rarely overlapped with Beta-II tubulin expression in (A) T/S mouse vs (B) Unm. mouse (arrowheads). Reporter expression was seen in cells with smooth muscle morphology (asteriks) as well as cells near the periphery of ganglia, possibly interstitial cells of Cajal, glia, or immune cells based on location, morphology and processes (arrows). 40x. Scale bar = 50 um. **E.** Representative flow cytometry analysis of *Rora* (YFP) expression in intestinal ILCs ($CD45^+Lin^-CD90^+$) and MCs ($CD45^+Lin^-CD117^+\alpha\text{-}IgE^+$) in *Rora*$^{cre/cre}$*ROSA*$^{YFP}$ mice.

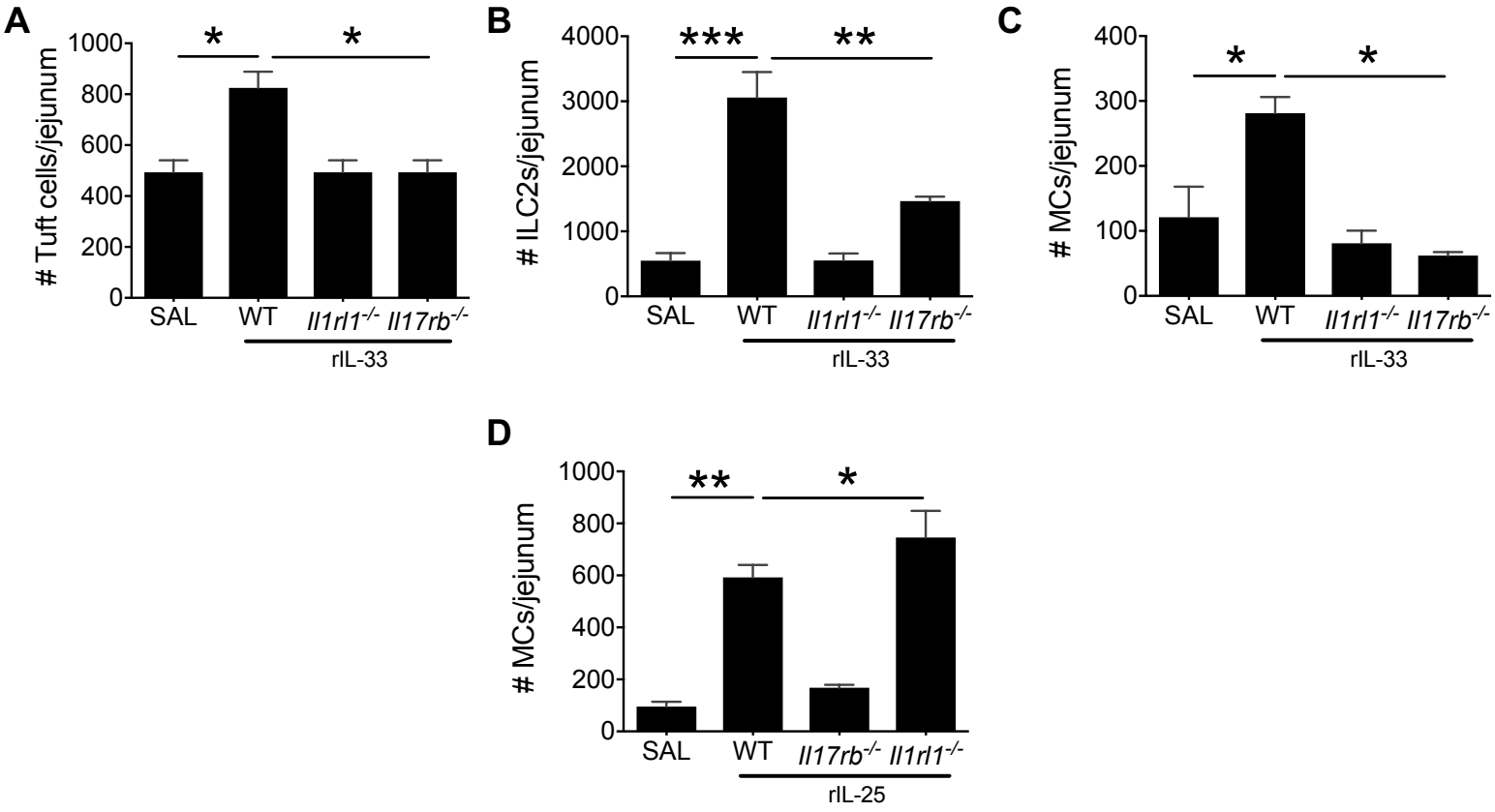

A
# Tuft cells/jejunum
1000
800
600
400
200
0
*
*
SAL
WT
Il1rl1-/-
Il17rb-/-
rIL-33
B
# ILC2s/jejunum
4000
3000
2000
1000
0
***
**
SAL
WT
Il1rl1-/-
Il17rb-/-
rIL-33
C
# MCs/jejunum
400
300
200
100
0
*
*
SAL
WT
Il1rl1-/-
Il17rb-/-
rIL-33
D
# MCs/jejunum
1000
800
600
400
200
0
**
*
SAL
WT
Il17rb-/-
Il1rl1-/-
rIL-25

**Figure S6**

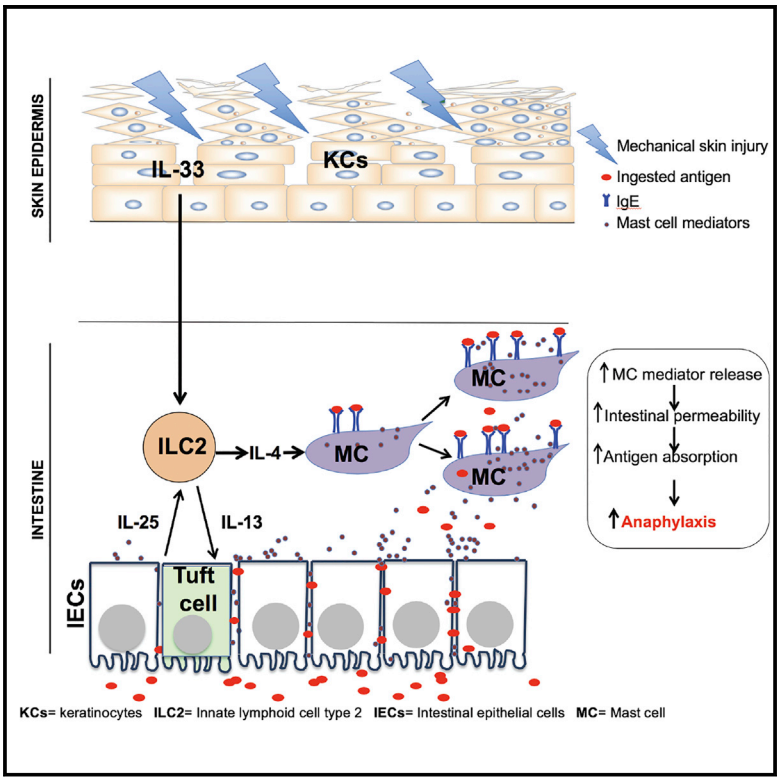
**Figure S6. Effect of i.v injection of rIL-33 and rIL-25 in the expansion of intestinal tuft cells, ILC2 and MCs, related to Figure 5. A-C.** Number of $CD45^{-}SiglecF^{+}EPCAM^{+}$ tuft cells (A), $CD45^{+}Lin^{-}CD90^{+}GATA3^{+}$ ILC2s (B) and $CD45^{+}Lin^{-}CD117^{+}\alpha\text{-}IgE^{+}$ MCs (C) in the jejunum of *Il1rl1*$^{-/-}$ and *Il17rb*$^{-/-}$ mice and WT controls injected with rIL-33. **D.** Number of MCs in the jejunum of *Il17rb*$^{-/-}$ and *Il1rl1*$^{-/-}$ mice and WT controls injected with rIL-25. Results are derived from 2 independent experiments with 3 to 5 mice/group. Columns and bars represent mean and SEM. * = $p < 0.05$, ** = $p < 0.01$, *** = $p < 0.001$.

Article

Immunity

# Mechanical Skin Injury Promotes Food Anaphylaxis by Driving Intestinal Mast Cell Expansion

## Graphical Abstract




## Highlights

- Mechanical skin injury promotes intestinal mast-cell expansion
- Intestinal mast-cell expansion requires skin-derived IL-33 and gut-derived IL-25
- Intestinal mast-cell expansion requires ILC2 activation by IL-33 and IL-25
- ILC2-derived IL-4 and IL-13 directly cause intestinal mast-cell expansion

## Authors

Juan-Manuel Leyva-Castillo, Claire Galand, Christy Kam, ..., Isaac Chiu, K. Frank Austen, Raif S. Geha

## Correspondence

raif.geha@childrens.harvard.edu

## In Brief

Atopic dermatitis is a pruritic inflammatory skin disease highly associated with food allergy. Leyva-Castillo and colleagues demonstrate that a skin-to-gut crosstalk initiated by mechanical skin injury promotes food anaphylaxis by increasing mast cells in the gut.

Leyva-Castillo et al., 2019, Immunity *50*, 1–14
May 21, 2019 © 2019 Elsevier Inc.
https://doi.org/10.1016/j.immuni.2019.03.023

CellPress

Please cite this article in press as: Leyva-Castillo et al., Mechanical Skin Injury Promotes Food Anaphylaxis by Driving Intestinal Mast Cell Expansion, Immunity (2019), https://doi.org/10.1016/j.immuni.2019.03.023



CellPress

# Mechanical Skin Injury Promotes Food Anaphylaxis by Driving Intestinal Mast Cell Expansion

Juan-Manuel Leyva-Castillo,[1,11] Claire Galand,[1,11,12] Christy Kam,[1] Oliver Burton,[1,13] Michael Gurish,[2,14] Melissa A. Musser,[3] Jeffrey D. Goldsmith,[4] Elizabeth Hait,[5] Samuel Nurko,[5] Frank Brombacher,[6] Chen Dong,[7] Fred D. Finkelman,[8] Richard T. Lee,[9] Steven Ziegler,[10] Isaac Chiu,[3] K. Frank Austen,[2] and Raif S. Geha[1,15,*]

[1]Division of Immunology, Boston Children's Hospital, Harvard Medical School, Boston, MA, USA
[2]Division of Rheumatology, Immunology and Allergy, Brigham and Women's Hospital, Harvard Medical School, Boston, MA, USA
[3]Department of Microbiology and Immunobiology, Harvard Medical School, Boston, MA 02115, USA
[4]Department of Pathology, Boston Children's Hospital, Boston, MA, USA
[5]Division of Gastroenterology, Boston Children's Hospital, Boston, MA, USA
[6]International Center for Genetic Engineering and Biotechnology & University of Cape Town & South Africa Medical Research Council, South Africa
[7]Institute for Immunology and School of Medicine, Tsinghua University, Beijing, China
[8]Department of Internal Medicine and Division of Immunobiology, Cincinnati Children's Hospital Medical Center, Cincinnati, OH, USA
[9]Department of Stem Cell and Regenerative Biology, Harvard University, Cambridge, MA, USA
[10]Immunology Program, Benaroya Research Institute, Seattle, WA, USA
[11]These authors contributed equally
[12]Present address: Agenus, Inc., 3 Forbes Rd, Lexington, MA 02421, USA
[13]Present address: VIB-KU Leuven Center for Brain & Disease Research, Leuven, Belgium
[14]Deceased
[15]Lead Contact
*Correspondence: raif.geha@childrens.harvard.edu
https://doi.org/10.1016/j.immuni.2019.03.023

## SUMMARY

**Mast cell (MC) mediator release after crosslinking of surface-bound IgE antibody by ingested antigen underlies food allergy. However, IgE antibodies are not uniformly associated with food allergy, and intestinal MC load is an important determinant. Atopic dermatitis (AD), characterized by pruritis and cutaneous sensitization to allergens, including foods, is strongly associated with food allergy. Tape stripping mouse skin, a surrogate for scratching, caused expansion and activation of small intestinal MCs, increased intestinal permeability, and promoted food anaphylaxis in sensitized mice. Tape stripping caused keratinocytes to systemically release interleukin-33 (IL-33), which synergized with intestinal tuft-cell-derived IL-25 to drive the expansion and activation of intestinal type-2 innate lymphoid cells (ILC2s). These provided IL-4, which targeted MCs to expand in the intestine. Duodenal MCs were expanded in AD. In addition to promoting cutaneous sensitization to foods, scratching may promote food anaphylaxis in AD by expanding and activating intestinal MCs.**

## INTRODUCTION

Food allergy affects 6% of children and 3% of adults in the US and is on the rise (Sicherer and Sampson, 2009). The life-threatening symptom of food allergy is anaphylaxis. The physiopathology of anaphylaxis involves mast cell (MC) degranulation and release of mediators and cytokines after recognition of antigen by immunoglobulin E (IgE) antibodies bound to high-affinity IgE receptors (FcεRI) on MCs (Galli and Tsai, 2012). Not all individuals who have food-specific IgE antibodies react upon oral challenge, and food-specific IgE serum concentrations do not necessarily predict the severity of food allergy (Fleischer et al., 2011). Thus, additional factors other than IgE antibody are required for food anaphylaxis. An important such factor is intestinal MC load, which controls intestinal permeability (Lee et al., 2013) and, thereby, systemic absorption of antigen, which is essential for food anaphylaxis (Strait et al., 2011). Importantly, gut MC expansion is associated with increased susceptibility to oral anaphylaxis (Vaali et al., 2012), and intestinal MC load modulates the severity of oral anaphylaxis (Ahrens et al., 2012). Cutaneous exposure to food allergens in infants and mice predisposes to IgE-mediated food allergy (Bartnikas et al., 2013; Lack et al., 2003), implicating the skin as an important route of sensitization. There is a high prevalence of IgE antibodies to foods in atopic dermatitis (AD), a chronic pruritic inflammatory skin disease affecting ~15% of children in the United States (Spergel, 2010). The association between IgE sensitization to food and food anaphylaxis is substantially higher in patients with AD than in the population at large (Salo et al., 2014). Intestinal $IgE^+$ cell numbers are increased in patients with AD (Caffarelli et al., 2001; Kalimo et al., 1988), but the nature of these $IgE^+$ cells is ill defined. Furthermore, intestinal permeability is increased in AD patients (Pike et al., 1986). Tape stripping the skin of mice is a surrogate for scratching. Intestinal MC expansion is observed after application of saline to tape-stripped skin (Bartnikas et al., 2013), suggesting a link between mechanical skin injury and intestinal MC expansion. In the present study,

we demonstrate that tape stripping mouse skin causes selective MC expansion in the small intestine (SI), increases intestinal permeability, and promotes food anaphylaxis. Interleukin (IL)-33 released by keratinocytes synergized with IL-25 released by intestinal tuft cells to expand intestinal type-2 innate lymphoid cells (ILC2s) and increase their expression of *Il4* and/or *Il13*. ILC2-derived IL-4 and IL-13 targeted MCs to cause their expansion in the SI. We demonstrated that duodenal MCs are expanded in children with AD, independent of overt food allergy. Our observations document a skin-to-gut crosstalk in which mechanical skin injury promotes food anaphylaxis by driving intestinal MC expansion, in addition to facilitating sensitization to food allergens. Thus, our results are directly relevant to food allergy in patients with AD.

## RESULTS

### Mechanical Skin Injury Elicits Expansion of Intestinal Mast Cells

To mimic mechanical skin injury caused by scratching, the shaved back skin of BALB/c mice was tape stripped six times on day 0 and three times on day 3, and the mice were studied on day 14 (Figure 1A). Tape stripping resulted in a 2-fold increase in chloroacetate esterase positive ($CAE^+$) MCs in the jejunum, including MCs in the submucosa, as well as the lamina propria (LP) (Figure 1B). Immunohistochemical staining demonstrated that tape stripping the skin caused an increase in mast cell protease-$1^+$ ($mMCPT1^+$) MCs and $mMCPT6^+$ MCs in the jejunum (Figure S1A). The increase in MC expansion in the jejunal LP of tape-stripped mice was confirmed by flow cytometric analysis of $CD45^+Lin^-$ $c\text{-}Kit^+IgE^+$ cells (Figure 1C). Tape stripping also caused MC expansion in the duodenum but not in the colon (Figure S1B). The total number of $CD45^+$ cells in the SI did not increase in tape-stripped mice (Figure S1C). MCs expanded at the site of tape stripping but not in distant skin sites, lungs, or spleen (Figure 1D).

Tape stripping the skin caused an increase in the granularity of jejunal $c\text{-}Kit^+IgE^+$ MCs (Figure 1E) and upregulated their surface expression of c-Kit and IgE binding (Figure 1F), as well as their expression of *Il13*, *Hdc*, *Alox5*, *Kit*, and *Fcer1a* but not *Il4* (Figure 1G). *Il5* and *Il9* mRNAs were not detectable in jejunal MCs. These results indicate that tape stripping causes selective expansion of mucosal and submucosal MCs in the SI with an increase in MC granularity, maturation, and potential ability to produce IL-13, histamine, and leukotrienes.

Expansion of intestinal MCs after mechanical skin injury was not specific to the BALB/c strain, as it was observed in C57BL/6 mice (Figures S1D and S1E). Furthermore, it was independent of the mouse housing facility. A comparable ~2-fold increase in jejunal MCs was observed after tape stripping the skin of BALB/c mice obtained from Taconic Biosciences (Figure S1E). Importantly, jejunal MC expansion induced by tape stripping was independent from the microbiota, as it was preserved in germ-free BALB/c mice (Figure S1E). Because of the differences in baseline numbers of intestinal MCs between mice of different strains and mice housed in different facilities, we subsequently expressed the numbers of intestinal MCs in tape-stripped mice relative to their numbers in genetically matched unmanipulated controls.

### Tape Stripping Increases Intestinal Permeability and Promotes Oral Anaphylaxis

MC numbers in mouse intestine correlate with intestinal permeability (Ahrens et al., 2012). Tape stripping mouse skin caused an increase in intestinal permeability, as evidenced by an increase in serum horseradish peroxidase (HRP) concentration after oral gavage of HRP (Figure 2A). The increase in intestinal permeability was dependent on MCs and, in particular, on intestinal MCs, as it was not observed in $Kit^{W\text{-}sh/W\text{-}sh}$ mice, which globally lack MCs, or $Itgb7^{-/-}$ mice, which are selectively deficient in intestinal MCs (Gurish et al., 2001) (Figure 2A).

We investigated whether the expansion, increased granularity, and activation of intestinal MCs elicited by mechanical skin injury was associated with enhancement of oral anaphylaxis. To that end, mice were tape stripped and i.p. immunized with ovalbumin (OVA) or saline in alum, then challenged orally with OVA (Figure 2B). As expected, mice i.p. immunized with OVA, but not saline, demonstrated a drop in body temperature and an increase in serum mMCPT1 concentrations after oral OVA challenge (Figure 2B). Tape stripping of the skin enhanced oral anaphylaxis in mice i.p. immunized with OVA, as evidenced by a greater drop in core body temperature and higher serum mMCPT1 concentrations after oral OVA challenge compared to non-tape-stripped controls (Figure 2B). Neither non-tape-stripped nor tape-stripped i.p.-immunized $Itgb7^{-/-}$ mice exhibited a drop in body temperature after oral OVA challenge (data not shown), demonstrating the critical role of intestinal MCs in food anaphylaxis. MC expansion after tape stripping was comparable in mice immunized with OVA and in controls injected with saline (Figure S2A). Tape stripping had no detectable effect on the IgE anti-OVA response to i.p. immunization (Figure S2B). These results indicate that that the more severe oral anaphylaxis in tape-stripped mice was not due to a greater IgE antibody response to OVA.

To circumvent other potential effects of tape stripping on the response to OVA immunization, we examined whether tape stripping of the skin enhances IgE-mediated passive food anaphylaxis. Mice were tape stripped and passively sensitized by i.v. administration of IgE anti-TNP (2,4,6-trinitrophenol) or saline as control, then challenged orally with TNP-BSA (bovine serum albumin) (Figure 2C). Mice sensitized with IgE anti-TNP, but not unsensitized controls, demonstrated a drop in body temperature and an increase in serum mMCPT1 concentrations after oral TNP-BSA challenge (Figure 2C). Anaphylaxis to oral antigen challenge following passive sensitization was more severe in tape-stripped mice compared to unmanipulated controls, as evidenced by a greater drop in core body temperature and higher serum concentrations of MCTP1 (Figure 2C). These results suggest that expansion of intestinal MCs after mechanical skin injury increases intestinal absorption of antigen and promotes oral anaphylaxis.

### Keratinocyte-Derived IL-33 and Intestinal-Cell-Derived IL-25 Are Essential for Intestinal MC Expansion Elicited by Mechanical Skin Injury

Keratinocytes upregulate the expression and/or release of the cytokines IL-33, thymic stromal lymphopoietin (TSLP), and IL-25 in response to injury (Leyva-Castillo et al., 2013; Oyoshi et al., 2010). Receptors for these cytokines are expressed by

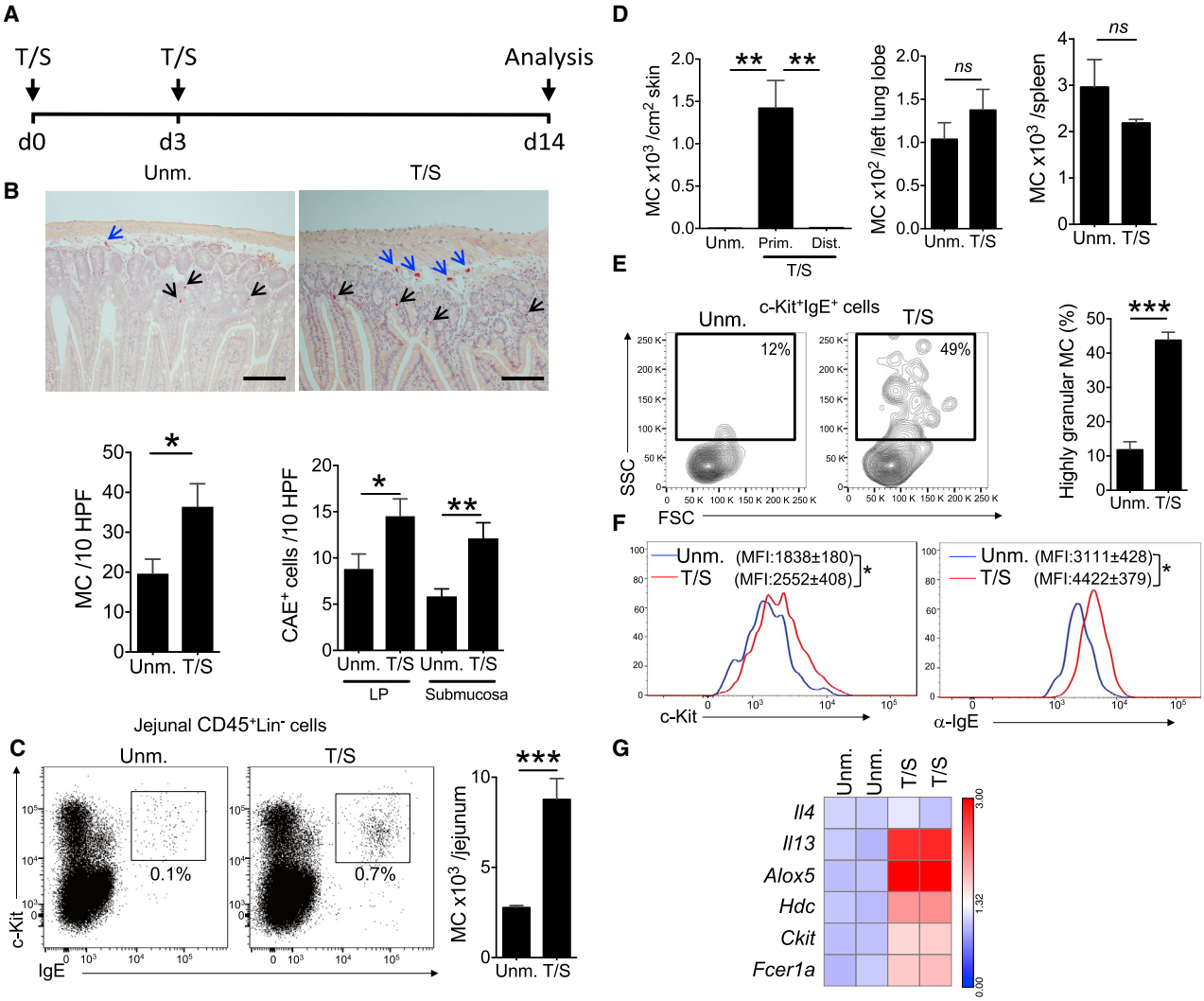



**Figure 1. Tape Stripping Mouse Skin Causes Expansion of Mast Cells (MCs) in the Small Intestine**

(A) Experimental protocol. BALB/C mouse skin was tape stripped (T/S) 6 times on day 0 and 3 times on day 3 using Tegaderm; mice were analyzed on day 14.

(B) Representative chloroacetate esterase (CAE) staining of jejunal sections, with scale bars representing 100 μM (top) and quantitation of MC numbers per 10 HPF in jejunum (bottom left) and jejunal LP and submucosa (bottom right) of T/S mice and unmanipulated (Unm.) controls. Results are derived from 2 independent experiments, each with 3 to 5 mice/group.

(C) Representative flow cytometry analysis of c-Kit$^+$IgE$^+$ MCs in the CD45$^+$Lin$^-$ fraction of jejunal LP cells from T/S mice and Unm. controls (left), and absolute numbers of jejunal CD45$^+$Lin$^-$c-Kit$^+$IgE$^+$ MCs (right). Results are derived from 2 independent experiments, each with 4 mice/group.

(D) Numbers of CD45$^+$Lin$^-$c-Kit$^+$IgE$^+$ MCs in primary (Prim.) skin sites subjected to tape stripping, distant (Dist.) skin site (left), lungs (middle), and spleen (right) of T/S mice and Unm. controls. Data are representative of 2 independent experiments, each with 3 to 4 mice/group.

(E) Representative flow cytometry analysis of the granularity (side scatter) and size (forward scatter) of CD45$^+$Lin$^-$c-Kit$^+$IgE$^+$ MCs (left) and percentage of SSC$^{high}$c-Kit$^+$IgE$^+$ MCs (right) in the jejunum of T/S mice and Unm. controls. Results are derived from 2 independent experiments, each with 4 mice/group.

(F) Representative flow cytometry analysis of surface expression of c-Kit or CD117 (left) and FcεR1 detected as IgE binding (right) by CD45$^+$Lin$^-$c-Kit$^+$IgE$^+$ MCs from the lamina propria (LP) of T/S mice and Unm. controls. Results are representative of 2 independent experiments, each with 4 mice/group.

(G) qPCR analysis of mRNA expression of select genes by CD45$^+$Lin$^-$c-Kit$^+$IgE$^+$ MCs sorted from the LP of T/S mice and Unm. controls expressed relative to the mean of Unm. controls. The lanes correspond to the groups from 2 different experiments in which MCs were pooled from 4 to 5 mice/group.

Columns and bars in B–E represent SEM. **p < 0.01, ***p < 0.001, ns: not significant. Please see also Figure S1.

ILC2s, MCs, and subsets of T cells (Saenz et al., 2008), rendering epithelial cytokines potential candidates for communicating signals from injured skin to the intestine. mRNA expression of *Il33* and *Tslp*, but not *Il25*, increased in mouse skin 6 h after tape stripping (Figure 3A). Explants of tape-stripped mouse skin released more IL-33 and TSLP than explants from unmanipulated skin, but no detectable amounts of IL-25 (Figure 3B). Importantly, there was a ~3-fold rise in the serum concentration of IL-33, but not TSLP, 1 h after tape stripping the skin (Figure 3C). IL-25 was not detected in the serum. IL-33 release by skin explants and the increase in IL-33 serum concentrations after tape stripping were abolished in *K14-cre*$^{Tg/0}$*Il33*$^{flox/flox}$

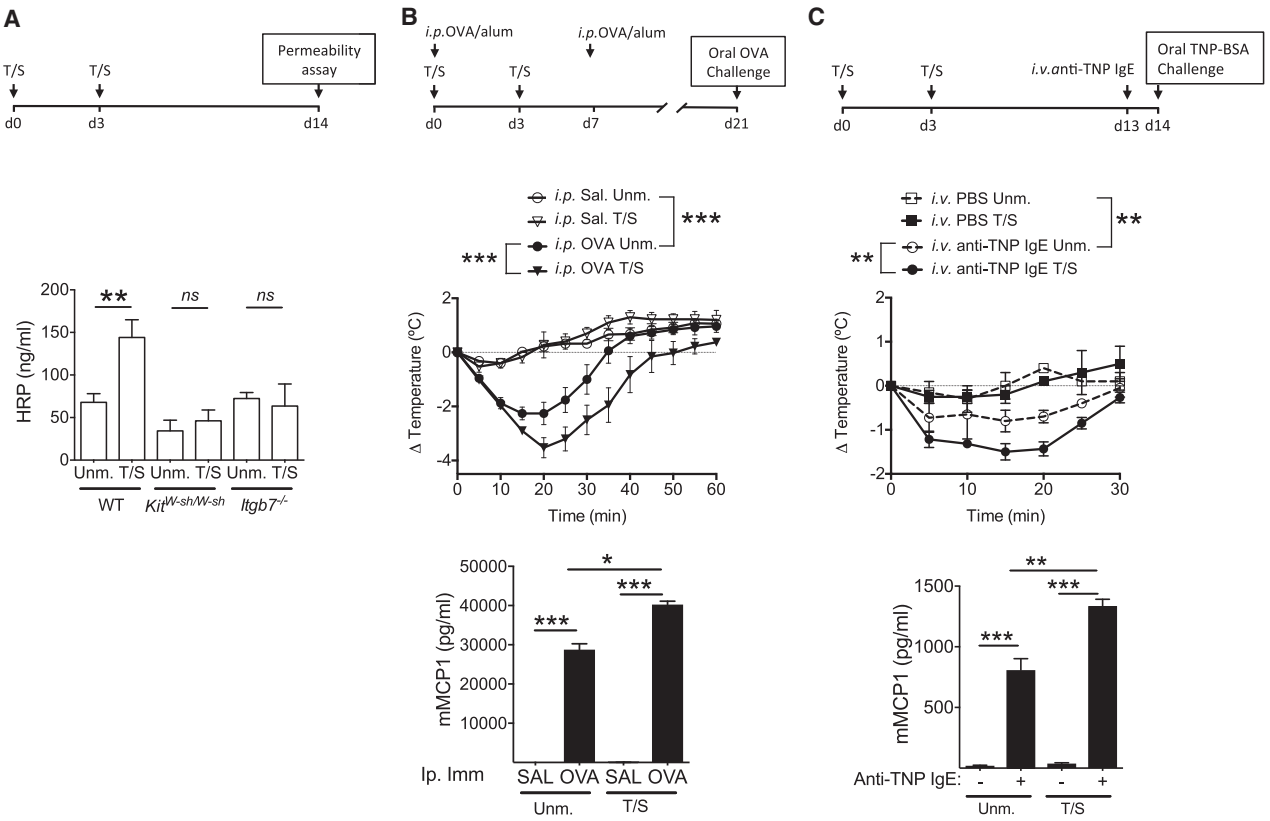



**Figure 2. Tape Stripping of the Skin Increases Intestinal Permeability and Promotes Anaphylaxis to Oral Antigen Challenge**

(A) Effect of tape stripping (T/S) the skin on intestinal permeability. Upper panel: Experimental protocol. Lower panel: serum HRP concentrations in T/S and Unm. wild-type (WT,) *Kit*$^{W\text{-}sh/W\text{-}sh}$, and *Itgb7*$^{-/-}$ mice. Results are derived from 3 independent experiments, each with 4 to 5 mice/group.

(B) Effect of tape stripping the skin on food anaphylaxis in i.p.-immunized T/S and Unm. WT mice. Upper panel: experimental protocol. Middle panel: change in core body temperature following oral OVA challenge. Lower panel: serum mMCPT1 concentrations. Data are representative of 2 independent experiments, each with 4 to 5 mice/group.

(C) Effect of tape stripping the skin on food anaphylaxis in T/S and Unm. mice passively sensitized with IgE anti-TNP. Upper panel: experimental protocol. Middle panel: change in core body temperature after oral challenge with TNP-BSA. Lower panel: serum mMCPT1 concentrations.

Data are representative of 2 independent experiments each with 4 to 5 mice/group. Columns and bars in (A) and symbols and bars in (B) and (C) represent SEM. **p < 0.01, ***p < 0.001, ns: not significant. Please see also Figure S2.

mice, which lack IL-33 specifically in keratinocytes (Figure 3D). These results suggest that mechanical injury to mouse skin results in the systemic release of the epithelial cytokine IL-33 from keratinocytes. In addition to keratinocytes, the *K14* transgene is expressed in mouse thymic epithelial cells (TECs) and oral epithelium (Li et al., 2001). We cannot rule out a potential contribution of these tissues in our model.

Expansion of intestinal MCs was abolished in *Il1rl1*$^{-/-}$ mice that lack the IL-33R and in *Il17rb*$^{-/-}$ mice that lack the high-affinity ligand-binding chain of the IL-25R but was preserved in *Tslpr*$^{-/-}$ mice (Figure 3E), indicating that IL-33 and IL-25, but not TSLP, play essential and non-redundant roles in intestinal MC expansion elicited by mechanical skin injury. Expansion of intestinal MCs was abolished in tape-stripped *K14-cre*$^{Tg/0}$ *Il33*$^{flox/flox}$ mice (Figure 3F). In contrast, it was preserved in *K14-cre*$^{Tg/0}$*Il25*$^{flox/flox}$ mice (Figure 3F). These results demonstrate that keratinocytes are the source of the IL-33, but not the IL-25, essential for intestinal MC expansion elicited by mechanical skin injury.

Tuft cells constitutively express IL-25 and are the only identified source of IL-25 in the intestine (von Moltke et al., 2016). They are characterized by intracellular expression of doublecortin like kinase 1 (DCLK1) and surface expression of epithelial cell adhesion molecule (EpCAM) and the C-type lectin receptor SiglecF (von Moltke et al., 2016). Immunofluorescence analysis of the jejunum revealed that tape stripping caused a ~2-fold increase in the number of DCLK1$^{+}$ tuft cells (Figure 3G). This was confirmed by flow cytometry analysis of CD45$^{-}$EpCAM$^{+}$SiglecF$^{+}$ tuft cells in jejunal IECs (Figure 3H). Tape stripping also caused a ~3-fold increase in *Il25* mRNA expression in jejunal IECs (Figure 3I). Upregulation of *Il25* mRNA expression after tape stripping of the skin was selective to IECs, as it was not observed in lung epithelial cells or skin epidermal layer (Figure S3). Importantly, expansion of jejunal MCs after tape stripping was abolished in *Vil1-cre*$^{Tg/0}$*Il25*$^{flox/flox}$ mice, which lack IL-25 in their IECs (von Moltke et al., 2016) (Figure 3J). These results demonstrate that tape stripping of the skin causes tuft-cell expansion and increased *Il25* expression by IECs and that IEC-derived

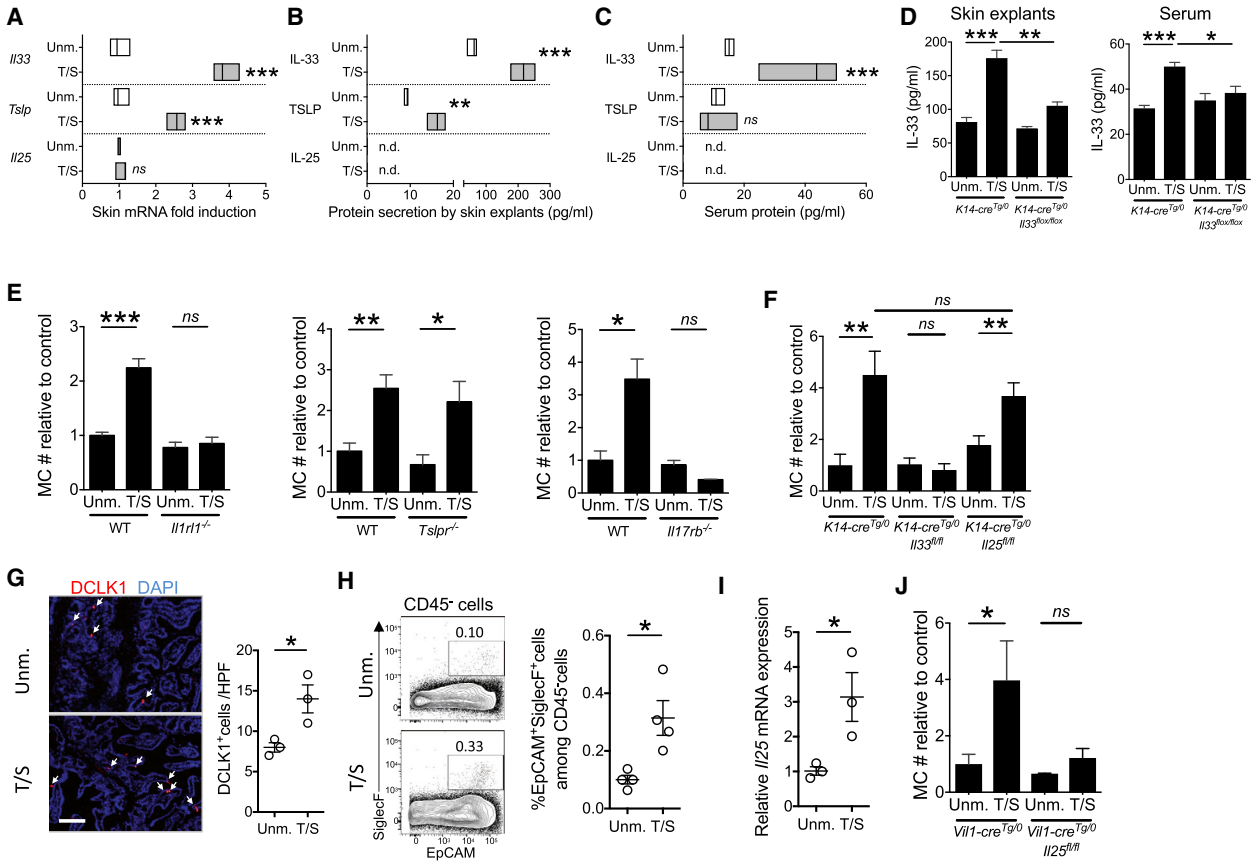



**Figure 3. Keratinocyte-Derived IL-33 and IEC-Derived IL-25 Are Necessary for Intestinal MC Expansion Elicited by Tape Stripping the Skin**

(A) *Il33*, *Tslp*, and *Il25* mRNA expression in skin. Values represent fold induction in tape-stripped skin relative to unmanipulated (Unm.) skin. Data are representative of 2 independent experiments, each with 3 mice/group.

(B) IL-33, TSLP, and IL-25 concentrations in the supernatants of skin explants from T/S and Unm. skin.

(C) Serum concentrations of IL-33, TSLP, and IL-25 in mice 1 h after tape stripping the skin and in Unm. controls. Data representative of 2 independent experiments, each with 3 mice/group.

(D) IL-33 concentrations in the supernatants of skin explants (left) and serum (right) of T/S and Unm*K14-cre*$^{Tg/0}$*Il33*$^{flox/flox}$ mice and *K14-cre*$^{Tg/0}$ controls.

(E) Jejunal MC numbers (#) in T/S and Unm. *Il1rl1*$^{-/-}$, *Tslpr* $^{-/-}$, and *Il17rb*$^{-/-}$ mice and genetically matched WT controls relative to the mean of unmanipulated controls. Results are derived from 2 independent experiments with 3 to 5 mice/group.

(F) Jejunal MC numbers (#) in T/S and Unm. *K14- cre*$^{Tg/0}$*Il33*$^{flox/flox}$, *K14-cre*$^{Tg/0}$*Il25*$^{flox/flox}$, and *K14-cre*$^{Tg/0}$ mice relative to the mean of the unmanipulated *K14-cre*$^{Tg/0}$ controls. Results are derived from 2 independent experiments with 3 to 5 mice/group.

(G) Representative immunofluorescence staining of jejunal sections for DCLK1 in red and DAPI in blue (left) and quantitation of DCLK1$^{+}$ tuft cells per HPF (right) in T/S WT mice and Unm. controls. Results are derived from 2 independent experiments, each with 1 and 2 mice/group, respectively.

(H) Representative flow cytometry analysis (left) and quantitation of the percentage (right) of SiglecF$^{+}$EPCAM$^{+}$ cells gating on CD45$^{-}$ cells from the jejunal epithelial layer. Results are derived from 2 independent experiments, each with 2 mice/group.

(I) *Il25* mRNA expression in intestinal epithelial cells from T/S WT mice and Unm. controls. Values represent fold induction relative to the mean of unmanipulated mice. Results are derived from 2 independent experiments, each with 1 and 2 mice/group, respectively.

(J) Jejunal MC numbers (#) in T/S and Unm. *Vil1-cre*$^{Tg/0}$*Il25*$^{flox/flox}$ mice and *Vil1-cre*$^{Tg/0}$ controls relative to unmanipulated *Vil1-cre*$^{Tg/0}$ controls. Results are derived from 2 independent experiments with 2 to 3 mice/group.

Circles in (G)–(I) represent individual mice. Floating bars in (A)–(C), columns and bars in (D)–(F) and (J), and horizontal lines and bars in (G)–(I) represent mean and SEM. *p < 0.05, **p <0.01, ***p< 0.001, ns: not significant. Please see also Figure S3.

IL-25 is essential for intestinal MC expansion elicited by mechanical skin injury.

## ILC2s Are Essential for Intestinal MC Expansion Elicited by Tape Stripping the Skin

ILC2s and adaptive Th2 cells are targets for IL-33 and IL25 (Saenz et al., 2008). Tape stripping of the skin caused intestinal MC expansion in *Rag2*$^{-/-}$ mice, which are deficient in mature T and B cells but sufficient in ILCs (Figure 4A). In contrast, it caused no expansion of intestinal MCs in *Rag2*$^{-/-}\gamma c^{-/-}$ mice, which, in addition, lack ILCs (Figure 4B). Tape stripping also failed to cause intestinal MC expansion in *Il7ra*$^{-/-}$ mice, which lack ILCs and are deficient in T and B cells (Figure 4B). These results indicate that ILCs, but not mature T or B cells, are important for the expansion of intestinal MCs elicited by mechanical skin injury.

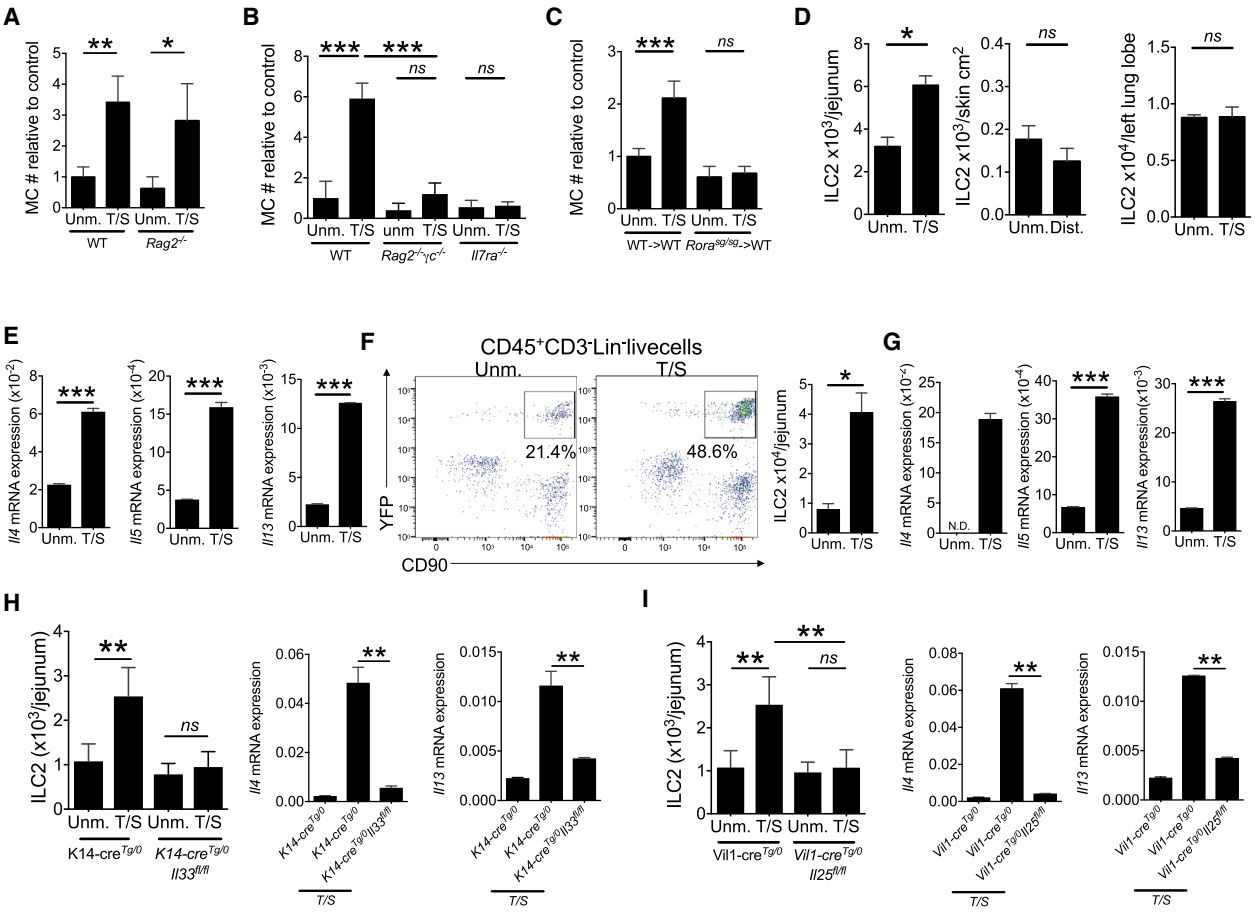



**Figure 4. ILC2s Are Necessary for Intestinal MC Expansion Elicited by Tape Stripping the Skin**

(A and B) Jejunal MC numbers in tape stripped (T/S) and unmanipulated (Unm.) *Rag2*$^{-/-}$, *Rag2*$^{-/-}\gamma c^{-/-}$, and *Il7ra*$^{-/-}$ mice (B) and genetically matched WT controls relative to the mean value of the unmanipulated control group. Results are derived from 2 independent experiments with 2 to 5 mice/group.

(C) Jejunal MC numbers (#) in T/S and Unm. *Rora*$^{sg/sg}\rightarrow$WT and WT$\rightarrow$WT chimeras, relative to the mean value of the unmanipulated WT$\rightarrow$WT chimera group. Results are derived from 2 independent experiments, each with 2 to 3 mice/group.

(D) ILC2 numbers in the jejunum (left), distant skin (middle), and lungs (right) in T/S BALB/c mice and Unm. controls. Data pooled from 2 independent experiments, each with 3 to 4 mice/group.

(E) Cytokine mRNA expression, relative to *B2m* in sorted CD45$^{+}$Lin$^{-}$CD90$^{+}$ ILCs from the jejunum of T/S mice and Unm. controls. Data pooled from 2 independent experiments, each with 3 to 4 mice/group.

(F) Representative flow cytometry analysis (left) and quantitation (right) of CD90$^{+}$YFP$^{+}$ ILC2s gating on CD45$^{+}$Lin$^{-}$ live cells from the jejunum of T/S and Unm. *Rora*$^{cre/cre}$*ROSA*$^{YFP}$ mice.

(G) Cytokine mRNA expression, relative to *B2m*, in Lin$^{-}$CD90$^{+}$YPF$^{+}$ cells (ILC2s) sorted from the jejunum of T/S and Unm. *Rora*$^{cre/cre}$*ROSA*$^{YFP}$ mice. Data pooled from 2 independent experiments, each with 3 to 4 mice/group.

(H and I) ILC2 numbers (left) and *Il4* and *Il13* mRNA expression, relative to *B2m*, in sorted CD45$^{+}$Lin$^{-}$CD90$^{+}$ ILCs (right) from the jejunum of T/S and Unm. *K14-cre*$^{Tg/0}$*Il33*$^{flox/flox}$ mice and *K14-cre*$^{Tg/0}$ controls (H) and T/S and Unm. *Vil1-cre Il25*$^{flox/flox}$ mice and *Vil1-cre* controls (I). Results are derived from 2 independent experiments with 3 to 5 mice/group.

Columns and bars represent mean and SEM. *p < 0.05, **p < 0.01, ***p < 0.001, ns: not significant. Please see also Figures S5 and S6.

ILC2s, but not ILC1s or ILC3s, express IL-25R and IL-33R (Spits et al., 2013). We directly examined the role of ILC2s in intestinal MC expansion after tape stripping of the skin. The transcription factor RAR-related orphan receptor alpha (RORα) is expressed selectively in ILC2s but not ILC1s or ILC3s (Spits et al., 2013). It is also expressed in cerebellar Purkinje cells and a subset of Th2 cells. *Rora*$^{sg/sg}$ mice carry a deletion that introduces a frameshift in the exon that encodes the ligand-binding domain of RORα (Dussault et al., 1998) and have no detectable ILC2s. However, they have neurologic abnormalities and a severely reduced lifespan. We therefore examined *Rora*$^{sg/sg}\rightarrow$ wild-type (WT) bone-marrow radiation chimeras, which are healthy and have a normal lifespan (Wong et al., 2012). GATA-3 is a transcription factor expressed in ILC2s but not ILC1s or ILC3s (Spits et al., 2013), allowing their identification by flow cytometry analysis as CD45$^{+}$Lin$^{-}$CD90$^{+}$CD3$^{-}$GATA-3$^{+}$ cells (Figure S4A). Intestinal ILC2s were virtually undetectable in *Rora*$^{sg/sg}\rightarrow$WT chimeras, but their numbers in control WT$\rightarrow$WT chimeras were comparable to those in WT mice (Figure S4B). Tape stripping caused no expansion of intestinal

MCs in *Rora*$^{sg/sg}$→WT chimeras but caused intestinal MC expansion in WT→WT chimeras comparable in magnitude to that in WT mice (Figure 4C). Because T cells are dispensable for intestinal MC expansion after tape stripping, these results indicate that ILC2s are critical for this expansion.

## Keratinocyte-Derived IL-33 and IEC-Derived IL-25 Drive the Expansion and Activation of Intestinal ILC2s after Mechanical Skin Injury

Tape stripping the skin caused a ~2-fold increase in the numbers of CD45$^+$Lin$^-$CD90$^+$CD3$^-$GATA-3$^+$ ILC2s in the LP of the jejunum of WT mice (Figure 4D). ILC2 expansion after mechanical skin injury was selective to the jejunum, because ILC2 numbers did not increase in distant skin sites, lungs, blood, skin draining lymph nodes, spleens, or visceral adipose tissue of tape-stripped mice (Figures 4D and S4C). We observed a 2-fold increase in ILC2s in tape-stripped skin (Figure S4D). Treatment with the sphingosine-1-phosphate (S1P) analogue FTY720 did not abolish the intestinal MC expansion induced by tape stripping (Figure S4E), suggesting that migration of ILC2s from tape-stripped skin is not required in our model.

There was an increase in Ki67$^+$ intestinal ILC2s at day 10, but not day 7, of our tape-stripping protocol (Figure S4F), suggesting that ILC2s are proliferating locally. IL-33 promotes the egress of ILC2 progenitors from the bone marrow (BM) (Stier et al., 2018). There was a decrease in Lin$^-$Sca1$^+$IL-25R$^+$CD25$^+$CD127$^+$ ILC2 progenitors (ILC2ps) in the BM at day 7, but not day 10, of our tape-stripping protocol (Figure S4G), but there was no increased expression of the gut-homing receptors CCR9 and integrin beta7 by these ILC2ps (data not shown). ILC2p mobilization from the BM may contribute to the ILC2 expansion in our model.

Activated ILC2s express type 2 cytokines (McKenzie et al., 2014; Spits et al., 2013). Tape stripping the skin upregulated expression of *Il4*, *Il5*, and *Il13* mRNA in CD45$^+$Lin$^-$CD90$^+$CD3$^-$ ILCs sorted from the jejunal LP (Figure 4E) but not in ILCs sorted from distant skin (Figure S4H). *Il4*, *Il5*, and *Il13* mRNA was not detectable in CD45$^+$Lin$^-$CD90$^+$CD3$^-$ ILCs sorted from the lungs. *Il9* mRNA was undetectable in jejunal ILCs (data not shown). In addition, tape stripping did not increase lung or visceral-adipose-tissue ILC2 numbers or their expression of IL-5 or IL-13 on day 7, 10, or 14 (Figures S4I and S4J; data not shown). Because CD45$^+$Lin$^-$CD90$^+$CD3$^-$ cells include ILCs other than ILC2s, we examined *Rora*$^{cre/cre}$*ROSA26*$^{YFP}$ mice in which ILC2s are identified as CD45$^+$Lin$^-$CD90$^+$CD3$^-$YFP$^+$ cells. Tape stripping the skin caused an increase in the numbers of CD45$^+$Lin$^-$CD90$^+$YFP$^+$ jejunal ILC2s in *Rora*$^{cre/cre}$*ROSA26*$^{YFP}$ mice (Figure 4F) and upregulated *Il4*, *Il5*, and *Il13* mRNA expression in yellow fluorescent protein$^+$ (YFP$^+$) ILC2s sorted from the jejunum of these mice (Figure 4G). *Il4*, *Il5*, and *Il13* mRNAs were not detectable in CD45$^+$Lin$^-$CD90$^+$CD3$^-$YFP$^-$ cells from the jejunum of tape-stripped *Rora*$^{cre/cre}$*ROSA26*$^{YFP}$ mice (data not shown). Serum IL-4 and IL-13 concentrations were increased 2-fold on day 4 after tape stripping, when jejunal expansion and activation are not yet observed, but returned to normal on day 7, before jejunal ILC2s were expanded and activated (Figure S4K; data not shown).

Jejunal ILC2 expansion and increased expression of *Il4* and *Il13* by ILCs were abolished in tape-stripped *K14-cre*$^{Tg/0}$ *Il33*$^{flox/flox}$ mice and *Vil1-cre*$^{Tg/0}$*Il25*$^{flox/flox}$ mice (Figures 4H and 4I), demonstrating that keratinocyte-derived IL-33 and IEC-derived IL-25 play non-redundant roles in the expansion and activation of jejunal ILC2s elicited by mechanical skin injury.

## IL-33 and IL-25 Act Directly on ILC2s to Cause Their Expansion and Activation after Mechanical Skin Injury

IL-33 and IL-25 act directly on ILC2s to cause proliferation and expression of type 2 cytokines (Spits et al., 2013). We investigated whether IL-33 and IL-25 act directly on ILC2s to cause their expansion in the intestines of tape-stripped mice. Tape stripping the skin caused a ~3-fold expansion of jejunal ILC2s and an increase in the expression of *Il4* and *Il13* mRNAs by jejunal ILCs in *Rora*$^{cre/cre}$ mice but not in *Rora*$^{cre/cre}$*Il17rb*$^{flox/flox}$ mice and *Rora*$^{cre/cre}$*Il1rl1*$^{flox/flox}$ mice, which lack IL-25R and IL-33R, respectively, in *Rora*-expressing cells (Figures 5A and 5B). Furthermore, tape stripping caused expansion of jejunal MCs in *Rora*$^{cre/cre}$ mice but not *Rora*$^{cre/cre}$*Il17rb*$^{flox/flox}$ or *Rora*$^{cre/cre}$*Il1rl1*$^{flox/flox}$ mice (Figure 5C). These results demonstrate that keratinocyte-derived IL-33 and IEC-derived IL-25 act directly and non-redundantly on intestinal ILC2s to cause their expansion and activation and to promote intestinal MC expansion after mechanical skin injury. YFP expression was detected in less than 2% of Beta III tubulin$^+$ intestinal neurons and was undetectable in intestinal MCs of *Rora*$^{cre/cre}$*ROSA26*$^{YFP}$ mice (Figure S5), demonstrating that *Rora*-driven *cre*-mediated ablation of gene expression is not operative in these cells.

Flow cytometry analysis demonstrated that IL-25R is expressed robustly on jejunal ILC2s and weakly on lung ILC2s, whereas IL-33R was expressed robustly on lung ILC2s and less strongly on intestinal ILC2s (Figure 5D). The strong expression of IL-25R on jejunal ILC2s, together with the selective increase in *Il25* mRNA in IECs after tape stripping of the skin, likely contributes to the selective expansion of ILC2s and MCs in the jejunum after mechanical skin injury.

## A Feedforward Loop Drives the Expansion and Activation of Intestinal ILC2s and Tuft Cells after Mechanical Skin Injury

Recent reports demonstrate the existence of a feedforward loop involving intestinal ILC2s and tuft cells in which IL-13 derived from ILC2s promotes the expansion of intestinal tuft cells and their expression of IL-25, which drives ILC2 expansion and activation (von Moltke et al., 2016). We used *Rora*$^{cre/cre}$*Il4/13*$^{flox/flox}$ and *Rag2*$^{-/-}$ mice to investigate whether expansion of intestinal tuft cells after tape stripping of the skin is dependent on ILC2-derived IL-13 and/or IL-4. Tape stripping of the skin caused expansion of EpCAM$^+$SiglecF$^+$ jejunal tuft cells, increased IL-25 mRNA expression by IECs, and expansion of ILC2s in *Rora*$^{cre/cre}$ mice but not *Rora*$^{cre/cre}$*Il4/13*$^{flox/flox}$ mice (Figures 5E–5G). Expansion of jejunal tuft cells, as well as expansion of intestinal ILC2s and their upregulation of *Il4* and *Il13* expression after tape stripping of the skin, was preserved in *Rag2*$^{-/-}$ mice (Figure 5H). Together with the dependence of intestinal ILC2 expansion and activation on IEC-derived IL-25 (Figure 4I), these results suggest that, after mechanical skin injury, IL-13 and/or IL-4 produced by ILC2s in response to keratinocyte-derived IL-33 activate a feedforward loop in which expansion and upregulation of IL-25 by tuft cells drives further the expansion and activation of small intestinal ILC2s. Injection of rIL-33 caused

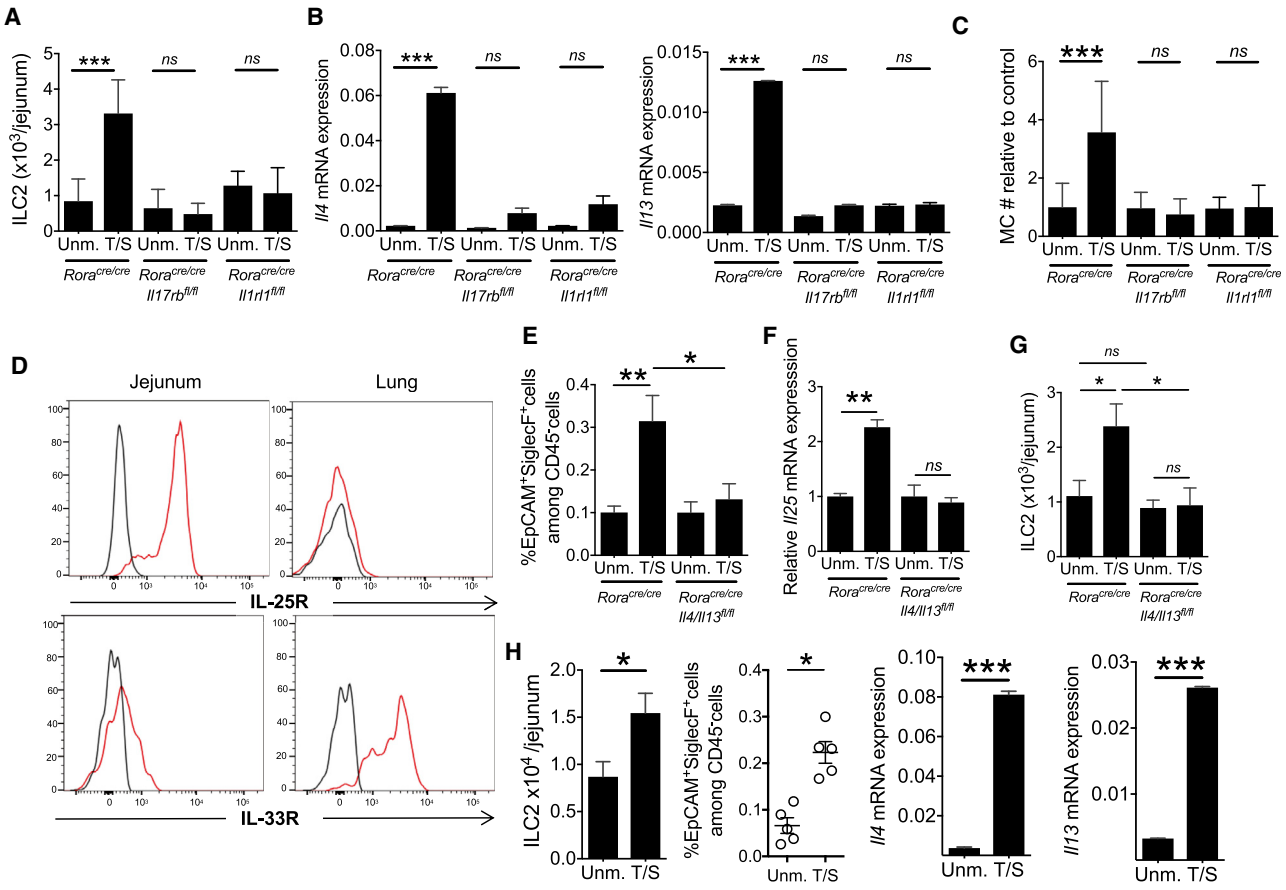



**Figure 5. IL-33 and IL-25 Directly Target ILC2s to Cause Their Expansion and to Activate a Feedforward ILC2 and Tuft-Cell Loop in the Intestine of Tape-Stripped Mice**

(A–C) ILC2 numbers (A), *Il4* and *Il13* mRNA expression relative to *B2m* in sorted CD45$^+$Lin$^-$CD90$^+$ ILCs (B) and MC numbers (C) in the jejunum of T/S and Unm. *Rora*$^{cre/cre}$*Il17rb*$^{flox/flox}$, *Rora*$^{cre/cre}$*Il1rl1*$^{flox/flox}$, and *Rora*$^{cre/cre}$ mice relative to Unm. *Rora*$^{cre/cre}$ controls. Results are derived from 3 independent experiments with 2 to 4 mice/group.

(D) Representative flow cytometry analysis of IL-25R (left) and IL-33R (right) expression by jejunal and lung CD45$^+$Lin$^-$ CD90$^+$YFP$^+$ ILC2s from *Rora*$^{cre/cre}$ *ROSA*$^{YFP}$ mice. Black lines represent isotype control. Similar results were obtained in two other independent experiments.

(E–G) Quantitation of the percentage of SiglecF$^+$EPCAM$^+$ cells gating on CD45$^-$ cells from the epithelial layer (E), *Il25* mRNA expression in IECs (F), and ILC2s numbers (G) in the jejunum of T/S and Unm. *Rora*$^{cre/cre}$*Il4/13*$^{flox/flox}$ mice and *Rora*$^{cre/cre}$ controls. Results are derived from 3 independent experiments with 2 to 4 mice/group.

(H) ILC2 numbers (left), percentage SiglecF$^+$EPCAM$^+$ cells gating on CD45$^-$ cells from the jejunal epithelial layer (center), and *Il4* and *Il13* mRNA expression relative to *B2m* in sorted CD45$^+$Lin$^-$CD90$^+$ ILCs (right) in the jejunum of T/S and Unm. *Rag2*$^{-/-}$ mice. Results are derived from 2 independent experiments with 3 to 4 mice/group.

Columns and bars represent mean and SEM. *p < 0.05, ***p< 0.001, ns: not significant. Please see also Figure S5.

an increase in the number of jejunal tuft cells, ILC2s, and MCs in WT mice that was abolished or markedly less in *Il17rb*$^{-/-}$ mice (Figures S6A–S6C), whereas injection of rIL-25 caused a comparable increase in the number of jejunal MCs in WT mice and *Il1rl1*$^{-/-}$ mice but no increase in *Il17rb*$^{-/-}$ mice (Figure S6D). These findings support the notion that keratinocyte-derived IL-33 initiates the intestinal ILC2-tuft-cell feedforward loop that results in intestinal MC expansion in our model.

## IL-4 and IL-13 Produced by ILC2s Target MCs to Cause MC Expansion after Mechanical Skin Injury

IL-4, IL-5, IL-9, and IL-13 promote the proliferation of bone-marrow-derived MCs *in vitro* (Okayama and Kawakami, 2006), whereas IL-4 and IL-9 can drive the expansion of MCs *in vivo* (Burton et al., 2013). Intestinal MC expansion elicited by tape stripping the skin of WT mice was abolished by administration of neutralizing monoclonal antibody (mAb) to IL-4 and IL-13 but not IL-5 and IL-9 (Figure 6A), indicating that IL-4 and IL-13 play essential and non-redundant roles in small intestinal MC expansion after mechanical skin injury.

To investigate whether ILC2s are the source of IL-4 and IL-13 important for intestinal MC expansion elicited by tape stripping the skin, we used *Rora*$^{cre/cre}$*Il4/13*$^{flox/flox}$ mice. Tape stripping caused no intestinal MC expansion in these mice but caused a ~2-fold expansion of intestinal MCs in *Rora*$^{cre/cre}$ controls (Figure 6B). The lack of intestinal MC expansion in *Rora*$^{cre/cre}$ *Il4/13*$^{flox/flox}$ mice was accompanied by attenuation of anaphylaxis in response to oral OVA challenge after i.p. sensitization

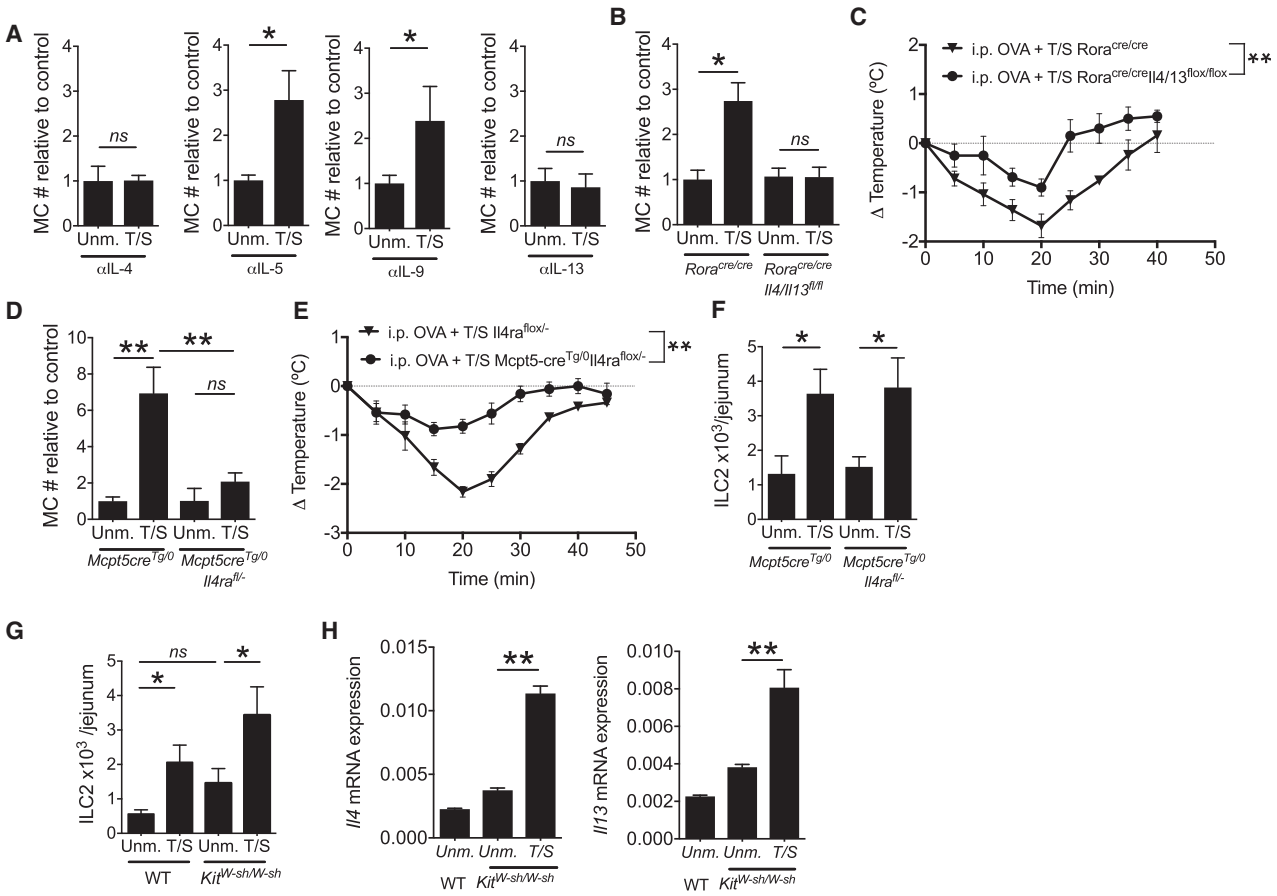



**Figure 6. ILC2-Derived IL-4 and IL-13 Directly Target MCs to Cause Their Expansion in the Intestine of Tape-Stripped Mice**

(A) Jejunal MC numbers (#) in T/S and Unm. WT mice treated with neutralizing anti-IL-4, anti-IL-5, anti-IL-9, or anti-IL-13 mAbs. MC values are relative to the mean value of the unmanipulated control group. Results are derived from 3 independent experiments with 2 to 4 mice/group.

(B) MC numbers relative to Unm. *Rora*$^{cre/cre}$ controls in the jejunum of T/S and Unm. *Rora*$^{cre/cre}$*Il4/13*$^{flox/flox}$ and *Rora*$^{cre/cre}$ mice. Results are derived from 3 independent experiments with 2 to 4 mice/group.

(C) Change in core body temperature after oral OVA challenge in T/S *Rora*$^{cre/cre}$*Il4/13*$^{flox/flox}$ mice and *Rora*$^{cre/cre}$ controls i.p. sensitized with OVA. Results are derived from 2 independent experiments with 3 to 5 mice/group.

(D and E) MC numbers relative to Unm. *Mcpt5-cre*$^{Tg/0}$ (D) and ILC2 numbers (E) in the jejunum of T/S and Unm. *Mcpt5-cre*$^{Tg/0}$*Il4ra*$^{flox/-}$ mice and *Mcpt5-cre*$^{Tg/0}$ mice. Results are derived from 2 independent experiments with 3 to 5 mice/group.

(F) Change in core body temperature following oral OVA challenge in T/S *Mcpt5-cre*$^{Tg/0}$*Il4ra*$^{flox/-}$ mice and *Mcpt5-cre*$^{Tg/0}$ controls i.p. sensitized with OVA. Results are derived from 2 independent experiments with 3 to 5 mice/group.

(G and H) ILC2 numbers (G) and *Il4* and *Il13* mRNA expression in sorted CD45$^+$Lin$^-$CD90$^+$ ILCs (H) in the jejunum of T/S and Unm. *Kit*$^{W\text{-}sh/W\text{-}sh}$ mice and genetically matched controls. Results are derived from 2 independent experiments with 3 to 5 mice/group.

Columns and bars represent mean and SEM. *p < 0.05, **p < 0.01, ns: not significant.

(Figure 6C). Given that intestinal MC expansion after tape stripping is maintained in *Rag2*$^{-/-}$ mice, these results suggest that ILC2-derived IL-4 and/or IL-13 are essential for intestinal MC expansion elicited by mechanical skin injury.

To examine whether IL-4 and/or IL-13 target MCs directly to mediate their expansion in the intestines of tape-stripped mice, we used *Mcpt5-cre*$^{Tg/0}$*Il4ra*$^{flox/-}$ mice, which selectively lack IL-4Rα and, thus, both IL-4R and IL-13R, in MCs. Tape stripping the skin caused no significant intestinal MC expansion in *Mcpt5-cre*$^{Tg/0}$*Il4ra*$^{flox/-}$ mice but caused robust intestinal MC expansion in *Mcpt5-cre*$^{Tg/0}$ controls (Figure 6D). Together with our previous findings, this result strongly suggests that IL-4 and/or IL-13 derived from intestinal ILC2s directly target intestinal MCs to cause their expansion. The lack of intestinal MC expansion in *Mcpt5-cre*$^{Tg/0}$*Il4ra*$^{flox/-}$ mice was accompanied by a decrease in food anaphylaxis in response to oral OVA challenge after i.p. sensitization (Figure 6E).

MCs release molecules that can drive the expansion and activation of ILC2s (Shimokawa et al., 2017). Intestinal ILC2 expansion after tape stripping of the skin was comparable in *Mcpt5-cre*$^{Tg/0}$*Il4ra*$^{flox/-}$ mice and *Mcpt5-cre*$^{Tg/0}$ controls (Figure 6F). Importantly, intestinal ILC2 expansion and increased expression of *Il4* and *Il13* mRNAs after tape stripping of the skin was comparable in MC-deficient *Kit*$^{W\text{-}sh/W\text{-}sh}$ mice and WT controls (Figures 6G and 6H). These results demonstrate that

A

**Characteristics of AD patients and non-AD controls**

| Subject | AD | Age (years) | Sex | Clinical Food Sensitivity | IgE (U/ml) | Food specific IgE |
|---|---|---|---|---|---|---|
| 1 | + | 3 | F | Anaphylaxis to milk | 1517 | + |
| 2 | + | 8 | F | Eosinophilic Esophagitis | 2348 | - |
| 3 | + | 13 | F | None | 41 | n.d. |
| 4 | + | 2 | M | None | 285 | + |
| 5 | - | 15 | F | None | n.d. | n.d. |
| 6 | - | 13 | F | None | n.d. | n.d. |
| 7 | - | 10 | M | Anaphylaxis to wheat | 784 | + |
| 8 | - | 4 | M | Eosinophilic Esophagitis | 715 | + |

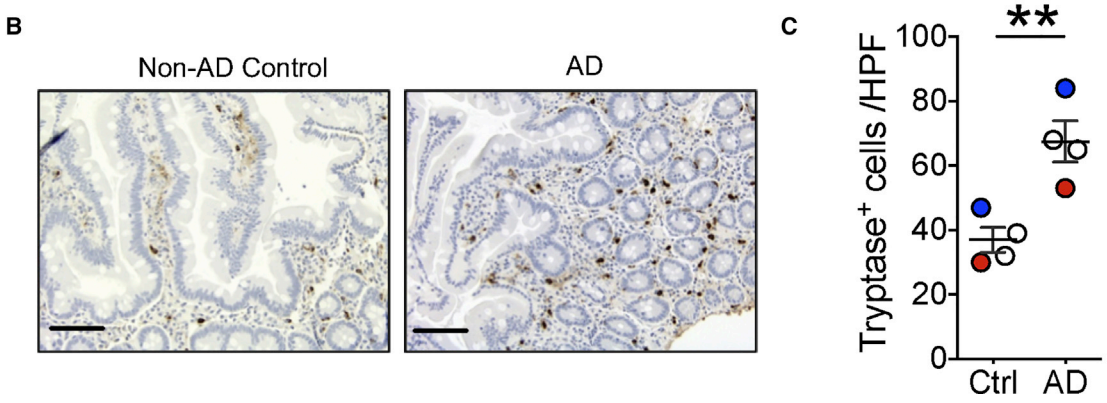



**Figure 7. Duodenal Mast Cells Are Increased in Patients with AD**

(A) Characteristics of AD patients and non-AD controls, n.d.: not done.

(B) Representative immunohistochemistry staining of duodenal sections with anti-tryptase mAb, with scale bars representing 100 μm (left) and numbers of tryptase$^+$ cells per HPF in the duodenum (right) of 4 children with active AD and scratching and 4 children with no AD and no scratching.

Circles represent individual patients. Open circle: no history of food sensitivity, red circle: anaphylaxis to food, blue circle: eosinophilic esophagitis. Horizontal lines and bars in (C) represent mean and SEM. **$p < 0.01$.

intestinal ILC2 expansion and activation after mechanical skin injury is independent of MCs.

## Duodenal Mast Cells Are Increased in Patients with AD

We next investigated whether intestinal MCs are increased in patients with AD. We examined MCs in archived duodenal biopsies from four children with active AD and four non-AD age-matched children. All patients underwent endoscopy with biopsy of the esophagus, stomach, and duodenum because of a history of recurrent upper abdominal pain and/or vomiting. History of food sensitivity, IgE serum concentrations, and IgE antibodies to food allergens in the patients are shown in Figure 7A. Two AD patients and two non-AD patients had no history of sensitivity to foods. One AD patient and one non-AD patient had a history of food anaphylaxis and IgE antibodies to the offending allergens but were on an avoidance diet and had no food allergy symptoms at the time of the study. One AD patient and one non-AD patient have been diagnosed clinically with eosinophilic esophagitis (EoE) and had IgE antibodies to multiple food allergens. MCs were identified in tissue sections by staining for the MC-specific enzyme tryptase. The number of tryptase-positive MCs in the LP of the duodenal mucosa was higher in

AD compared to non-AD controls (Figures 7B and 7C). Duodenal biopsies did not include the submucosa. Except for the increased MC numbers in the AD patients and the confirmation of the clinical diagnosis of EoE in one AD patient and one non-AD patient by the presence of more than 15 eosinophils per HPF in the esophagus LP, no other abnormalities were evident in the patients' biopsies. IgE can promote MC proliferation (Oettgen and Burton, 2015). The increased number of MCs in the duodenums of AD patients could not be simply due to higher serum IgE concentrations, because two of the four AD patients had lower serum IgE than the two non-AD patients on whom serum IgE concentrations were determined, one AD patient had a serum IgE in the normal range, and the mean serum IgE concentrations were not significantly different between the AD and non-AD patients: mean ± SEM, 1048 ± 540 IU/mL for AD patients, n = 4, versus 750 ± 35 IU/mL for non-AD patients, n = 2 ($p = 0.73$, unpaired t test). These results suggest that AD is associated with intestinal MC expansion independent of the presence of food allergy or EoE and that this expansion is not simply the result of elevated serum IgE.

## DISCUSSION

We unraveled the mechanisms of a crosstalk between skin and gut in which mechanical skin injury elicits expansion of intestinal MCs and thereby promotes IgE-mediated food anaphylaxis.

Tape stripping of the skin caused selective expansion of both mucosal and submucosal MCs in the jejunum, independently of the microbiota. This suggests that danger signals released in response to mechanical skin injury activate a skin-gut crosstalk that culminates in the expansion of intestinal MCs. Expansion of intestinal MCs was accompanied by phenotypic changes that included increased MC granularity; maturation, with increased c-Kit and FcεRI expression; and activation, with increased expression of genes that encode for IL-13 and enzymes involved in histamine and leukotriene synthesis.

MCs regulate homeostatic intestinal epithelial barrier function (Groschwitz et al., 2009). Tape stripping the skin increased intestinal permeability. This was dependent on intestinal MCs, as no increase in permeability was observed in tape-stripped *Igtb7*$^{-/-}$ mice that lack these cells. More importantly, tape stripping the skin concurrently with i.p. immunization with OVA potentiated anaphylaxis to oral antigen challenge. This was not due to an effect on the IgE antibody response to OVA or other aspects of the immune response to OVA immunization, because tape stripping also potentiated anaphylaxis to oral antigen challenge in mice that were passively sensitized with IgE antibodies. The finding that intestinal MC expansion after mechanical skin injury was associated with increased severity of anaphylaxis to oral challenge is consistent with previous reports that intestinal MC numbers control the severity of oral anaphylaxis (Ahrens et al., 2012). MC-mediated intestinal permeability predisposes to oral antigen hypersensitivity (Forbes et al., 2008). Thus, increased intestinal permeability associated with MC expansion likely contributed to the increased susceptibility to oral anaphylaxis caused by mechanical skin injury.

Tape stripping the skin caused increased local expression of the epithelial cytokine genes *Il33* and *Tslp*, but not *Il25*, and release of IL-33 and TSLP; however, only IL-33 was released systemically into the blood. Examination of *K14-cre*$^{Tg/0}$ *Il33*$^{flox/flox}$ mice revealed that keratinocytes were the source of the increased IL-33 released by skin explants and increased serum IL-33 in tape-stripped mice. Experiments using receptor-deficient mice demonstrated that both IL-33 and IL-25 are required for intestinal MC expansion after mechanical skin injury. Studies in mice with selective deficiency of IL-33 or IL-25 in keratinocytes demonstrated that keratinocyte-derived IL-33 was important for elicitation of intestinal MC expansion by mechanical skin injury. In contrast, keratinocyte-derived IL-25 played no evident role, consistent with the failure to detect IL-25 in the blood. Intestinal MC expansion after tape stripping was abolished in *Vil1-cre*$^{Tg/0}$*Il25*$^{flox/flox}$ mice, which lack IL-25 in their IECs, demonstrating that tuft cells, the only IECs known to produce IL-25, are the relevant source of IL-25 in our model. The finding that tape stripping caused an increase in the numbers of intestinal tuft cells and upregulated *Il25* mRNA expression by IECs suggests that mechanical skin injury causes proliferation and activation of tuft cells.

ILC2s were essential mediators of skin-to-gut crosstalk in our model. This was evidenced by the observation that lack of ILC2s in *Rora*$^{sg/sg}$ → WT BM chimeras abrogated the ability of tape stripping the skin to elicit intestinal MC expansion. Tape stripping caused expansion of intestinal ILC2s and their activation, as evidenced by marked upregulation of expression of the type 2 cytokines *Il4*, *Il5*, and *Il13*. rIL-33 and rIL-25 synergize to cause ILC2 expansion *in vivo* and ILC2 proliferation and cytokine secretion *in vitro* (Salimi et al., 2013). Expansion and activation of intestinal ILC2 after tape stripping was abrogated in *Rora*$^{cre/cre}$*Il17rb*$^{flox/flox}$ mice and *Rora*$^{cre/cre}$*Il1rl1*$^{flox/flox}$ mice that lack IL-33R or IL-25R, respectively, in ILC2s. This demonstrates that IL-33 and IL-25 play non-redundant roles in our model, suggesting that *in vivo* synergy between these two cytokines is necessary to optimally drive intestinal ILC2 expansion and activation in our model. Importantly, intestinal MC expansion after tape stripping was also abrogated in *Rora*$^{cre/cre}$*Il17rb*$^{flox/flox}$ mice and *Rora*$^{cre/cre}$*Il1rl1*$^{flox/flox}$ mice, indicating that expansion and activation of intestinal ILC2s is required for intestinal MC expansion. The selective upregulation of *Il25* expression in IECs and the high expression of IL-25R by intestinal ILC2s, but not in lung or skin ILC2s (Ricardo-Gonzalez et al., 2018), may underlie the selective expansion and activation of ILC2s in the small intestine after tape stripping. IL-33 acts on MCs to promote food anaphylaxis (Galand et al., 2016). IL-33 action on MCs cannot account by itself for the MC expansion and activation in tape-stripped mice, as these are strictly dependent on IL-4. However, IL-33 could act in synergy with IL-4 on MCs in our model.

We provide evidence that, after mechanical skin injury, intestinal ILC2s and tuft cells participate in a feedforward loop that amplifies their expansion and activation. We propose that, after tape stripping the skin, increased serum IL-33 activates intestinal ILC2s to produce IL-13 and IL-4, which drive the expansion of tuft cells and upregulate their production of IL-25, which amplifies ILC2 production of IL-13 and IL-4 in a feedforward loop. ILC2-derived IL-4 then drives intestinal MC expansion and activation. Such a feedforward loop has been demonstrated in intestinal helminth infection (Howitt et al., 2016; von Moltke

et al., 2016) and may have evolved to protect the intestine from helminths that infect it directly or via the skin as a portal of entry, as in the case of hookworms, and to provide concomitant immunity. In line with this hypothesis, oral administration of sodium succinate, a metabolite from protists and helminths, promotes expansion of intestinal-tuft-cell ILC2s and intestinal mast cells (Schneider et al., 2018; data not shown). ILC2-derived IL-4 and/or IL-13 drove intestinal MC expansion in our model by directly targeting MCs, as intestinal MC expansion after tape stripping was abolished in *Rora*$^{cre/cre}$*Il4/13*$^{flox/flox}$ mice and *Mcpt5-cre*$^{Tg/0}$*Il4ra*$^{flox/-}$ mice.

MCs play a protective role against microbes and helminths (Mukai et al., 2017). The crosstalk that we describe between mechanically injured skin and intestine may have evolved as a system to alert the gut to react to agents breaching the skin barrier. Importantly, intestinal MC expansion elicited by mechanical skin injury is likely relevant to food anaphylaxis in patients with AD. We tape stripped ~10% of the mouse body surface area in our model. A similar or greater percentage of body area is commonly affected and subject to scratching in patients with AD (Sugarman et al., 2003). Skin and serum IL-33 concentrations are increased in our model and in patients with AD (Galand et al., 2016; Savinko et al., 2012), and *Il33* mRNA expression increases in the skin of healthy individuals after scratching (Galand et al., 2016). We observed intestinal MC expansion in patients with AD, independent of food allergy history, serum IgE, or the presence of EOE. Moreover, increased intestinal permeability has been documented in patients with AD (Caffarelli et al., 2001; Kalimo et al., 1988). Taken together, our findings suggest that increased intestinal MCs and permeability elicited by mechanical skin injury inflicted by scratching may play an important role in promoting food anaphylaxis in patients with AD. Interventions that inhibit scratching may be useful in dampening the severity of food allergy in these patients by decreasing their intestinal MC load.

## STAR★METHODS

Detailed methods are provided in the online version of this paper and include the following:

- KEY RESOURCES TABLE
- CONTACT FOR REAGENT AND RESOURCE SHARING
- EXPERIMENTAL MODEL AND SUBJECT DETAILS
  - Mice
  - Human Subjects
- METHOD DETAILS
  - Mechanical Skin Injury, EC Sensitization, and Oral Antigen Challenge
  - Passive Sensitization
  - Intraperitoneal Sensitization
  - Histology
  - Cell Suspension Preparation and Flow Cytometry Analysis
  - Intestinal Permeability
  - *Il33, Il25,* and *Tslp* mRNA Expression and Its Release Upon Tape Stripping
- QUANTIFICATION AND STATISTICAL ANALYSIS

## SUPPLEMENTAL INFORMATION

Supplemental Information can be found online at https://doi.org/10.1016/j.immuni.2019.03.023.

## ACKNOWLEDGMENTS

We thank Dr. T. Chatila for his gift of *Mcpt5-cre*$^{Tg/0}$ mice; Dr. Andrew N.J. McKenzie for his gift of *Il1rl1*$^{-/-}$ and *Il17rb*$^{-/-}$ mice; Dr. Dennis O'Leary for his gift of *Rora*$^{cre/cre}$ mice; Dr. Nicolas Severe for help in immunofluorescence imaging; and Drs. T. Chatila, H. Oettgen, and J. Chou for reading the manuscript and for useful discussions. This work was supported by NIH grants AI113294-01A1 and U19 AI117673. J.-M.L.-C. is supported by NIAID T32 training grant (5T32AI007512).

## AUTHOR CONTRIBUTIONS

J.-M.L.-C., C.G., and R.S.G designed experiments. J.-M.L.-C., C.G., C.K., O.B., M.G., J.G., E.H., and S.N. performed experiments and analyzed data. F.B., C.D., F.D.F., R.T.L., S.Z. and K.F.A. contributed with critical reagents, mice, or analytic tools. J.-M.L.-C., C.G. and R.S.G interpreted data and wrote the manuscript.

## DECLARATION OF INTERESTS

The authors declare no competing interests.

Received: August 17, 2018
Revised: January 17, 2019
Accepted: March 25, 2019
Published: April 23, 2019

## REFERENCES

Ahrens, R., Osterfeld, H., Wu, D., Chen, C.Y., Arumugam, M., Groschwitz, K., Strait, R., Wang, Y.H., Finkelman, F.D., and Hogan, S.P. (2012). Intestinal mast cell levels control severity of oral antigen-induced anaphylaxis in mice. Am. J. Pathol. *180*, 1535–1546.

Al-Shami, A., Spolski, R., Kelly, J., Keane-Myers, A., and Leonard, W.J. (2005). A role for TSLP in the development of inflammation in an asthma model. J. Exp. Med. *202*, 829–839.

Angkasekwinai, P., Chang, S.H., Thapa, M., Watarai, H., and Dong, C. (2010). Regulation of IL-9 expression by IL-25 signaling. Nat. Immunol. *11*, 250–256.

Bartnikas, L.M., Gurish, M.F., Burton, O.T., Leisten, S., Janssen, E., Oettgen, H.C., Beaupre, J., Lewis, C.N., Austen, K.F., Schulte, S., et al. (2013). Epicutaneous sensitization results in IgE-dependent intestinal mast cell expansion and food-induced anaphylaxis. J Allergy Clin Immunol *131*, 451–460.e1–6.

Burton, O.T., Darling, A.R., Zhou, J.S., Noval-Rivas, M., Jones, T.G., Gurish, M.F., Chatila, T.A., and Oettgen, H.C. (2013). Direct effects of IL-4 on mast cells drive their intestinal expansion and increase susceptibility to anaphylaxis in a murine model of food allergy. Mucosal Immunology *6*, 740–750.

Caffarelli, C., Cavagni, G., Romanini, E., Caruana, P., and de Angelis, G. (2001). Duodenal IgE-positive cells and elimination diet responsiveness in children with atopic dermatitis. Ann. Allergy Asthma Immunol. *86*, 665–670.

Chou, S.J., Babot, Z., Leingärtner, A., Studer, M., Nakagawa, Y., and O'Leary, D.D. (2013). Geniculocortical input drives genetic distinctions between primary and higher-order visual areas. Science *340*, 1239–1242.

Dussault, I., Fawcett, D., Matthyssen, A., Bader, J.A., and Giguère, V. (1998). Orphan nuclear receptor ROR alpha-deficient mice display the cerebellar defects of staggerer. Mech. Dev. *70*, 147–153.

Fleischer, D.M., Bock, S.A., Spears, G.C., Wilson, C.G., Miyazawa, N.K., Gleason, M.C., Gyorkos, E.A., Murphy, J.R., Atkins, D., and Leung, D.Y. (2011). Oral food challenges in children with a diagnosis of food allergy. J Pediatr *158*, 578–583.e1.

Forbes, E.E., Groschwitz, K., Abonia, J.P., Brandt, E.B., Cohen, E., Blanchard, C., Ahrens, R., Seidu, L., McKenzie, A., Strait, R., et al. (2008). IL-9- and mast

cell-mediated intestinal permeability predisposes to oral antigen hypersensitivity. J. Exp. Med. *205*, 897–913.

Galand, C., Leyva-Castillo, J.M., Yoon, J., Han, A., Lee, M.S., McKenzie, A.N.J., Stassen, M., Oyoshi, M.K., Finkelman, F.D., and Geha, R.S. (2016). IL-33 promotes food anaphylaxis in epicutaneously sensitized mice by targeting mast cells. J. Allergy Clin. Immunol. *138*, 1356–1366.

Galli, S.J., and Tsai, M. (2012). IgE and mast cells in allergic disease. Nat. Med. *18*, 693–704.

Gerbe, F., Sidot, E., Smyth, D.J., Ohmoto, M., Matsumoto, I., Dardalhon, V., Cesses, P., Garnier, L., Pouzolles, M., Brulin, B., et al. (2016). Intestinal epithelial tuft cells initiate type 2 mucosal immunity to helminth parasites. Nature *529*, 226–230.

Groschwitz, K.R., Ahrens, R., Osterfeld, H., Gurish, M.F., Han, X., Abrink, M., Finkelman, F.D., Pejler, G., and Hogan, S.P. (2009). Mast cells regulate homeostatic intestinal epithelial migration and barrier function by a chymase/Mcpt4-dependent mechanism. Proc. Natl. Acad. Sci. USA *106*, 22381–22386.

Gurish, M.F., Tao, H., Abonia, J.P., Arya, A., Friend, D.S., Parker, C.M., and Austen, K.F. (2001). Intestinal mast cell progenitors require CD49dbeta7 (alpha4beta7 integrin) for tissue-specific homing. J. Exp. Med. *194*, 1243–1252.

Herbert, D.R., Hölscher, C., Mohrs, M., Arendse, B., Schwegmann, A., Radwanska, M., Leeto, M., Kirsch, R., Hall, P., Mossmann, H., et al. (2004). Alternative macrophage activation is essential for survival during schistosomiasis and downmodulates T helper 1 responses and immunopathology. Immunity *20*, 623–635.

Howitt, M.R., Lavoie, S., Michaud, M., Blum, A.M., Tran, S.V., Weinstock, J.V., Gallini, C.A., Redding, K., Margolskee, R.F., Osborne, L.C., et al. (2016). Tuft cells, taste-chemosensory cells, orchestrate parasite type 2 immunity in the gut. Science *351*, 1329–1333.

Kalimo, K., Lammintausta, K., Klemi, P., Leino, R., Panula, P., and Kalimo, H. (1988). Mast cells and IgE in intestinal mucosa in adult atopic dermatitis patients. Br. J. Dermatol. *119*, 579–585.

Lack, G., Fox, D., Northstone, K., and Golding, J.; Avon Longitudinal Study of Parents and Children Study Team (2003). Factors associated with the development of peanut allergy in childhood. N. Engl. J. Med. *348*, 977–985.

Lee, H., Park, J.H., Park, D.I., Kim, H.J., Cho, Y.K., Sohn, C.I., Jeon, W.K., Kim, B.I., and Chae, S.W. (2013). Mucosal mast cell count is associated with intestinal permeability in patients with diarrhea predominant irritable bowel syndrome. J. Neurogastroenterol. Motil. *19*, 244–250.

Leisten, S., Oyoshi, M.K., Galand, C., Hornick, J.L., Gurish, M.F., and Geha, R.S. (2013). Development of skin lesions in filaggrin-deficient mice is dependent on adaptive immunity. J Allergy Clin Immunol *131*, 1247–1250.

Leyva-Castillo, J.M., Hener, P., Jiang, H., and Li, M. (2013). TSLP produced by keratinocytes promotes allergen sensitization through skin and thereby triggers atopic march in mice. J. Invest. Dermatol. *133*, 154–163.

Li, M., Chiba, H., Warot, X., Messaddeq, N., Gérard, C., Chambon, P., and Metzger, D. (2001). RXR-alpha ablation in skin keratinocytes results in alopecia and epidermal alterations. Development *128*, 675–688.

Mathias, C.B., Hobson, S.A., Garcia-Lloret, M., Lawson, G., Poddighe, D., Freyschmidt, E.J., Xing, W., Gurish, M.F., Chatila, T.A., and Oettgen, H.C. (2011). IgE-mediated systemic anaphylaxis and impaired tolerance to food antigens in mice with enhanced IL-4 receptor signaling. J Allergy Clin Immunol *127*, 795–805.e1–6.

McKenzie, A.N.J., Spits, H., and Eberl, G. (2014). Innate lymphoid cells in inflammation and immunity. Immunity *41*, 366–374.

Mukai, K., Karasuyama, H., Kabashima, K., Kubo, M., and Galli, S.J. (2017). Differences in the Importance of Mast Cells, Basophils, IgE, and IgG versus That of $CD4^+$ T Cells and ILC2 Cells in Primary and Secondary Immunity to Strongyloides venezuelensis. Infect. Immun. *85*, e00053-17.

Oettgen, H.C., and Burton, O.T. (2015). IgE and Mast Cells: The Endogenous Adjuvant. Adv. Immunol. *127*, 203–256.

Okayama, Y., and Kawakami, T. (2006). Development, migration, and survival of mast cells. Immunol. Res. *34*, 97–115.

Oyoshi, M.K., Larson, R.P., Ziegler, S.F., and Geha, R.S. (2010). Mechanical injury polarizes skin dendritic cells to elicit a T(H)2 response by inducing cutaneous thymic stromal lymphopoietin expression. J Allergy Clin Immunol *126*, 976–984.

Pike, M.G., Heddle, R.J., Boulton, P., Turner, M.W., and Atherton, D.J. (1986). Increased intestinal permeability in atopic eczema. J. Invest. Dermatol. *86*, 101–104.

Ricardo-Gonzalez, R.R., Van Dyken, S.J., Schneider, C., Lee, J., Nussbaum, J.C., Liang, H.E., Vaka, D., Eckalbar, W.L., Molofsky, A.B., Erle, D.J., and Locksley, R.M. (2018). Tissue signals imprint ILC2 identity with anticipatory function. Nat. Immunol. *19*, 1093–1099.

Rickel, E.A., Siegel, L.A., Yoon, B.-R.P., Rottman, J.B., Kugler, D.G., Swart, D.A., Anders, P.M., Tocker, J.E., Comeau, M.R., and Budelsky, A.L. (2008). Identification of functional roles for both IL-17RB and IL-17RA in mediating IL-25-induced activities. J Immunol *181*, 4299–4310.

Saenz, S.A., Taylor, B.C., and Artis, D. (2008). Welcome to the neighborhood: epithelial cell-derived cytokines license innate and adaptive immune responses at mucosal sites. Immunol. Rev. *226*, 172–190.

Salimi, M., Barlow, J.L., Saunders, S.P., Xue, L., Gutowska-Owsiak, D., Wang, X., Huang, L.C., Johnson, D., Scanlon, S.T., McKenzie, A.N., et al. (2013). A role for IL-25 and IL-33-driven type-2 innate lymphoid cells in atopic dermatitis. J. Exp. Med. *210*, 2939–2950.

Salo, P.M., Arbes, S.J., Jr., Jaramillo, R., Calatroni, A., Weir, C.H., Sever, M.L., Hoppin, J.A., Rose, K.M., Liu, A.H., Gergen, P.J., et al. (2014). Prevalence of allergic sensitization in the United States: results from the National Health and Nutrition Examination Survey (NHANES) 2005-2006. J. Allergy Clin. Immunol. *134*, 350–359.

Savinko, T., Matikainen, S., Saarialho-Kere, U., Lehto, M., Wang, G., Lehtimäki, S., Karisola, P., Reunala, T., Wolff, H., Lauerma, A., and Alenius, H. (2012). IL-33 and ST2 in atopic dermatitis: expression profiles and modulation by triggering factors. J. Invest. Dermatol. *132*, 1392–1400.

Schneider, C., O'Leary, C.E., von Moltke, J., Liang, H.E., Ang, Q.Y., Turnbaugh, P.J., Radhakrishnan, S., Pellizzon, M., Ma, A., and Locksley, R.M. (2018). A Metabolite-Triggered Tuft Cell-ILC2 Circuit Drives Small Intestinal Remodeling. Cell *174*, 271–284.

Scholten, J., Hartmann, K., Gerbaulet, A., Krieg, T., Müller, W., Testa, G., and Roers, A. (2008). Mast cell-specific Cre/loxP-mediated recombination in vivo. Transgenic Res. *17*, 307–315.

Shimokawa, C., Kanaya, T., Hachisuka, M., Ishiwata, K., Hisaeda, H., Kurashima, Y., Kiyono, H., Yoshimoto, T., Kaisho, T., and Ohno, H. (2017). Mast Cells Are Crucial for Induction of Group 2 Innate Lymphoid Cells and Clearance of Helminth Infections. Immunity *46*, 863–874.e4.

Sicherer, S.H., and Sampson, H.A. (2009). Food allergy: recent advances in pathophysiology and treatment. Annu. Rev. Med. *60*, 261–277.

Spergel, J.M. (2010). From atopic dermatitis to asthma: the atopic march. Ann Allergy Asthma Immunol *105*, 99–106.

Spits, H., Artis, D., Colonna, M., Diefenbach, A., Di Santo, J.P., Eberl, G., Koyasu, S., Locksley, R.M., McKenzie, A.N., Mebius, R.E., et al. (2013). Innate lymphoid cells–a proposal for uniform nomenclature. Nat. Rev. Immunol. *13*, 145–149.

Stier, M.T., Zhang, J., Goleniewska, K., Cephus, J.Y., Rusznak, M., Wu, L., Van Kaer, L., Zhou, B., Newcomb, D.C., and Peebles, R.S., Jr. (2018). IL-33 promotes the egress of group 2 innate lymphoid cells from the bone marrow. J. Exp. Med. *215*, 263–281.

Strait, R.T., Mahler, A., Hogan, S., Khodoun, M., Shibuya, A., and Finkelman, F.D. (2011). Ingested allergens must be absorbed systemically to induce systemic anaphylaxis. J Allergy Clin Immunol *127*, 982–989.e1.

Sugarman, J.L., Fluhr, J.W., Fowler, A.J., Bruckner, T., Diepgen, T.L., and Williams, M.L. (2003). The objective severity assessment of atopic dermatitis score: an objective measure using permeability barrier function and stratum corneum hydration with computer-assisted estimates for extent of disease. Arch. Dermatol. *139*, 1417–1422.

Townsend, M.J., Fallon, P.G., Matthews, D.J., Jolin, H.E., and McKenzie, A.N. (2000). T1/ST2-deficient mice demonstrate the importance of T1/ST2 in developing primary T helper cell type 2 responses. J Exp Med *191*, 1069–1076.

Vaali, K., Lappalainen, J., Lin, A.H., Mäyränpää, M.I., Kovanen, P.T., Berstad, A., and Eklund, K.K. (2012). Imatinib mesylate alleviates diarrhea in a mouse model of intestinal allergy. Neurogastroenterol. Motil. *24*, e325–e335.

von Moltke, J., Ji, M., Liang, H.E., and Locksley, R.M. (2016). Tuft-cell-derived IL-25 regulates an intestinal ILC2-epithelial response circuit. Nature *529*, 221–225.

Wong, S.H., Walker, J.A., Jolin, H.E., Drynan, L.F., Hams, E., Camelo, A., Barlow, J.L., Neill, D.R., Panova, V., Koch, U., et al. (2012). Transcription factor RORα is critical for nuocyte development. Nat. Immunol. *13*, 229–236.

# STAR★METHODS

## KEY RESOURCES TABLE

| REAGENT or RESOURCE | SOURCE | IDENTIFIER |
|---|---|---|
| Antibodies | | |
| eBioscience Fixable Viability Dye eFluor 506 | Thermo Fisher | Cat# 65-0866-18 |
| Alexa Fluor 700 anti-mouse CD45 Antibody | Biolegend | Cat# 103128; RRID: AB_493715 |
| Biotin anti-mouse/human CD45R/B220 Antibody | Biolegend | Cat# 103204; RRID: AB_312989 |
| Biotin anti-mouse/human CD11b Antibody | Biolegend | Cat# 101204; RRID: AB_312787 |
| CD11c Monoclonal Antibody (N418), Biotin, | Thermo Fisher | Cat# 13-0114-85; RRID: AB_493715 |
| CD19 Monoclonal Antibody (eBio1D3 [1D3]) | Thermo Fisher | Cat# 13-0193-85; RRID: AB_657658 |
| F4/80 Monoclonal Antibody (BM8), Biotin | Thermo Fisher | Cat# 13-4801-85; RRID: AB_466658 |
| Ly-6G/Ly-6C Monoclonal Antibody (RB6-8C5), Biotin | Thermo Fisher | Cat# 13-5931-85; RRID: AB_466801 |
| CD335 (NKp46) Monoclonal Antibody (29A1.4), Biotin, | Thermo Fisher | Cat# 13-3351-82; RRID: AB_2572784 |
| CD3 Monoclonal Antibody (17A2), PerCP-eFluor 710 | Thermo Fisher | Cat# 46-0032-82; RRID: AB_1834427 |
| CD117 (c-Kit) Monoclonal Antibody (ACK2) | Thermo Fisher | Cat# 17-1172-83; RRID: AB_469434 |
| BV421 Rat Anti-Mouse IgE | BD Biosciences | Cat# 564207; RRID: AB_2738668 |
| CD31 (PECAM-1) Monoclonal Antibody (390), PE-Cyanine7 | Thermo Fisher | Cat# 25-0311-82; RRID: AB_2716949 |
| PE Rat Anti-Mouse Siglec-F | BD Biosciences | Cat# 552126; RRID: AB_394341 |
| Rabbit anti-DCAMKL1 | Abcam | Cat# ab31704; RRID: AB_873537 |
| Biological Samples | | |
| anti-trinitrophenyl (TNP) IgE monoclonal antibody | Finkelman FD | PMID: 22465213 |
| Chemicals, Peptides, and Recombinant Proteins | | |
| Peroxidase from horseradish | Sigma | P8375 |
| Albumin from chicken egg white | Sigma | A5503 |
| Imject Alum Adjuvant | Thermo Fisher | 77161 |
| Sodium succinate hexahydrate | Alfa Aesar | Cat# 41983 |
| Critical Commercial Assays | | |
| RNeasy Micro Kit | QIAGEN | Cat# 74004 |
| MCPT-1 (mMCP-1) Mouse Uncoated ELISA Kit | Thermo fisher | Cat# 7400488-7503-86 |
| Mouse/Rat IL-33 Quantikine ELISA Kit | R&D | Cat# 74004M3300 |
| Mouse TSLP Quantikine ELISA Kit | R&D | Cat# 74004MTLP00 |
| RNAqueous Total RNA Isolation Kit | Thermo Fisher | Cat# 74004AM1912 |
| Experimental Models: Organisms/Strains | | |
| Mouse, BALB/cAnNCrl | Charles River | Strain code: 028 |
| Mouse, C57BL/6NCrl | Charles River | Strain code: 027 |
| Mouse, BALB/cAnNTac | Taconic | Model# BALB-F |
| Mouse, Balb/c *Kit*$^{W\text{-}sh/W\text{-}sh}$ | Michael Stassen, Johannes Gutenberg University | N/A |
| Mouse, Balb/c *Itgb7*$^{-/-}$ | In this paper | N/A |
| *K14-Cre*$^{Tg/0}$*Il33*$^{flox/flox}$ | In this paper | N/A |
| Mouse, Balb/c *Il1rl1*$^{-/-}$ | Andrew N.J. McKenzie | N/A |
| Mouse, Balb/c *Il17rb*$^{-/-}$ | Amgen | N/A |
| Mouse, Balb/c *Tslpr*$^{-/-}$ | Steve F. Ziegler | N/A |
| *K14-Cre*$^{Tg/0}$*Il25*$^{flox/flox}$ | In this paper | N/A |
| *Vil1-Cre*$^{Tg/0}$*Il25*$^{flox/flox}$ | In this paper | N/A |
| Mouse, Balb/c *Rag2*$^{-/-}$ | Taconic | 601 |
| *Rag2*$^{-/-}\gamma c^{-/-}$ | Taconic | 4111 |

(*Continued on next page*)

**Continued**

| REAGENT or RESOURCE | SOURCE | IDENTIFIER |
|---|---|---|
| *Il7ra*$^{-/-}$ | JAX | Stock Number 002295 |
| *Rora*$^{sg/sg}$ | JAX | 000237 |
| *Rora*$^{Cre/Cre}$*ROSA26*$^{YFP}$ | Raif Geha, Boston Children's Hospital | N/A |
| *Rora*$^{Cre/Cre}$*Il17rb*$^{flox/flox}$ | In this paper | N/A |
| *Rora*$^{Cre/Cre}$*Il1rl1*$^{flox/flox}$ | In this paper | N/A |
| *Rora*$^{Cre/Cre}$ | Dennis O'Leary | N/A |
| *Rora*$^{Cre/Cre}$*Il4/13*$^{flox/flox}$ | In this paper | N/A |
| Mouse, Balb/c *Mcpt5-Cre*$^{Tg/0}$*Il4ra*$^{flox/-}$ | In this paper | N/A |
| Mouse, Balb/c *Mcpt5-Cre*$^{Tg/0}$ | Talal Chatila, Boston Children's Hospital | N/A |
| Oligonucleotides | | |
| Hdc TaqMan Assays | Thermo Fisher | Assay ID Mm00456104_m1 |
| Alox5 TaqMan Assays | Thermo Fisher | Mm01182747_m1 |
| Il13 TaqMan Assays | Thermo Fisher | Mm00434204_m1 |
| Kit TaqMan Assays | Thermo Fisher | Mm00445212_m1 |
| Fcerla TaqMan Assays | Thermo Fisher | Mm00438867_m1 |
| Il4 TaqMan Assays | Thermo Fisher | Mm00445259_m1 |
| Il9 TaqMan Assays | Thermo Fisher | Mm00434305_m1 |
| Il33 TaqMan Assays | Thermo Fisher | Mm00505403_m1 |
| TSLP TaqMan Assays | Thermo Fisher | Mm01157588_m1 |
| Il25 TaqMan Assays | Thermo Fisher | Mm00499822_m1 |
| Il5 TaqMan Assays | Thermo Fisher | Mm00439646_m1 |
| Software and Algorithms | | |
| GraphPad Prism 7 | GraphPad Software | N/A |
| FlowJo 10.4.2 | Tree Star | https://www.flowjo.com/solutions/flowjo/downloads |
| Morpheus | Broad Institute | https://software.broadinstitute.org/morpheus/ |

## CONTACT FOR REAGENT AND RESOURCE SHARING

Further information and requests for resources and reagents should be directed to and will be fulfilled by the Lead Contact, Raif S. Geha (raif.geha@childrens.harvard.edu).

## EXPERIMENTAL MODEL AND SUBJECT DETAILS

### Mice

WT BALB/c, C57BL/6, and B6.SJL mice were purchased from Charles River Laboratories. BALB/c, Rag2-deficient mice, Rag2-gamma chain-deficient mice were obtained from Taconic. ST2-deficient *Il1rl1*$^{-/-}$ mice obtained from Dr. Andrew N.J. McKenzie (Townsend et al., 2000); IL-25R-deficient *Il17rb*$^{-/-}$ mice obtained from Amgen (Rickel et al., 2008); IL-25R-floxed *Il17rbfl/fl* mice and TSLPR-deficient mice (Al-Shami et al., 2005) were obtained from Dr. Steve F. Ziegler; Il4Rα-floxed mice were obtained from Dr. Frank Brombacher on BALB/c background (Herbert et al., 2004). Mcpt5-cre mice (Scholten et al., 2008), obtained from Dr. Talal Chatila, were derived for >6 generations on BALB/c background. Integrin beta7 *Itgb7*$^{-/-}$, *K14-creTg/0*, *Vil1-cre Tg/0*, Il7R -deficient, RORα-deficient mice, on C57Bl/6 background and IL-4Rα-deficient mice, on a Balb/c background, were obtained from Jax. Integrin beta7 *Itgn7*$^{-/-}$ were derived for >6 generations on BALB/c background in the laboratory. ST2-floxed *Il1rl1fl/fl* mice and IL-33-floxed mice obtained from Dr. Richard T Lee; IL-25-floxed mice obtained from Dr. Chen Dong (Angkasekwinai et al., 2010); and Rora-cre mice obtained from Dr. Dennis O'Leary (Chou et al., 2013), on a C57Bl/6 background were crossed once with mice on BALB/c background. All mice were housed in a specific pathogen-free environment and fed an OVA-free diet. All procedures were performed in accordance with the Animal Care and Use Committee of Boston Children's Hospital.

### Human Subjects

Excess of duodenal biopsy samples from children endoscoped because of abdominal pain, were collected during routine clinical care. Subjects were divided in 2 groups: active AD and scratching and subjects with no AD and no scratching based on history and clinical examination recorded by their gastroenterologist (E.H.). Samples were submitted in a blinded fashion to the pathologist (J.G.).

## METHOD DETAILS

### Mechanical Skin Injury, EC Sensitization, and Oral Antigen Challenge

Mechanical skin injury consists in two cycles of tape stripping, one at day 0 and one at day 3 (scheme in Figure 1A). For the first cycle, 6- to 8-week-old female mice were anesthetized; their back skin was shaved and tape-stripped with a film dressing (TegadermTM, 3M) 6 times. For the other cycle, mice were tape stripped 3 times. Finally, mice were sacrificed at different time points.

### Passive Sensitization

6- to 8-week-old female mice were injected intravenously with 10 μg of anti-trinitrophenyl (TNP) IgE monoclonal antibody (mAb). The following day, mice were challenged intragastrically with 12.5mg of TNP conjugated bovine serum albumin (TNP-BSA). Temperature changes were measured every 5 min following OVA challenge using the DAS-6001 Smart Probe and IPTT-300 transponders (Bio Medic Data Systems) injected subcutaneously.

### Intraperitoneal Sensitization

6- to 8-week-old female mice were injected intraperitoneally (i.p.) with 50 μg of OVA and 1 mg of alum at day 0 and day 7. At day 14, mice were challenged intragastrically with 100 mg of OVA. Temperature changes were measured as described above.

### Histology

For the chloroacetate esterase (CAE) staining, 1 cm pieces of mouse jejunum were fixed in 4% paraformaldehyde overnight at 4°C and embedded in paraffin. Paraffin sections were stained with CAE. $CAE^+$ cells were counted by an investigator who was blinded to the experimental groups. For the tryptase staining, duodenal biopsy samples were stained with an anti-tryptase antibody. Ten HPFs in areas of high-density MCs were evaluated blinded per the criteria used in evaluating EOE. For DCLK1 staining, the whole SI were treated as previously described (von Moltke et al., 2016), rolled and frozen in OCT. 10μM slices were first incubated with rat serum then stained with purified mAb anti-DCLK1 (ab31704) from Abcam, and with secondary Ab anti-rabbit IgG. Slices were fixed with a mounting medium containing DAPI (Prolon Gold) from ThermoFisher Scientific.

### Cell Suspension Preparation and Flow Cytometry Analysis

Cell isolation from the jejunum was performed as previously described (Galand et al., 2016). In brief, the jejuna were harvested, flushed with PBS supplemented with 2% fetal calf serum, opened longitudinally, and cut in 1 cm long pieces. Then, intestinal pieces were incubated in HBSS without Ca2+ and Mg2+ supplemented with 10 mM EDTA, 10 mM HEPES, 0.5% fetal calf serum, and 1.5 mM DTE, for 20 min at 37°C twice. Intestinal pieces were digested in HBSS with Ca2+ and Mg2+, 20% fetal calf serum, 100 U/mL collagenase VIII (Sigma-Aldrich), and 5 μg/mL DNase (Sigma-Aldrich) for 60 min at 37°C. Immune cells were purified with a 40% Percoll gradient (GE Healthcare).

Cell isolation from the skin was performed as previously described (Leisten et al., 2013). One-centimer squares of back skin were harvested; the layer of fat under the dermis was scrapped. Lower left lobes of lung were harvested. Skin remaining tissue and lung lobes were chopped finely and incubated for 60 and 30 min, respectively, at 37°C in complete RPMI media complemented with 100U Liberase DL (Roche) and 5 μg/mL DNase (Sigma-Aldrich). Red blood cells of the lung suspensions were lysed with ACK buffer. The cell suspensions were washed, incubated with TruStain FcX (anti-CD16/32 antibody; 10 μg/ml; Biolegend) and stained with the eF506 viability dye from eBioscience to exclude dead cells and the following murine fluorochrome labeled-monoclonal antibodies: B220 (RA3-6B2), CD3 (17A2), CD4 (GK1.5), CD11c (N418), CD19 (1D3), CD45 (30F11), CD90.2 (53-2.1), c- Kit (ACK2), Gr1 (RB6-8C5), IL-13Rα1 (13MOKA), ST2 (RMST2-2) from eBioscience, CD11b (M1/70), F4/80 (BM8), FcεRI (MAR-1), IgE (RME-1) and IL-17RB (9B10) from Biolegend. BV605 Streptavidin from Biolegend was used to detect biotinylated antibodies. For transcription factor staining, cells were fixed and permeabilized (eBiosicence fix/perm kit) and stained in permeabilization solution with GATA-3 (TWAJ) and Rorc (B2D) antibodies from eBioscience. For cytokine staining, cells were stimulated with Ionomycin (0.5ug/ml; Sigma), Phorbol 12,13- dibutyrate (1ug/ml; Sigma), Brefeldin A (eBioscience), Monensin (eBioscience) in complete RPMI for 3 h before surface staining. Then, cells were fixed and permeabilized (BD Biosciences Cytofix/Cytoperm) and stained in permeabilization solution with IL-4 (11B11), IL-5 (TRFK5), IL-9 (RM9A4) antibodies from Biolegend and IL-13 (eBio13A) antibodies from eBioscience. Cells were analyzed by flow cytometry using an LSRFortessa machine (BD Biosciences). The data were analyzed with FlowJo software.

### Intestinal Permeability

Intestinal permeability was determined as previously (Mathias et al., 2011). Briefly, mice were gavaged at day 14 with 400 μl of a 1 mg/ml horseradish peroxidase solution (HRP, MW 44 kDa; Sigma). Blood was obtained 4h later and the concentration of HRP was measured in the serum using the TMB substrate system.

### *Il33, Il25,* and *Tslp* mRNA Expression and Its Release Upon Tape Stripping

The back skin of anesthetized mice was shaved and subjected to tape stripping six times with a film dressing (TegadermTM, 3M). 6 h later, RNA was extracted from the skin with Total RNA isolation kit (Ambion). Intestinal epithelial cells were isolated from the duodenum as previously described (Gerbe et al., 2016). cDNA was prepared with iscript cDNA synthesis kit (Biorad). Quantitative real-time PCR was done with the Taqman gene expression assay, universal PCR master mix and ABI prism 7300 sequence detection system (Applied Biosystems). *Il25*, *Il33* and *tslp* mRNA fold induction was calculated using delta-delta ct with normalization to the internal control *β2microglobulin*. An arbitrary unit of 1 was assigned to the mean value of unmanipulated skin samples or intestinal epithelial cells from unmanipulated mice. For measuring IL-33, IL-25 and TSLP release, patches of ~1cm2 skin were excised from unmanipulated back or immediately post-tape stripping. Subcutaneous fat was removed, and the patches were cultured for 1 hr in complete RPMI. IL-25, IL-33 and TSLP in the supernatant and the sera, harvested 1 hr after tape stripping, was measured using Quantikine ELISA kit (R&D Systems) for IL-33 and Ready-set- go ELISA kit (eBioscience) for IL-25 and TSLP.

## QUANTIFICATION AND STATISTICAL ANALYSIS

All experiments were performed using randomly assigned mice without investigator blinding. Results of allergen challenge studies were analyzed using two-way ANOVA. Other results were analyzed by one-way ANOVA or non-parametric t tests using Prism 7 (GraphPad). A p value of less than 0.05 was considered significant.

**Immunity, Volume *50***

## Supplemental Information

# Mechanical Skin Injury Promotes Food Anaphylaxis by Driving Intestinal Mast Cell Expansion

**Juan-Manuel Leyva-Castillo, Claire Galand, Christy Kam, Oliver Burton, Michael Gurish, Melissa A. Musser, Jeffrey D. Goldsmith, Elizabeth Hait, Samuel Nurko, Frank Brombacher, Chen Dong, Fred D. Finkelman, Richard T. Lee, Steven Ziegler, Isaac Chiu, K. Frank Austen, and Raif S. Geha**

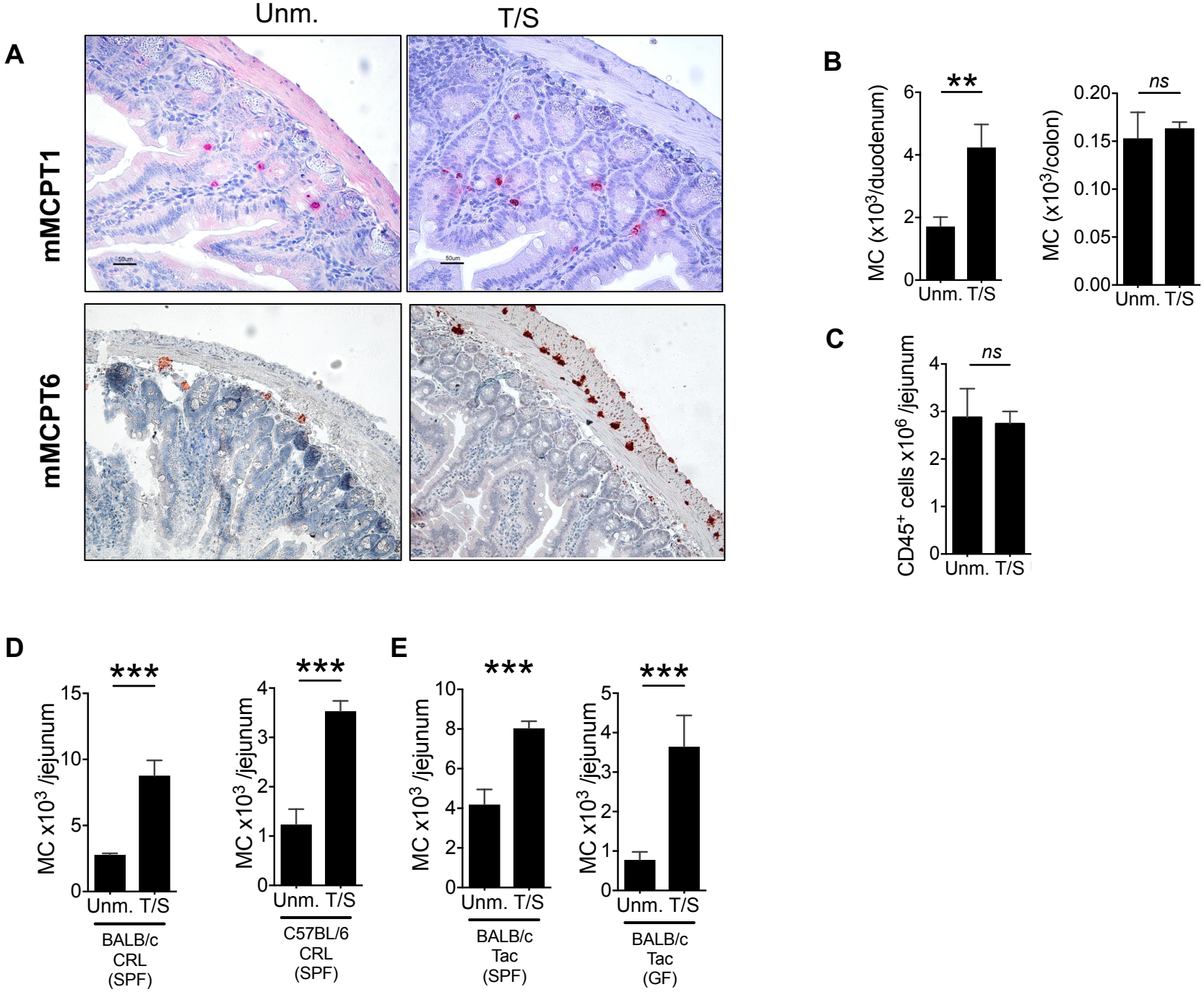

A
Unm.
T/S
mMCPT1
mMCPT6
B
**
ns
MC (x10³/duodenum)
MC (x10³/colon)
Unm. T/S
C
ns
CD45⁺ cells x10⁶ /jejunum
Unm. T/S
D
***
***
MC x10³ /jejunum
Unm. T/S
BALB/c CRL (SPF)
C57BL/6 CRL (SPF)
E
***
***
MC x10³ /jejunum
Unm. T/S
BALB/c Tac (SPF)
BALB/c Tac (GF)

**Figure S1**

**Figure S1. Tape stripping causes expansion of intestinal submucosal and mucosal MCs and of intestinal MCs in different mice strains and independently of the microbiota, related to Figure 1. A.** Representative immunohistochemistry staining for mMCPT1 (top) and mMCPT6 (bottom) of jejunal sections from tape stripped (T/S) mice and unmanipulated (Unm.) controls. **B.** Absolute numbers of c-kit$^+$IgE$^+$ MCs in duodenum (left) and colon (right) of T/S mice and Unm. controls. Results are derived from 2 independent experiments with 3 to 5 mice/group. **C.** Numbers of CD45$^+$ cells in the jejunum of T/S mice and Unm. controls. Results are derived from 2 independent experiments with 3 to 5 mice/group. **D.** Absolute numbers of jejunal c-kit$^+$IgE$^+$ MCs in T/S and Unm. BALB/c (left) and C57BL/6 (right) mice from Charles River Labs (CRL) kept at Children's Hospital Boston specific pathogen free (SPF) facility. Data representative of 2 independent experiments each with 3 to 4 mice/group. **E.** Absolute numbers of jejunal c-kit$^+$IgE$^+$ MCs in T/S and Unm. BALB/c mice from Taconic Biosciences (Tac) kept at Children's Hospital Boston SPF (left) or germ free (GF) facility. Data representative of 2 independent experiments each with 3 to 4 mice/group. Columns and bars represent mean and SEM. ** = $p < 0.01$, *** = $p < 0.001$, ns: not significant.

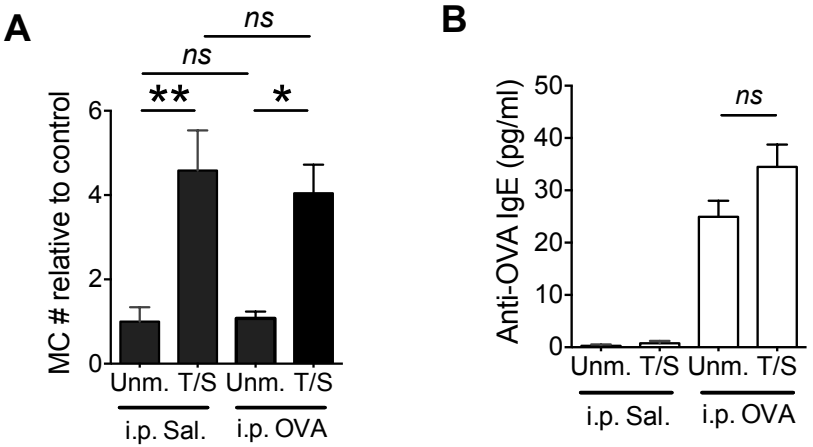

A
ns
ns
**
*
MC # relative to control
6
4
2
0
Unm.
T/S
Unm.
T/S
i.p. Sal.
i.p. OVA
B
ns
Anti-OVA IgE (pg/ml)
50
40
30
20
10
0
Unm.
T/S
Unm.
T/S
i.p. Sal.
i.p. OVA

**Figure S2**

**Figure S2. Intestinal MC expansion and antigen specific IgE in mice tape stripped and i.p. immunized with OVA, related to Figure 2. A-B.** Relative numbers (#) of jejunal MCs (A) and Serum anti-OVA IgE antibody concentrations (B) in WT BALB/c mice *i.p.* immunized with OVA or saline and tape stripped (T/S) or left unmanipulated (Unm.) as per the protocol in Fig. 2B. Data representative of 2 independent experiments each with 4-5 mice/group. Columns and bars represent mean and SEM. * = $p < 0.05$, ** = $p < 0.01$, ns: not significant.

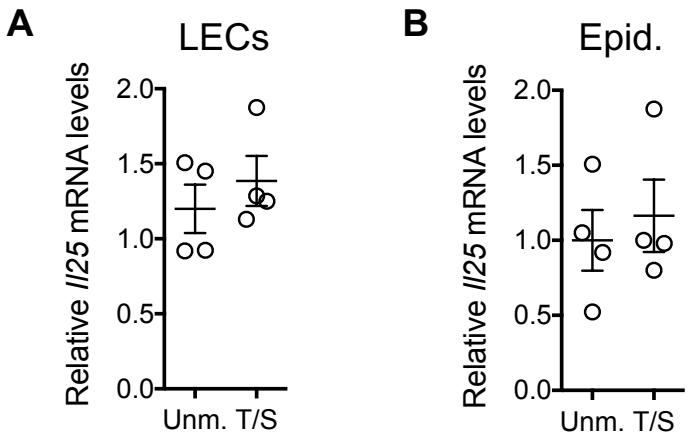

A
LECs
Relative Il25 mRNA levels
2.0
1.5
1.0
0.5
0.0
Unm.
T/S
B
Epid.
Relative Il25 mRNA levels
2.0
1.5
1.0
0.5
0.0
Unm.
T/S

**Figure S3**

**Figure S3**. **Effect of tape stripping on *Il25* mRNA expression in lung and skin epithelial cells, related to Figure 3. A.** *Il25* mRNA expression in lung epithelium cells (LECs) and skin epidermal layer (Epid.) from ears of mice tape stripped on back skin or unmanipulated controls. ns: not significant. Values represent fold induction relative to the mean value in unmanipulated mice. Results are derived from 2 independent experiments each with respectively 3 -5 mice/group.

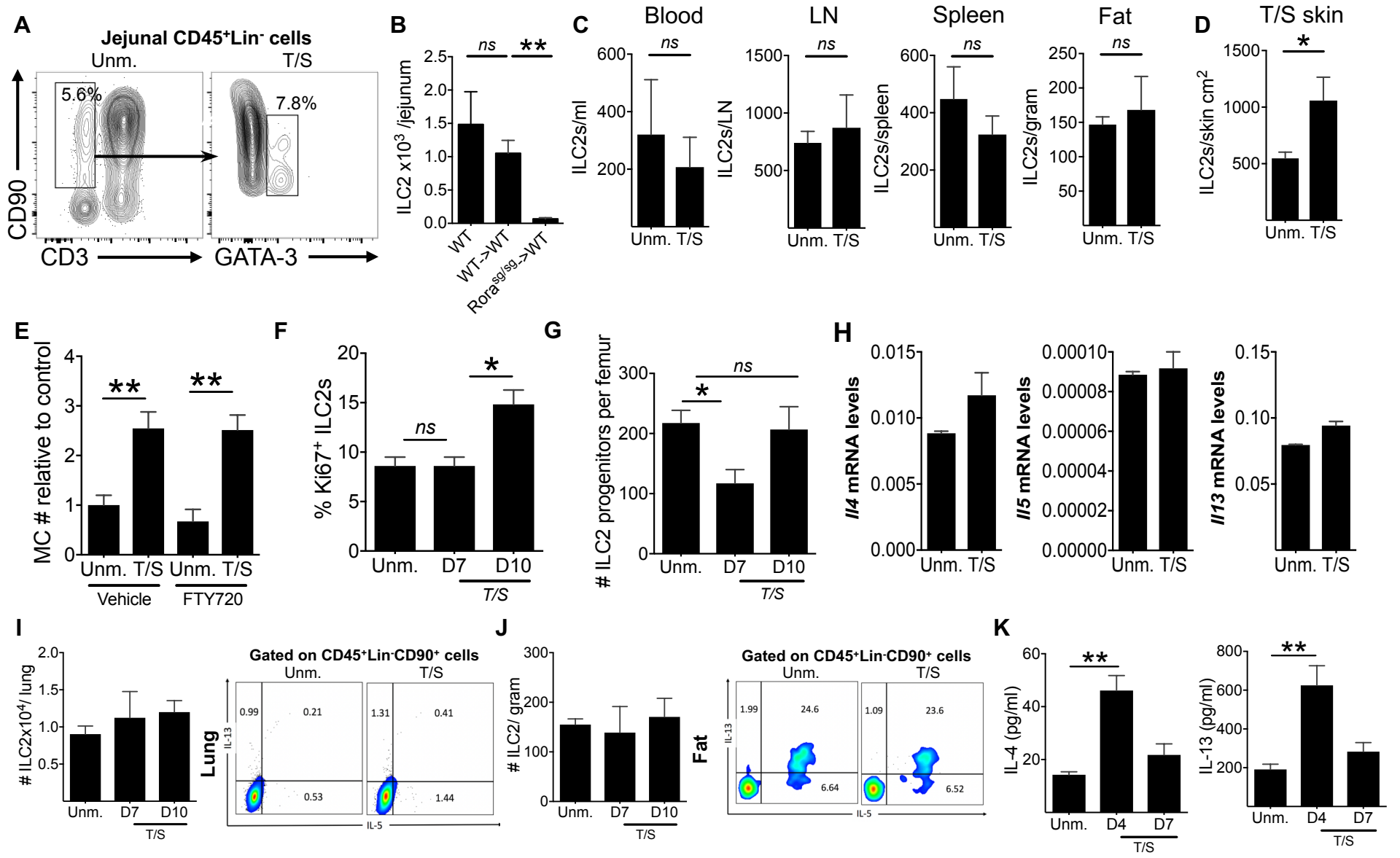
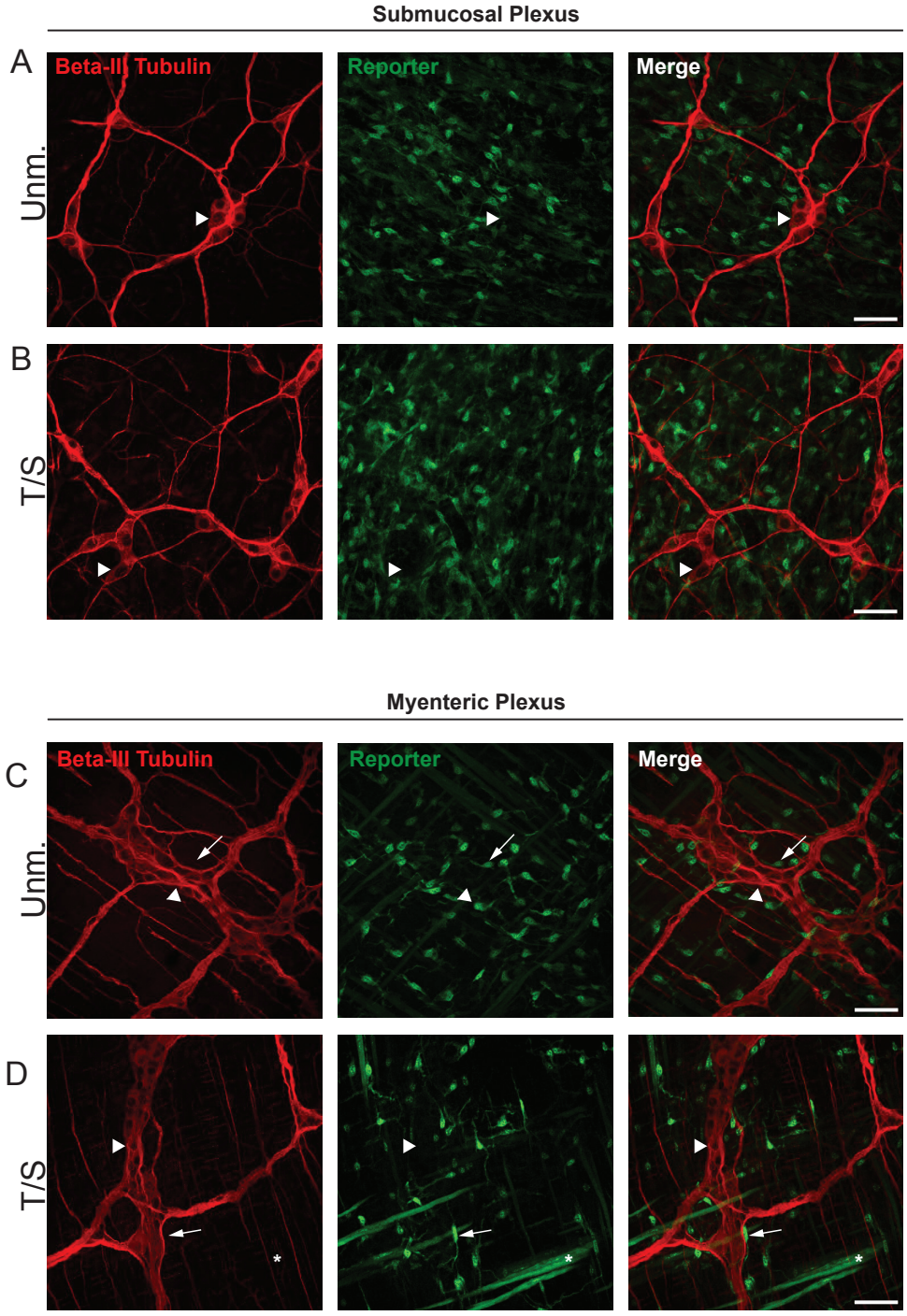

A
Jejunal CD45+Lin- cells
Unm.
T/S
5.6%
7.8%
CD90
CD3
GATA-3
B
ILC2 x10^3 /jejunum
ns
**
WT
WT->WT
Rora sg/sg->WT
C
Blood
LN
Spleen
Fat
ILC2s/ml
ILC2s/LN
ILC2s/spleen
ILC2s/gram
ns
Unm. T/S
D
T/S skin
ILC2s/skin cm2
*
E
MC # relative to control
**
Unm. T/S Unm. T/S
Vehicle
FTY720
F
% Ki67+ ILC2s
ns
*
Unm. D7 D10
T/S
G
# ILC2 progenitors per femur
ns
*
Unm. D7 D10
T/S
H
Il4 mRNA levels
Il5 mRNA levels
Il13 mRNA levels
Unm. T/S
I
# ILC2x10^4/ lung
Unm. D7 D10
T/S
Gated on CD45+Lin-CD90+ cells
Unm.
T/S
Lung
IL-13
IL-5
0.99
0.21
0.53
1.31
0.41
1.44
J
# ILC2/ gram
Unm. D7 D10
T/S
Gated on CD45+Lin-CD90+ cells
Unm.
T/S
Fat
IL-13
IL-5
1.99
24.6
6.64
1.09
23.6
6.52
K
IL-4 (pg/ml)
IL-13 (pg/ml)
**
Unm. D4 D7
T/S

**Figure S4**

**Figure S4**. **Gating strategy for intestinal ILC2s, absence of ILC2s in the intestine of *Rora*$^{sg/sg}$->WT, number of ILC2s in different tissues, effect of the sphingosine-1-phosphate (S1P) analogue FTY720 on intestinal MC expansion , effect of tape stripping on proliferation of jejunal ILC2s and mobilization of ILC2 progenitors from the bone marrow, type 2 cytokine expression in ILCs from distant skin sites, lungs and fat and Serum IL-4 and IL-13 are increased by tape stripping prior to intestinal ILC2 expansion related to Figure 4. A.** Representative flow cytometry analysis of CD90$^+$CD3$^-$GATA-3$^+$ ILC2s in the CD45$^+$Lin$^-$ fraction of LP cells from the jejunum. **B.** Numbers of jejunal ILC2s in unmanipulated *Rora*$^{sg/sg}$->WT chimeras, WT-WT chimeras and WT mice controls. **C-D.** Numbers of CD45$^+$Lin$^-$CD90$^+$GATA3$^+$ ILC2s in blood, lymph node (LN), spleen, visceral adipose tissue (C) and in the unmanipulated and tape stripped skin (D) of unmanipulated (Unm) and tape stripped (T/S) WT BALB/c mice. **E.** Jejunal MC numbers (#) in unmanipulated (Unm) and tape stripped (T/S) BALB/c mice treated with FTY720 or vehicle. **F.** Percentage of CD45$^+$Lin$^-$CD90$^+$GATA3$^+$Ki67$^+$ cells in the jejunum of unmanipulated (Unm) and tape stripped (T/S) WT mice. **G.** Numbers (right) of Lin$^-$Sca1$^+$IL-25R$^+$CD25$^+$CD127$^+$ ILC2 progenitors (ILC2p) in bone marrow cells from T/S or Unm. mice. **H.** *Il4, Il5 and Il13 mRNA* expression, relative to *B2m*, in sorted CD45$^+$Lin$^-$CD90$^+$ ILCs from distant skin sites of T/S mice and skin from Unm. controls. Data pooled from 2 independent experiments each with 3-4 mice/group. Columns and bars represent mean and SEM. **I-J.** ILC2 quantitation in lungs and visceral adipose tissue of WT BALB/c mice mice on Days 0, 7 and 10 post tape stripping (left panels) and representative flow cytometry analysis of the expression of IL-5 and IL-13 by CD45$^+$Lin$^-$CD90$^+$ ILCs in the lungs and visceral adipose tissue of Unmanipulated (Unm) mice and mice on Day 7 after tape stripping (right panels).

**K.** Serum concentration of IL-4 (left) and IL-13 (right) in tape stripped (T/S) or left unmanipulated (Unm.) WT mice at different time points. Results are derived from 2 independent experiments.


Submucosal Plexus
A
Unm.
Beta-III Tubulin
Reporter
Merge
B
T/S
Myenteric Plexus
C
Unm.
Beta-III Tubulin
Reporter
Merge
D
T/S

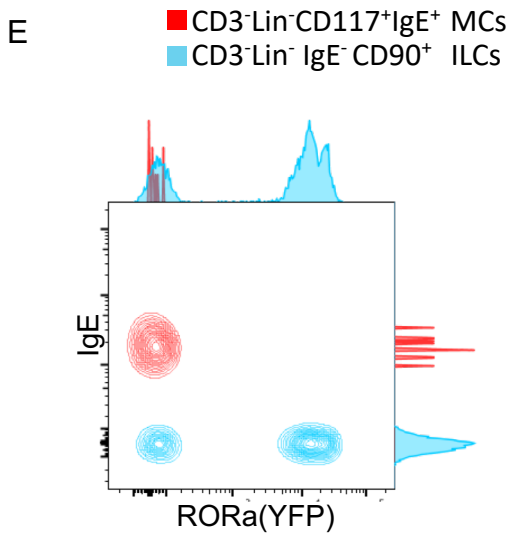

E
CD3⁻Lin⁻CD117⁺IgE⁺ MCs
CD3⁻Lin⁻ IgE⁻ CD90⁺ ILCs
IgE
RORa(YFP)

**Figure S5**

**Figure S5. RORα is not expressed in intestinal neurons or MCs, related to Figure 5. A-D.** Representative images from jejunum of tape stripped unmanipulated (Unm) and tape stripped (T/S) *Rora*$^{cre/cre}$*ROSA*$^{YFP}$ mice. Beta-III tubulin is a pan-neuronal marker, labeling neuron bodies and processes. In the submucosal plexus, YFP expression rarely, if ever, overlapped with Beta-III tubulin expression in (A) T/S mouse submucosal plexus vs (B) Unm. mouse submucosal plexus (arrowheads). Similar to the submucosal plexus, reporter expression very rarely overlapped with Beta-II tubulin expression in (A) T/S mouse vs (B) Unm. mouse (arrowheads). Reporter expression was seen in cells with smooth muscle morphology (asteriks) as well as cells near the periphery of ganglia, possibly interstitial cells of Cajal, glia, or immune cells based on location, morphology and processes (arrows). 40x. Scale bar = 50 um. **E.** Representative flow cytometry analysis of *Rora* (YFP) expression in intestinal ILCs ($CD45^+Lin^-CD90^+$) and MCs ($CD45^+Lin^-CD117^+\alpha\text{-}IgE^+$) in *Rora*$^{cre/cre}$*ROSA*$^{YFP}$ mice.

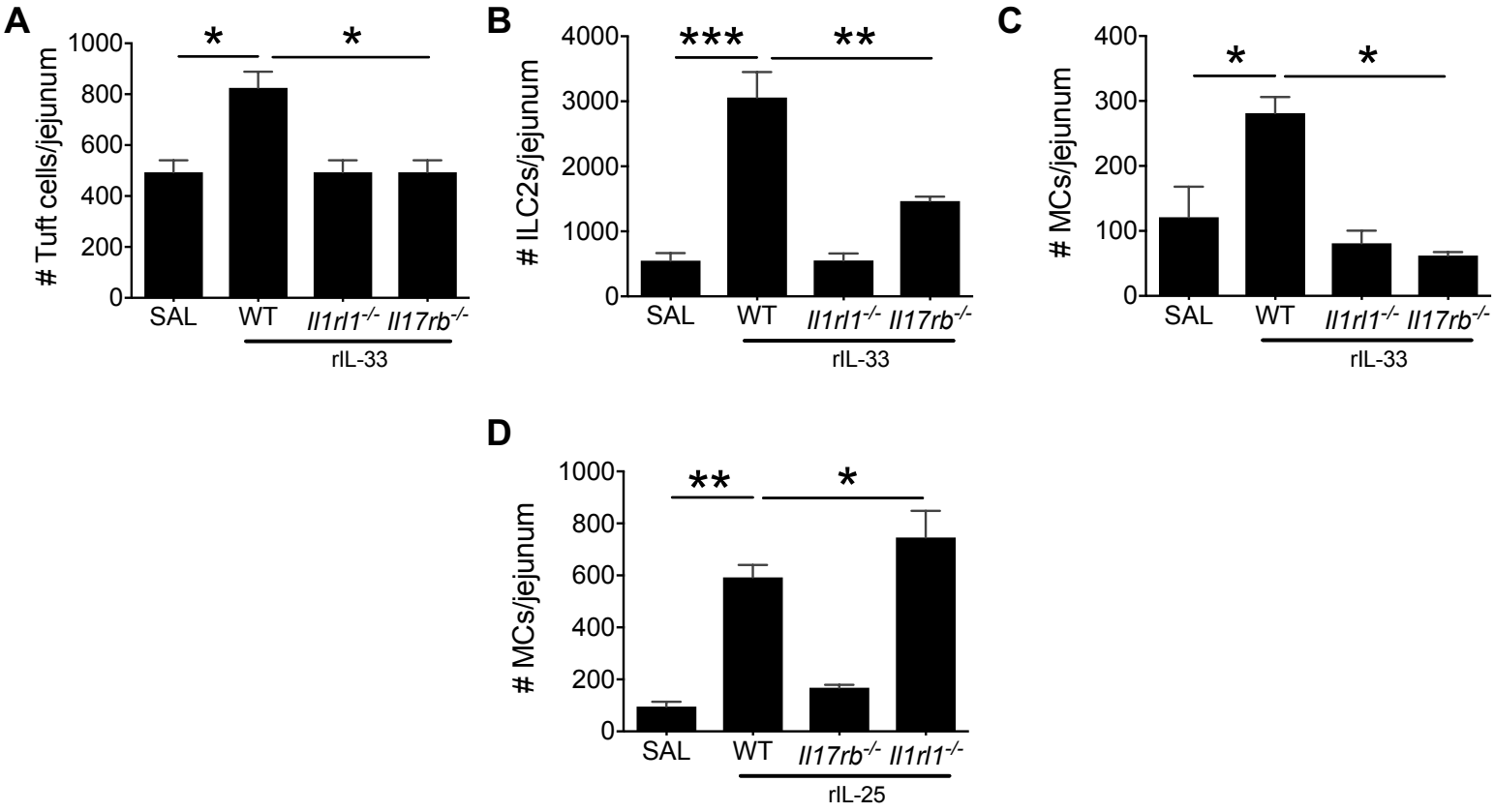

A
# Tuft cells/jejunum
1000
800
600
400
200
0
*
*
SAL
WT
Il1rl1-/-
Il17rb-/-
rIL-33
B
# ILC2s/jejunum
4000
3000
2000
1000
0
***
**
SAL
WT
Il1rl1-/-
Il17rb-/-
rIL-33
C
# MCs/jejunum
400
300
200
100
0
*
*
SAL
WT
Il1rl1-/-
Il17rb-/-
rIL-33
D
# MCs/jejunum
1000
800
600
400
200
0
**
*
SAL
WT
Il17rb-/-
Il1rl1-/-
rIL-25

**Figure S6**

**Figure S6. Effect of i.v injection of rIL-33 and rIL-25 in the expansion of intestinal tuft cells, ILC2 and MCs, related to Figure 5. A-C.** Number of $CD45^{-}SiglecF^{+}EPCAM^{+}$ tuft cells (A), $CD45^{+}Lin^{-}CD90^{+}GATA3^{+}$ ILC2s (B) and $CD45^{+}Lin^{-}CD117^{+}\alpha\text{-}IgE^{+}$ MCs (C) in the jejunum of *Il1rl1*$^{-/-}$ and *Il17rb*$^{-/-}$ mice and WT controls injected with rIL-33. **D.** Number of MCs in the jejunum of *Il17rb*$^{-/-}$ and *Il1rl1*$^{-/-}$ mice and WT controls injected with rIL-25. Results are derived from 2 independent experiments with 3 to 5 mice/group. Columns and bars represent mean and SEM. * = $p < 0.05$, ** = $p < 0.01$, *** = $p < 0.001$.